NACA RM L55L13

NACA

RESEARCH MEMORANDUM

INVESTIGATION OF JET EFFECTS ON A FLAT SURFACE DOWNSTREAM OF THE EXIT OF A SIMULATED TURBOJET NACELLE AT A FREE-STREAM MACH NUMBER OF 1.39

By Walter E. Bressette and Abraham Leiss

Langley Aeronautical Laboratory
Langley Field, Va.

NATIONAL ADVISORY COMMITTEE
FOR AERONAUTICS

WASHINGTON

April 2, 1956
Declassified February 10, 1959

NACA RM L55L13

NATIONAL ADVISORY COMMITTEE FOR AERONAUTICS

RESEARCH MEMORANDUM

INVESTIGATION OF JET EFFECTS ON A FLAT SURFACE DOWNSTREAM OF THE EXIT OF A SIMULATED TURBOJET NACELLE AT A FREE-STREAM MACH NUMBER OF 1.39

By Walter E. Bressette and Abraham Leiss

SUMMARY

An investigation at a free-stream Mach number of 1.39 utilizing a blowdown-type tunnel was made to determine the effects of a propulsive jet on a zero angle-of-attack wing surface located in the vicinity of both a choked convergent nozzle and a convergent-divergent nozzle. Static-pressure surveys were made on a flat surface that was located in the vicinity of the propulsive jet. The nozzles were operated over a varied range of both exit static- and total-pressure ratios at different, fixed vertical distances from the flat surface.

Within the scope of this investigation, it was found that shock waves, formed in the external flow because of the presence of the jet exhaust, impinged on the flat surface and greatly altered the pressure distribution. An integration of this pressure distribution for the choked convergent nozzle, with the location of the propulsive-jet exit varied from 1.747 jet-exit diameters to 4.981 jet-exit diameters below the wing surface, resulted in a positive incremental normal force on the wing at all positions.

INTRODUCTION

It has been shown previously that a propulsive jet issuing from the rear of a nacelle into free-stream supersonic flow produced strong disturbances which were responsible for the formation of shock waves in the free stream downstream of the jet exit. Reference 1 shows that, at a free-stream Mach number of 2.02, when these shock waves in the external flow impinged upon an adjacent surface, a positive pressure rise was produced and resulted in an induced lift on the adjacent surface. The present report is a continuation, in a more detailed manner, of the investigation of reference 1 at a free-stream Mach number of 1.39.

The investigation was conducted in the preflight jet of the Langley Pilotless Aircraft Research Station at Wallops Island, Va. A small-scale nacelle mounted beneath a flat plate was used to simulate a turbojet engine and wing combination. The nacelle was both vertically and horizontally adjustable with respect to the flat surface. The nacelle was operated with both hot and cold exhaust jets utilizing a convergent nozzle as well as a convergent-divergent nozzle.

The data presented were obtained over a range of jet total-pressure ratios from 2 to 15 at a free-stream Mach number of 1.39 and at angles of attack and sideslip of 0°. The Reynolds number per foot for the tests was approximately 10×10^6.

SYMBOLS

ΔC_N	incremental normal-force coefficient, $\frac{(\text{Normal force})_n - (\text{Normal force})_f}{q_o S_j}$
C_T	gross thrust coefficient, $T/q_o S_j$
D	diameter, in.
D_B	diameter of nacelle base, in.
H	total pressure, lb/sq in.
H_j/p_o	nacelle-exit total-pressure ratio
M	Mach number
p	static pressure, lb/sq in.
p_j/p_o	nacelle-exit static-pressure ratio
P	pressure coefficient, $\frac{p_w - p_o}{q_o}$
q	dynamic pressure, $\gamma p M^2/2$, lb/sq in.
S	area, sq in.
T	gross thrust, $\gamma p_j M_j^2 S_j + p_j S_j - p_o S_j$, lb

x	chordwise distance from nacelle exit (downstream is positive), in.
y	spanwise distance from nacelle center line, in.
α	secondary jet-on wave angle, deg
γ	specific-heat ratio, 1.40 for air, 1.67 for helium, and 1.27 for the hot test
θ	primary jet-on wave angle, deg
θ'	angle of inclination of a straight line between nacelle exit and impingement point on wing of primary shock wave, deg

Subscripts:

f	propulsive jet off
j	nacelle exit
j^*	sonic throat
l	local conditions
n	propulsive jet on
o	free stream
w	wing

APPARATUS

The tests were made in the preflight jet facility of the Langley Pilotless Aircraft Research Station at Wallops Island, Va. (ref. 2). A Mach number 1.39, 27- by 27-inch nozzle was used for all the tests. A photograph of the nacelle mounted in the test position beneath the flat-surface wing at the exit of the 27- by 27-inch nozzle is shown as figure 1.

Nacelle

A sketch of the nacelle with its principal dimensions is shown as figure 2. Also shown and tabulated in figure 2 are the different components of the nacelle used in the hot and cold tests.

The nacelle was designed to produce a hot propulsive jet (burning of hydrogen and air) or a cold propulsive jet. In the hot tests, metering flow nozzles were used to determine the fuel and air rates and ignition was accomplished with a black-powder squib in combination with a magnesium burnout restriction mounted at the exit of the nacelle. Immediately after ignition, the restriction was burned and blown from the nacelle.

The body of the nacelle had a maximum diameter of 1.12 inches with an overall length of 11.65 inches. Two types of interchangeable nacelle-exit nozzles were used for the tests, a convergent nozzle providing a sonic exit and a convergent-divergent nozzle providing a supersonic exit. The physical dimensions of both nozzles are given in figure 2.

The nacelle was mounted on a hollow strut which served as a housing for the fuel, air, and pressure tubes as well as a support for the nacelle. The leading edge of the strut was swept back at a 25° angle, while the trailing edge was swept back at a 40° angle and the strut had a hexagonal cross section as shown in figure 2.

Wing

The wing used in the tests consisted of a 1-inch maximum thickness built-up steel section that completely spanned the exit of the preflight-jet nozzle as shown in figure 1. The wing had welded supports that were bolted to the exit of the preflight-jet nozzle. The leading edge of the wing was 2.5 inches inside the nozzle as shown in figure 3, and approximately one-half of the total vertical distance up from the lower nozzle plate. The wing had a flat under surface and was of rectangular plan form with a 16.5-inch chord and an 8° bevel on the upper surfaces of the leading edge.

Figure 3 also shows the location of the nacelle with respect to the wing and preflight-jet-nozzle exit for all the positions tested.

INSTRUMENTATION

The internal static pressure of the nacelle was measured for all tests through a 0.03-inch-diameter orifice shown in figure 2. Also shown in figure 2 is the manifolded total-pressure tube used in recording the internal total pressure of the nacelle for all cold tests. A ±150-pound maximum thrust-drag balance was used to measure both the total drag (nacelle jet off) and the net thrust (nacelle jet on).

The static pressure on the wing was measured through 47 static-pressure orifices 0.06 inch in diameter. The position of each of these orifices with respect to the nacelle exit is shown in figure 4.

Tunnel pressures measured were the free-stream total pressure in the section upstream of the 27- by 27-inch nozzle, and the stream static pressure on the wall 1/2 inch upstream from the nozzle exit. All pressures were recorded by electrical pressure recorders of the strain-gage type. A 10-cps timer correlated all time histories on paper records. Shadowgraphs, which were photographed at an exposure of approximately 0.003 second, were obtained by using a carbon-arc light source and an opaque-glass screen.

TEST AND METHODS

The tests were made at a free-stream Mach number of 1.39 with a Reynolds number per foot of approximately 10×10^6.

With the arrangement shown in figure 3, the complete test field was within the Mach wedge of the preflight-jet nozzle with the upper half of nozzle flow being diverted by the wing. For all tests, the nacelle-exit center line was located vertically below the center line of the wing. The only variation between individual tests was the vertical distance between wing and nacelle center line at position I and the horizontal distance between the nacelle exit and the wing trailing edge at positions I_b and II_b, as shown in figure 3. At all times the nacelle was at an angle of attack and sideslip of 0° with respect to both the wing surface and the center line of the preflight jet.

A high-frequency strain-gage balance was used to measure both the total drag (nacelle jet off) and the net thrust (nacelle jet on). The gross thrust was then obtained by an algebraic summation of these measurements. From the gross thrust, the static pressure at the exit of the nacelle was calculated by using the one-dimensional-flow theory applied to the momentum equation as follows:

$$T = \gamma p_j M_j^2 S_j + p_j S_j - p_o S_j$$

Therefore

$$p_j = \frac{T + p_o S_j}{S_j\left(\gamma M_j^2 + 1\right)}$$

A nacelle static pressure was measured (fig. 2) for all test runs as well as a total pressure for all cold test runs, and the thrust determined from these measurements was used as a check on the strain-gage balance readings for the different nacelle positions tested.

The static pressure at the exit of the nacelle for the hot, the air, and the helium sonic propulsive jets is different for the same gross thrust because the values of γ are different for each of these gases. Since p_j varies with γ and H_j is not constant, a plot of the variation of p_j/p_o with H_j/p_o for all test runs is presented in figure 5. Figure 5 also indicates the ranges of pressure ratios covered in these tests. Although the nacelle could be operated with a hot propulsive jet, the short pressure-ratio range obtainable from the hot jet plus the excessive heating of the nacelle components in repeated tests was considered undesirable. Therefore, in order to expedite the investigation, a cold helium propulsive jet was used for most of the tests. A cold air propulsive jet was also tested for comparative purposes. Both helium and air propulsive jets were tested at position I_b (fig. 3) to determine which could more nearly duplicate the pressure distribution on the wing as obtained from the hot propulsive jet. From the results of these tests, as discussed later in the "jet-on" section of this paper, it was decided to use helium for most of the tests.

The incremental normal force due to the presence of the propulsive jet was determined from an integration of the measured pressures on the lower wing surface.

ACCURACY

By accounting for the instrument error of 1 percent of full-scale range, the probable error is believed to be within the following limits:

M_o	± 0.02
P_f and P_n	± 0.02
H_j/p_o and p_j/p_o	± 0.05

All measured angles are believed to be accurate to $\pm 1^o$. The magnitude of error in the force-balance measurements was ± 1 percent for full-scale deflection. The estimated error of the air-flow and fuel-flow measurements was ± 2 percent.

RESULTS AND DISCUSSION

Jet-Off Pressure Coefficients

The measured jet-off pressure coefficients P_f on the wing surface are tabulated in table I and are plotted in figure 6 as a function of distance from the nacelle exit x/D_j for four spanwise positions. The value of P_f as obtained in these tests includes all the interference effects on the wing pertaining to this particular investigation. The chordwise pressure distributions on the wing for positions I_a, I_b, I_c, and II_b along the nacelle center line (fig. 6(a)) in general are characterized first by the expansion to a low negative pressure region near the vicinity of the exit of the nacelle and second by a pressure rise to a positive pressure through the shock wave originating from the nacelle wake (fig. 7). As the nacelle is lowered from position I_a, the low pressure regions although moved farther to the rear on the wing are of the same magnitude. In turn, the pressure rise through the shock waves also takes place farther to the rear on the wing and the profiles are generally of the same shape, with the fall off in positive pressure increasing until a common pressure point is reached just forward of the wing trailing edge. This common point of pressure indicates an influence on the jet-off pressure from the flow over the upper surface of the wing similar to base pressure effect at supersonic speeds. Although the maximum positive pressure is of approximately the same value for each position along the nacelle center line (fig. 6(a)), there is a gradual reduction in this pressure at each position as the spanwise distance is increased. (Compare figs. 6(a), 6(b), 6(c), and 6(d).) A typical jet-off pressure field on the wing is presented in figure 8.

Jet-On Pressure Coefficients

Effect of jet properties.- Tabulated in table II (parts (a) to (g)), are the experimental jet-on pressure coefficient P_n obtained with a helium jet for individual orifice locations at all the test positions investigated as well as two other types of jets tested at position I_b. For reasons explained, in the test and methods section, it was considered necessary to use a simple cold propulsive jet for the majority of tests in this investigation. Therefore, both helium and air propulsive jets were tested at position I_b to determine which could more nearly duplicate the P_n distribution on the wing as obtained from the hot propulsive jet.

Presented in figure 9 are the shadowgraph pictures of the flow field about the nacelle exit for $H_j/p_o = 7$ from the three types of sonic

propulsive jets at test position I_b. Clearly visible, downstream of the nacelle exit, in each of the three pictures presented in figure 9 are two shock waves that impinge upon the wing surface and then are reflected. The aerodynamics of the formation and existence of these shock waves is discussed in reference 3. In keeping with the nomenclature of this investigation, the first part of which has already been published in reference 1, the first and second shock waves downstream from the nacelle exit will be called the primary and secondary shock waves, respectively.

Figure 10 presents the chordwise variation of P_n on the wing along the nacelle center line and at $1.40D_j$ spanwise from the nacelle center for the three types of sonic propulsive jets tested at $H_j/p_o = 7$. The chordwise profiles of P_n for all the propulsive jets tested at $H_j/p_o = 7$ differ in magnitude and position only in the immediate vicinity of the first and second P_n rises in both figures 10(a) and 10(b). The orifices located approximately one D_j behind the first and second P_n rise show essentially the same value of P_n. This indicates that the fall off in P_n behind the intersection of the shock waves on the wing takes place at a similar rate.

In reference 3 it is shown that both p_j/p_o and γ have an effect upon the initial inclination of the propulsive jet boundary and this boundary together with M_l distribution determines θ. In the case for the primary shock wave, the M_l distribution for the three propulsive jets tested should be the same because the geometry of the components used in the tests is the same. The combined effects of both p_j/p_o and γ are visible in figure 10, but in order to separate the effects of these parameters a plot of the variation of P_n with H_j/p_o is presented in figure 11 for the orifices located at $2.43D_j$ behind the nacelle exit for the three propulsive jets tested. The general trend of the curves in figure 11 shows the effect on P_n from the movement of the primary shock wave when H_j/p_o is increased. When H_j/p_o is increased at a constant value of γ (for $M_j = 1$) p_j/p_o will also increase. As p_j/p_o is increased, θ will increase and the point of intersection with the wing will move toward the nacelle exit. The result of this forward movement of the impingement on the wing of the primary shock wave is shown in figure 11 by the rapid P_n rise at the stationary orifice position when the shock wave passes over. This P_n rise apparently begins at a lower value of H_j/p_o for the hot tests and is progressively delayed in the air test and helium test. Also shown in figures 11(a) and 11(b) is the progressive decrease in P_n at a constant value of H_j/p_o for

the hot jet, air jet, and helium jet. These significant differences in P_n with a variation or a constant value of H_j/p_o for the three types of propulsive jets indicate that θ is progressively greater as the value of p_j/p_o is increased and also as γ is decreased. This trend is also shown by theoretical calculations in reference 3.

In order to eliminate the effects on P_n due to the increase in p_j/p_o while decreasing γ (p_j/p_o increases proportionally with a decrease in γ when $M_j = 1$) a plot of the variation of P_n with p_j/p_o is presented in figure 12 for the orifices located at $2.43D_j$ behind the nacelle exit from the three propulsive jets tested. The smaller differences in P_n visible in figure 12 as compared with figure 11 indicates that a variation of p_j/p_o is the main reason for the variation of the primary shock location on the wing in these tests and that the effect of γ is of secondary order.

The general trend of the curves as presented in figure 13 shows the effect on P_n from the movement of the secondary shock wave when H_j/p_o is increased. As H_j/p_o is increased, the secondary shock wave, which is formed in the propulsive jet structure (ref. 3), moves downstream as shown in figure 13 by the rapid P_n drop at the stationary orifice position when the shock wave passes over.. This P_n drop begins at a lower value of H_j/p_o for the air jet than for both the hot jet and the helium jet. As in the case of the primary shock wave, M_l as well as H_j/p_o and γ will determine the intersection point on the wing of the secondary shock wave. However, unlike the conditions of equal M_l in front of the primary shock wave, the M_l distribution in front of the secondary shock wave will be influenced by the mixing of the propulsive jet and free stream at their interface. A plot of P_n against p_j/p_o will not isolate the effect of p_j at the secondary shock wave as it did in the vicinity of the primary shock wave, because the values of P_n in figure 13 are not in the same systematic order with the variation of both H_j/p_o and γ as they were in figure 11. Therefore, along with the possible expected effects of both H_j/p_o and γ on P_n from the secondary shock wave, the data indicate by inspection that there is a variation of P_n from a change in M_l distribution.

A light gas, such as helium, has high sonic velocities comparable to those of a hot jet and the duplication of the effect due to mixing on the M_l distribution should be closely approximated. The limited comparable data between the three types of propulsive jets tested indicate this to be so in both figures 10 and 13 with the resulting P_n

distribution from the secondary shock wave in close agreement with the hot jet when a helium jet is used.

From the results as indicated in figures 10, 11, 12, and 13, a reasonable approximation of a hot jet's influence on the wing pressure distribution can be obtained by the use of a cold helium propulsive jet. This can be done by plotting the P_n profile with H_j/p_o and then correcting the profile for the maximum forward position of the primary shock wave from the variation of θ' with p_j/p_o, as presented in figure 14.

Effect of nacelle position.- In figure 15, the chordwise variation of P_n is plotted at four spanwise positions as a function of distance from the nacelle exit x/D_j for test positions I_a, I_b, and I_c at H_j/p_o of 7. There are two separate positive pressure rises on the wing at each position caused by the interaction on the wing of both the primary and the secondary shock waves visible in the jet-on shadowgraph pictures in figure 16. Figure 15 shows a reduction in the maximum positive pressure and a rearward movement of the complete pressure profile as the nacelle is lowered in position as well as a general reduction in pressure at each position as the spanwise distance is increased. This reduction at each position as the spanwise distance is increased, as well as the impingement on the wing of both the primary and secondary shock waves, is shown in a sketch of a typical jet-on pressure field on the wing presented in figure 17.

Presented in figure 18 is the chordwise variation of P_n along the nacelle center line for positions I_b and II_b at $H_j/p_o = 7$. In figure 18 both positive pressure rises on the wing appear to take place for each position at the same distance downstream of the nacelle exit indicating that both the primary and secondary shock waves are duplicated at each position. The small variation in P_n at some of the locations indicates the effects of different wing surface conditions because P_n for the two positions at the same value of x/D_j was measured at different locations on the wing. Also visible in figure 18 is the effect on P_n from the location of the wing trailing edge. The value of P_n behind the secondary shock wave for position II_b falls off more rapidly than it does for position I_b until a similar value of P_n is obtained at an equal distance from the wing trailing edge.

Effect of jet exit Mach number.- In figures 19(a) to 19(e) is presented the chordwise variation of P_n along the wing center line, at test position I_b for both the sonic and supersonic nacelle exits, at H_j/p_o of 4, 6, 8, 10, and 12. Also included in figure 19 are

shadowgraph pictures taken at these same values of H_j/p_o. In general, the P_n profiles for both the sonic and supersonic nacelle exits are similar in that they both normally have two positive P_n rises. Note in figures 19(a) to 19(e) the upstream movement of the first positive P_n rise for both the sonic and supersonic nacelle exits as H_j/p_o is increased. This indicates that θ is increasing for both the sonic and supersonic exits when p_j/p_o is increased by increasing H_j/p_o.

The first rise which is caused by the intersection on the wing of the primary shock wave, visible in all of the pictures, begins farther forward on the wing and is higher for the sonic exit than for the supersonic exit at the same value of H_j/p_o. With an increase in H_j/p_o, the secondary shock wave moves downstream for both the sonic and supersonic exit at what appears to be nearly the same rate.

Other differences between the sonic and supersonic exit P_n plots of figure 19 (best examples, 19(d) and 19(e)) are the more gradual fall off in P_n behind the primary shock wave for the supersonic exit than for the sonic exit, and the more pronounced negative P_n values in front of the secondary shock wave for the sonic exit.

In reference 3 it is shown from characteristic calculations that a jet boundary increases in size with an increase in nozzle divergence angle at the same value of p_j/p_o. Therefore, it could be expected that the supersonic nacelle exit in these tests, with a nozzle divergence angle of approximately 5°, would create at the same value of p_j/p_o a larger value of θ than would be obtained from the sonic exit. Another variable that might change θ at the same value of p_j/p_o in these tests is the effect of base annulus area. This might account for a larger value of θ for the supersonic exit than for the sonic exit because D_j/D_B is greater for the supersonic exit than it is for the sonic exit. The effect of either or both nozzle divergence angle and base annulus area on P_n at the same value of p_j/p_o can be seen in figure 20 by observing the value of P_n for the orifice located at $x/D_j = 2.43$ for both the sonic and supersonic exits. A value of P_n of approximately -0.086 was obtained for the sonic exit while a value of P_n of approximately 0.124 was obtained for the supersonic exit. This shows that for a given value of p_j/p_o, θ is larger for the supersonic exit and intersects the wing upstream of the orifice location.

Shock Waves

From the shadowgraph pictures in conjunction with the measured wing pressure data over the nacelle center line, it was possible to locate the point of impingement of the shock waves on the flat-surface wing. In the jet-off case, the rise in P_f in figure 6 indicates the intersection on the wing of a possible shock wave, but the shadowgraph pictures as presented in figure 7 are not definite enough to establish an angle measurement. In the jet-on case for the sonic exit, two shock waves impinged on the wing as shown by the pressure rise in figure 15 and the shadowgraph pictures in figure 16. In the shadowgraph pictures for position I_a (fig. 16(a)), it can be seen that as H_j/p_o is increased the primary shock wave and its accompanying reflected shock wave from the wing is rapidly changing shape until a nearly normal shock-wave condition is visible in the shadowgraph picture for $H_j/p_o = 14$. This rapid change of the primary shock wave and its accompanying reflected shock wave from opposite oblique shock waves to a condition of a single nearly normal shock wave is not visible in either of the series of shadowgraph pictures presented for position I_b and I_c (figs. 16(b) and 16(c)). In chapter 4 of reference 4, a discussion on the analysis of the reflection of an oblique shock wave from a rigid wall indicates that if the Mach number behind the oblique shock wave is of such a low value that a reflecting shock wave is not possible then the only shock wave possible at the wall is a normal shock wave. In the case for position I_a, the proximity of the maximum diameter of the propulsive jet to the undersurface of the wing could be restricting the flow to such an extent that the required pressure rise in the free stream must be generated by a stronger shock wave which becomes nearly normal for the high jet pressure ratios.

Because the jet-on shock waves did not have a fixed origin in these tests, the angular variation between the wing surface and a straight line drawn along the shock wave was measured representing the angular variation between the nacelle center line and the shock wave. The primary jet-on wave angle, θ, as presented for the present tests in figure 21 was obtained only from the shadowgraph pictures for test positions I_b and I_c. Figure 21 shows that θ for the sonic exit from the present tests varied from approximately 44° at $p_j/p_o = 1$ to approximately 49° at $p_j/p_o = 4$ and then seems to level out. This leveling out of θ appears to occur simultaneously with a change in the shape of the primary shock wave from a pure oblique shock wave to one having two legs at the nacelle exit (figs. 16(b) and 16(c)). After the bifurcated oblique shock wave is formed, then a further increase in p_j/p_o only tends to increase the angle between the legs and cause the leading leg to form farther up on the nacelle boattail.

The secondary jet-on shock wave for the sonic exit, although moving farther downstream with an increase in H_j/p_o (fig. 16), appeared to have a constant wave angle α of approximately 47°.

Also presented in figure 21 are the measurements of θ and α as obtained at $M_o = 2.02$ from reference 1. As can be seen in figure 21, both θ and α decreased with an increase in M_o at a constant value of p_j/p_o throughout the comparable range of p_j/p_o obtained in both tests.

When using the pressure data presented in the tables to estimate lift, it is necessary to locate the apex for both the primary and secondary shock waves at the nacelle center line. From this apex location, approximate intersections of both shock waves on the wing can be determined from a simple conical projection. Therefore, the variation of p_j/p_o with the angle of inclination of a line drawn from the point of intersection on the wing of the primary shock wave to the nacelle exit is presented in figure 22 for positions I_a, I_b, and I_c. Figure 22 again indicates a difference in the primary shock wave at position I_a from both positions I_b and I_c as discussed previously because θ' varies similarly for positions I_b and I_c, while for position I_a there is a distinct difference.

In figure 23 is presented the variation of the point of intersection on the wing center line of the secondary shock wave from the nacelle exit with H_j/p_o for positions I_a, I_b, and I_c. The measurements in figure 23 can be used in conjunction with α as presented in figure 21 to determine a good approximate intersection on the wing of the secondary shock wave by a simple conical projection.

Incremental Normal Force

As previously discussed in the jet-off section, P_f as measured in these tests must include all the interference effects on the wing pertaining to this particular investigation. It can be expected that these same jet-off interference effects combined with the effects from the propulsive jet will be included in the P_n measurements. Therefore, to isolate the effects of the propulsive jet an incremental pressure coefficient $(P_n - P_f)$ was obtained. It seems reasonable that this incremental pressure coefficient could be applied to estimate the propulsive jet effects on different missile and airplane configurations when the conditions for the propulsive jet are the same.

In order to determine whether $P_n - P_f$ would remain the same when P_f was different for the same propulsive jet conditions, a test was performed at position II_b. As can be seen in figures 6(a) to 6(d), the P_f profiles on the wing are different for position II_b than they are for position I_b. Also as shown in figure 18, the axial P_n profile for position II_b is different from the one obtained for position I_b, but the axial $P_n - P_f$ profile as presented in figure 24 for both of these positions is for all practical purposes the same.

The major significance of the plot in figure 24 is that it indicates that the profiles of $P_n - P_f$ from these tests at each vertical position can be used to determine ΔC_N on a surface with the trailing edge at any position less than $x/D_j = 11.4$. As mentioned in the shock-wave section of this paper, the points of intersection on a surface of both the primary and secondary shock waves can be determined at a given vertical distance from the nacelle center line by a simple conical projection. Once these intersections are located the values of $P_n - P_f$ from table III at the given vertical distance can be fitted to the intersections and the profiles terminated for any value of trailing edge less than $x/D_j = 11.4$ before integrating for ΔC_N.

In figure 25 is presented the chordwise variation of $P_n - P_f$ at two spanwise stations for positions I_a, I_b, and I_c at $H_j/p_o = 7$. When jet-on and jet-off wing pressure data were combined to form the incremental pressure data, positive $P_n - P_f$ resulted immediately behind the intersection on the wing of the jet-on primary shock wave. This positive $P_n - P_f$ gradually decreases until it becomes negative upstream of the intersection on the wing of the secondary shock wave, rises in a positive direction through the secondary shock wave, and then becomes more negative again to the end of the wing. As was the case with the P_n profiles for the same vertical positions, the maximum values of $P_n - P_f$ gradually decrease both as the nacelle is lowered in position (fig. 25(a)) and also as the spanwise distance is increased at the same position (figs. 25(a) and 25(b)). Because the data from table III were obtained by using helium, it is necessary to correct the data for a change in the inclination of the primary shock wave due to the high value of γ. The dotted lines in figure 25 represent a correction of the data obtained with helium to a value of γ of a hot jet (1.27). Presented in figure 26 is a typical chordwise and spanwise variation of $P_n - P_f$.

Shown in figure 27 is the variation of incremental normal-force coefficient ΔC_N, based on S_j, with H_j/p_o for test positions I_a,

I_b, and I_c. The values of ΔC_N were calculated from an integration of the $P_n - P_f$ profiles for $x/D_j = 11.4$ corrected to a γ of 1.27; ΔC_N represents the change in normal force due to the presence of the propulsive jet. Positive ΔC_N resulted at each of the positions with a gradual positive rise as H_j/p_o is increased from a value of 2 to a value of approximately 6. As H_j/p_o is further increased to a value of 14, the increase of ΔC_N first becomes more rapid at each of the positions with position I_a subsequently leveling out, position I_b tending to level out, and position I_c appearing to be unaffected. It is obvious from inspection of figures 25 and 26 that the positive $P_n - P_f$ behind the intersection on the wing of the primary shock wave is responsible for the positive values of ΔC_N. It can be expected that as H_j/p_o is increased this positive $P_n - P_f$ will also increase, because the inclination of the primary shock wave will increase. However, with an increase in H_j/p_o, the negative $P_n - P_f$ is also increasing. The combination of both increasing positive and negative $P_n - P_f$ as H_j/p_o is increased resulted in the leveling out of ΔC_N in figure 27 first for position I_a and then for position I_b while position I_c continued to rise.

The calculated gross thrust coefficient C_T, based on S_j, is presented in figure 28 as it varies with H_j/p_o for a sonic propulsive jet having a γ of 1.27. Shown in figure 29 is the variation of $\Delta C_N/C_T$ with H_j/p_o at positions I_a, I_b, and I_c for the sonic exit. The incremental normal force to thrust ratio decreased rapidly from a maximum of 2.9 at $H_j/p_o = 2$ for test position I_a to a minimum of 0.55 at $H_j/p_o = 6$ for test position I_c. The difference in the variation of $\Delta C_N/C_T$ with H_j/p_o is consistent with the difference in the variation of ΔC_N with H_j/p_o for test positions I_a, I_b, and I_c since C_T is a constant for any given H_j/p_o at any position.

CONCLUDING REMARKS

Within the limits of the present tests conducted in a Mach number 1.39, free jet of a small-scale propulsive jet operated with both a choked convergent nozzle and a convergent-divergent nozzle located in the vicinity of a flat-surface wing, the results may be summarized as follows:

1. Shock waves, formed in the external flow because of the presence of the propulsive jet, impinged on the flat-surface wing and greatly altered the pressure distribution.

2. An integration of this pressure distribution, for the choked convergent nozzle, with the location of the propulsive jet exit varied from 1.747 propulsive jet exit diameters to 4.981 propulsive jet exit diameters below the wing resulted in a positive incremental normal force on the wing at all positions.

3. The pressure distribution on the wing was altered when a convergent-divergent nozzle was used but not as severely as when a choked convergent nozzle was used over the same range of propulsive-jet total pressure ratios.

4. A helium sonic propulsive jet can be used to approximate closely the pressure distribution on the wing from a hot sonic propulsive jet at the same value of exit total pressure, provided that the maximum forward position of the impingement on the wing of the primary shock wave is corrected for the variation in exit static pressure due to the difference in γ between the helium gas and the hot exhaust gas.

Langley Aeronautical Laboratory,
National Advisory Committee for Aeronautics,
Langley Field, Va., November 29, 1955.

REFERENCES

1. Bressette, Walter E.: Investigation of the Jet Effects on a Flat Surface Downstream of the Exit of a Simulated Turbojet Nacelle at a Free-Stream Mach Number of 2.02. NACA RM L54E05a, 1954.

2. Faget, Maxime A., Watson, Raymond S., and Bartlett, Walter A., Jr.: Free-Jet Tests of a 6.5-Inch-Diameter Ram-Jet Engine at Mach Numbers of 1.81 and 2.00. NACA RM L50L06, 1951.

3. Love, Eugene S., and Grigsby, Carl E.: Some Studies of Axisymmetric Free Jets Exhausting From Sonic and Supersonic Nozzles Into Still Air and Into Supersonic Streams. NACA RM L54L31, 1955.

4. Ferri, Antonio: Elements of Aerodynamics of Supersonic Flows. The Macmillan Co., 1949.

TABLE I

VALUES OF JET-OFF PRESSURE COEFFICIENTS FOR ALL WING ORIFICE POSITIONS

Orifice ordinates							
x/D_j	y/D_j	I_a	$I_{b(helium)}$ *	$I_{b(air)}$ *	$I_{b(hot)}$ *	I_c	II_b
10.76	0.00	-0.018	-0.021	-0.017	-0.017	-0.012	
9.72	.00	.030	.034	.037	.037	.046	
8.68	.00	.058	.064	.067	.067	.075	-0.012
7.63	.00	.066	.086	.085	.085	.090	.056
6.59	.00	.079	.095	.095	.095	.102	.081
5.55	.00	.063	.080	.078	.078	-.066	.106
4.51	.00	.070	.010	.010	.010	-.047	.070
3.47	.00	.092	-.086	-.086	-.086	-.117	-.073
2.43	.00	-.035	-.084	-.083	-.083	-.056	-.086
1.39	.00	-.122	-.127	-.128	-.128	-.041	-.130
.35	.00	-.096	.004	0	0	-.008	-.020
-.69	.00	-.200	0	0	0	.010	-.020
-1.73							.005
-2.77							0
10.76	1.40	-.016	-.024	-.021	-.021	-.014	
9.72	1.40	.026	.028	.028	.028	.038	
8.68	1.40	.048	.053	.055	.055	.065	-.018
7.63	1.40	.062	.082	.076	.076	.086	.058
6.59	1.40	.058	.076	.074	.074	.084	.069
5.55	1.40	.060	.073	.073	.073	-.073	.103
4.51	1.40	.080	-.093	-.090	-.090	-.046	-.024
3.47	1.40	.068	-.083	-.087	-.087	-.119	-.074
2.43	1.40	-.118	-.100	-.101	-.101	-.049	-.101
1.39	1.40	-.075	-.092	-.095	-.095	-.027	-.104
.35	1.40	-.140	0	0	0	-.010	-.024
-.69	1.40	-.060	0	0	0	.010	0
-1.73							0
-2.77							0
10.76	4.17	-.002	-.008	-.012	-.012	.006	
9.72	4.17	.009	.005	0	0	.020	
8.68	4.17	0	.007	.006	.006	.015	.001
7.63	4.17	.009	.018	.020	.020	-.050	.010
6.59	4.17	.012	-.051	-.047	-.047	-.099	-.007
5.55	4.17	-.040	-.101	-.101	-.101	-.072	-.088
4.51	4.17	-.080	-.060	-.065	-.065	-.079	-.108
3.47	4.17	-.042	-.070	-.071	-.071	.005	-.128
2.43	4.17	-.060	.010	.010	.010	.010	-.026
1.39	4.17	-.010	.020	.020	.020	.010	.021
.35	4.17	-.010	-.010	-.010	-.010	.020	.010
-.69							.020
-1.73							-.010
10.76	6.94	.018	.010	.006	.006	.030	
9.72	6.94	-.009	-.007	-.009	-.009	.047	
8.68	6.94	-.007	-.072	-.075	-.075	-.064	-.049
7.63	6.94	-.099	-.097	-.102	-.102	-.098	-.060
6.59	6.94	-.139	-.151	-.156	-.156	-.070	-.094
5.55	6.94	-.163	-.137	-.143	-.143	-.110	-.096
4.51	6.94	-.100	-.060	-.060	-.060	-.070	-.094
3.47	6.94	-.010	0	-.010	-.010	0	-.101
2.43							-.060
1.39							0
10.76	11.11	-.106	-.115	-.120	-.120	-.083	
9.72	11.11	-.080	-.072	-.073	.073	-.058	
8.68	11.11	-.057	-.048	-.051	-.051	-.042	-.067
7.63	11.11	-.04	-.030	-.030	-.030	-.040	-.030
6.59							-.044
5.55							-.030

*Actual measured pre-run values used in obtaining incremental pressure coefficients tabulated in table III.

TABLE II

VALUES OF JET-ON PRESSURE COEFFICIENTS FOR ALL WING ORIFICE POSITIONS FOR TOTAL-PRESSURE RATIOS OF 2 TO 15

(a) Helium at test position I_a (sonic exit)

Orifice ordinates		Pressure coefficients for nacelle-exit total-pressure ratio H_j/p_o of –													
x/D_j	y/D_j	2	3	4	5	6	7	8	9	10	11	12	13	14	15
10.76	0.00	-0.034	-0.032	-0.031	-0.029	-0.027	-0.026	-0.025	-0.028	-0.030	-0.025	-0.020	-0.015	-0.010	-0.006
9.72	.00	.012	.014	.015	.019	.025	.021	.012	.019	.021	.023	.033	.035	.037	.033
8.68	.00	.038	.042	.045	.047	.049	.050	.047	.053	.062	.067	.067	.056	.028	.012
7.63	.00	.050	.051	.052	.052	.054	.057	.062	.061	.047	.020	.009	.013	.024	.035
6.59	.00	.060	.060	.060	.060	.062	.069	.055	.025	.029	.039	.052	.070	.092	.112
5.55	.00	.038	.038	.039	.041	.023	.014	.024	.042	.064	.086	.109	.131	.143	.144
4.51	.00	.025	.031	.034	.023	.019	.048	.075	.097	.109	.093	-.095	-.188	-.205	-.217
3.47	.00	.040	.054	.040	.065	.085	.092	-.116	-.128	-.135	-.139	-.143	-.145	-.147	-.147
2.43	.00	.070	.081	.090	-.038	-.050	-.043	-.037	-.031	-.025	-.018	-.011	-.002	.008	.017
1.39	.00	.080	.051	.075	.099	.120	.141	.159	.177	.194	.212	.229	.245	.260	.272
.35	.00	-.096	.096	-.096	-.096	-.095	-.089	-.030	.064	.125	.155	.195	.215	.240	.259
-.69	.00	-.200	-.200	-.200	-.200	-.200	-.200	-.200	-.200	-.200	-.200	-.200	-.200	-.200	-.200
10.76	1.40	-.035	-.032	-.030	-.028	-.024	-.025	-.025	-.030	-.029	- 016	-.020	-.017	-.014	-.010
9.72	1.40	.006	.010	.013	.015	.019	.014	.009	.014	.019	.020	.030	.033	.030	.022
8.68	1.40	.035	.036	.037	.038	.039	.040	.042	.048	.051	.051	.043	.020	.004	.005
7.63	1.40	.051	.051	.052	.053	.055	.058	.060	.055	.031	.015	.016	.024	.038	.050
6.59	1.40	.044	.048	.044	.048	.052	.050	.020	.021	.029	.028	.055	.070	.089	.110
5.55	1.40	.028	.029	.030	.031	.012	.013	.035	.057	.077	.094	.108	.114	.099	.004
4.51	1.40	.031	.034	.031	.020	.039	.060	.076	.085	-.047	-.154	-.167	-.174	-.178	-.180
3.47	1.40	.047	.044	.057	.069	.070	-.084	-.096	-.095	-.094	-.095	-.094	-.092	-.089	-.087
2.43	1.40	.071	.098	-.011	-.014	-.004	.001	.009	.020	.027	.031	.039	.049	.054	.064
1.39	1.40	-.075	-.058	.064	.111	.141	.164	.183	.199	.207	.214	.227	.243	.257	.269
.35	1.40	-.140	-.140	-.140	-.140	-.140	-.130	-.120	-.110	-.060	-.030	.020	.070	.110	.140
-.69	1.40	-.060	-.060	-.060	-.060	-.060	-.060	-.060	-.060	-.060	-.060	-.060	-.060	-.060	-.060
10.76	4.17	-.020	-.013	-.022	-.021	-.012	-.019	-.021	-.018	-.015	-.013	-.018	-.027	-.035	-.037
9.72	4.17	-.014	-.016	-.017	-.016	-.009	-.017	-.016	-.018	-.030	-.033	-.035	-.035	-.031	-.020
8.68	4.17	-.015	-.015	-.015	-.015	-.015	-.017	-.030	-.033	-.030	-.023	-.015	-.008	-.003	0
7.63	4.17	-.009	-.009	-.009	-.009	-.017	-.019	-.009	0	.006	.010	.010	.004	-.026	-.066
6.59	4.17	-.014	-.011	-.016	-.021	-.010	..000	-.007	-.048	-.095	-.115	-.120	-.122	-.123	-.123
5.55	4.17	-.002	-.004	-.003	0	-.032	-.067	-.076	-.076	-.076	-.075	-.075	-.074	-.073	-.072
4.51	4.17	.040	.046	.021	.007	.007	.009	.012	.014	.015	.017	.018	.020	.021	.022
3.47	4.17	-.039	-.030	-.003	.039	.073	.090	.101	.108	.112	.116	.119	.122	.125	.128
2.43	4.17	-.060	-.060	-.060	-.060	-.060	-.040	-.020	.010	.060	.100	.130	.150	.160	.160
1.39	4.17	-.010	-.010	-.010	-.010	-.010	-.010	-.010	-.010	-.010	-.010	-.010	-.010	-.010	-.010
-.35	4.17	-.010	-.010	-.010	-.010	-.010	-.010	-.010	-.010	-.010	-.010	-.010	-.010	-.010	-.010
10.76	6.94	-.004	-.007	-.006	-.002	.003	-.009	-.015	-.010	-.006	.003	-.001	.001	.004	.002
9.72	6.94	.007	.006	.006	.009	.014	.010	.006	.006	.021	.036	.051	.065	.077	.088
8.68	6.94	-.007	-.007	-.007	-.006	-.003	-.022	-.048	-.057	-.060	-.061	-.060	-.060	-.059	-.058
7.63	6.94	-.028	-.028	-.028	-.038	-.047	-.053	-.056	-.056	-.054	-.053	-.051	-.049	-.048	-.046
6.59	6.94	-.122	-.099	-.099	-.081	-.065	-.061	-.059	-.057	-.055	-.054	-.052	-.083	-.089	-.083
5.55	6.94	-.163	-.163	-.163	-.163	-.155	-.134	-.092	-.063	-.050	-.047	-.040	-.035	-.032	-.028
4.51	6.94	-.100	-.100	-.100	-.100	-.090	-.090	-.090	-.080	-.070	-.060	-.050	-.030	-.010	0
3.47	6.94	-.010	-.010	-.010	-.010	-.010	-.010	-.010	-.010	-.010	-.010	-.010	-.010	-.010	-.010
10.76	11.11	-.109	-.109	-.092	-.074	-.054	-.048	-.043	-.040	-.037	-.036	-.034	-.033	-.032	-.030
9.72	11.11	-.080	-.080	-.080	-.080	-.074	-.063	-.047	-.027	-.013	-.005	0	.003	.006	.007
8.68	11.11	-.057	-.057	-.057	-.055	-.052	-.054	-.059	-.055	-.051	-.044	-.028	-.015	.002	.014
7.63	11.11	-.040	-.040	-.040	-.040	-.040	-.040	-.040	-.040	-.040	-.040	-.040	-.040	-.040	-.030

TABLE II.- Continued

VALUES OF JET-ON PRESSURE COEFFICIENTS FOR ALL WING ORIFICE POSITIONS FOR TOTAL-PRESSURE RATIOS OF 2 TO 15

(b) Helium at test position I_b (sonic exit)

Orifice ordinates		Pressure coefficients for nacelle-exit total-pressure ratio H_j/p_o of –													
x/D_j	y/D_j	2	3	4	5	6	7	8	9	10	11	12	13	14	15
10.76	0.00	-0.035	-0.032	-0.028	-0.031	-0.029	-0.025	-0.028	-0.026	-0.020	-0.017	-0.025	-0.025	-0.052	-0.053
9.72	.00	.015	-.020	.023	.023	.022	.018	.019	.021	.016	.006	-.010	-.012	-.011	-.007
8.68	.00	.050	.050	.055	.050	.050	.051	.050	.039	.024	.027	.033	.042	.051	.062
7.63	.00	.070	.065	.066	.065	.067	.053	.040	.054	.060	.075	.090	.104	.118	.130
6.59	.00	.065	.065	.065	.065	.050	.064	.080	.095	.113	.130	.127	.002	-.091	-.100
5.55	.00	.045	.050	.040	.050	.070	.082	.035	-.086	-.093	-.094	-.095	-.095	-.096	.095
4.51	.00	.045	.049	.068	.040	-.044	-.044	-.043	-.041	-.039	-.035	-.033	-.029	-.028	-.025
3.47	.00	.057	.078	.026	.034	.038	.051	.058	.065	.072	.072	.083	.090	.095	.099
2.43	.00	-.086	-.086	-.086	-.085	-.039	.064	.130	.155	.174	.189	.200	.215	.217	.225
1.39	.00	-.127	-.127	-.127	-.127	-.127	-.127	-.123	-.120	-.117	-.115	-.114	-.114	-.113	-.114
.35	.00	.004	.004	.003	.004	.004	0	.004	-.001	.004	.004	.004	-.001	.004	.001
-.69	.00	0	0	0	0	0	0	0	0	0	0	0	0	0	0
10.76	1.40	-.040	-.035	-.033	-.032	-.031	-.033	-.031	-.033	-.027	-.027	-.028	-.039	-.063	-.059
9.72	1.40	.012	.017	.019	.019	.013	.012	.013	.015	.010	-.011	-.016	-.015	-.011	-.008
8.68	1.40	.041	.041	.042	.041	.041	.043	.041	.025	.019	.026	.032	.040	.050	.058
7.63	1.40	.061	.061	.060	.061	.061	.059	.042	.054	.070	.083	.095	.100	.119	.127
6.59	1.40	.046	.050	.052	.035	.037	.052	.067	.084	.095	.092	-.001	-.082	-.097	-.099
5.55	1.40	.039	.037	.027	.049	.066	.067	-.074	-.084	-.086	-.087	-.087	-.086	-.086	-.086
4.51	1.40	-.005	.033	.068	-.028	-.033	-.031	-.028	-.026	-.023	-.020	-.017	-.014	-.012	-.009
3.47	1.40	.046	.044	.033	.045	.056	.064	.071	.076	-.084	.090	.096	.102	.107	.112
2.43	1.40	-.101	-.102	-.102	-.102	-.100	-.079	.015	.100	.154	.181	.198	.214	.220	.227
1.39	1.40	-.092	-.092	-.092	-.092	-.092	-.092	.092	-.092	-.092	-.092	-.092	-.092	-.092	-.092
.35	1.40	0	0	0	0	0	0	0	0	0	0	0	0	0	0
-.69	1.40	0	0	0	0	0	0	0	0	0	0	0	0	0	0
10.76	4.17	-.027	-.018	-.015	-.017	-.028	-.029	-.029	-.030	-.040	-.048	-.047	-.038	-.032	-.022
9.72	4.17	-.010	-.011	-.009	-.013	-.015	-.019	-.031	-.034	-.030	-.021	-.015	-.003	.004	.015
8.68	4.17	-.017	-.014	-.011	-.011	-.025	-.026	-.017	-.006	.003	.012	.018	.017	-.003	-.060
7.63	4.17	-.007	-.002	-.007	-.012	-.001	.009	.013	-.034	-.093	-.102	-.102	-.102	-.101	-.101
6.59	4.17	-.010	-.005	.005	.005	-.058	-.075	-.076	-.075	-.075	-.073	-.073	-.072	-.071	-.069
5.55	4.17	.001	.014	-.026	-.030	-.027	-.025	-.022	-.020	-.017	-.015	-.013	-.012	-.010	-.009
4.51	4.17	-.063	-.064	-.042	.032	.057	.066	.071	.074	.079	.082	.086	.089	.091	.094
3.47	4.17	-.070	-.070	-.070	-.070	-.069	-.069	-.065	-.052	-.018	.037	.096	.137	.165	.180
2.43	4.17	.010	.010	.010	.010	.010	.010	.010	.010	.010	.010	.010	.010	.010	.010
1.39	4.17	.020	.020	.020	.020	.020	.020	.020	.020	.020	.020	.020	.020	.020	.020
.35	4.17	-.010	-.010	-.010	-.010	-.010	-.010	-.010	-.010	-.010	-.010	-.010	-.010	-.010	-.010
10.76	6.94	-.013	-.008	-.003	-.007	-.020	-.021	-.014	-.007	-.003	-.002	-.007	-.036	-.051	-.074
9.72	6.94	.006	.010	.009	.006	0	0	.025	.053	.068	.075	.078	.079	.078	.077
8.68	6.94	-.004	-.002	0	-.015	-.040	-.045	-.045	-.045	-.047	-.045	-.043	-.042	-.040	-.039
7.63	6.94	-.040	-.038	-.035	-.035	-.034	-.033	-.030	-.029	-.027	-.025	-.022	-.020	-.016	-.014
6.59	6.94	-.154	-.152	-.150	-.139	-.106	-.068	-.040	-.030	-.024	-.019	-.017	-.012	-.011	-.008
5.55	6.94	-.142	-.142	-.140	-.141	-.141	-.140	-.141	-.140	-.133	-.125	-.102	-.067	-.035	-.018
4.51	6.94	-.060	-.060	-.060	-.060	-.060	-.060	-.060	-.060	-.060	-.060	-.060	-.060	-.060	-.060
3.47	6.94	0	0	0	0	0	0	0	0	0	0	0	0	0	0
10.76	11.11	-.116	-.108	-.105	-.087	-.067	-.048	-.041	-.034	-.031	-.028	-.026	-.021	-.019	-.014
9.72	11.11	-.075	-.075	-.075	-.075	-.075	-.075	-.067	-.055	-.038	-.013	.005	.015	.025	.056
8.68	11.11	-.052	-.052	-.052	-.052	-.052	-.052	-.052	-.052	-.052	-.052	-.052	-.044	-.040	-.029
7.63	11.11	-.030	-.030	-.030	-.030	-.030	-.030	-.030	-.030	-.030	-.030	-.030	-.030	-.030	-.030

TABLE II.- Continued

VALUES OF JET-ON PRESSURE COEFFICIENTS FOR ALL WING ORIFICE POSITIONS FOR TOTAL-PRESSURE RATIOS OF 2 TO 15

(c) Helium at test position I_c (sonic exit)

Orifice ordinates		Pressure coefficients for nacelle-exit total-pressure ratio H_j/p_o of –													
x/D_j	y/D_j	2	3	4	5	6	7	8	9	10	11	12	13	14	15
10.76	0.00	-0.027	-0.025	-0.024	-0.024	-0.026	-0.027	-0.023	-0.023	-0.028	-0.038	-0.042	-0.040	-0.036	-0.032
9.72	.00	.027	.027	.027	.027	.027	.027	.021	.006	.007	.015	.023	.032	.040	.048
8.68	.00	.054	.056	.051	.057	.049	.033	.042	.049	.065	.076	.090	.097	.104	.105
7.63	.00	.060	.065	.067	.042	.058	.071	.083	.093	.099	.005	-.066	-.070	-.071	-.070
6.59	.00	.072	.076	.082	.089	.099	-.005	-.023	-.023	-.023	-.023	-.023	-.023	-.023	-.022
5.55	.00	.050	.068	.036	0	.004	.007	.009	.011	.013	.015	.017	.019	.021	.023
4.51	.00	-.030	.034	.049	.057	.066	.072	.078	.082	.088	.094	.098	.100	.105	.108
3.47	.00	-.117	-.117	-.115	-.114	-.114	-.107	-.040	.035	.112	.153	.170	.180	.195	.200
2.43	.00	-.056	-.056	-.057	-.057	-.057	-.057	-.058	-.059	-.060	-.061	-.061	-.061	-.062	-.062
1.39	.00	-.041	-.041	-.041	-.041	-.041	-.041	-.041	-.041	-.041	-.041	-.041	-.041	-.041	-.041
.35	.00	-.008	-.008	-.008	-.008	-.008	-.008	-.008	-.008	-.008	-.008	-.008	-.008	-.008	-.008
-.69	.00	.010	.010	.010	.010	.010	.010	.010	.010	.010	.010	.010	.010	.010	.010
10.76	1.40	-.037	-.034	-.027	-.030	-.031	-.030	-.026	-.025	-.035	-.044	-.044	-.040	-.034	-.029
9.72	1.40	.024	.025	.021	.020	.021	.021	.008	0	.006	.014	.019	.029	.040	.049
8.68	1.40	.047	.047	.044	.049	.036	.028	.039	.051	.062	.072	.082	.091	.097	.065
7.63	1.40	.056	.060	.059	.041	.058	.075	.087	.094	.038	-.053	-.062	-.064	-.065	-.064
6.59	1.40	.052	.057	.064	.075	.075	-.022	-.025	-.025	-.025	-.024	-.024	-.024	-.023	-.022
5.55	1.40	.044	.064	.003	.001	.005	.008	.011	.013	.015	.017	.019	.021	.023	.026
4.51	1.40	-.046	-.038	.050	.062	.071	.078	.085	.091	.096	.102	.106	.110	.113	.116
3.47	1.40	-.119	-.119	-.119	-.119	-.119	-.119	-.118	-.095	-.015	.075	.130	.150	.179	.190
2.43	1.40	-.049	-.049	-.049	-.049	-.049	-.050	-.052	-.052	-.052	-.052	-.054	-.055	-.056	-.056
1.39	1.40	-.027	-.027	-.027	-.027	-.027	-.027	-.027	-.027	-.027	-.027	-.027	-.027	-.027	-.027
.35	1.40	-.010	-.010	-.010	-.010	-.010	-.010	-.010	-.010	-.010	-.010	-.010	-.010	-.010	-.010
-.69	1.40	.010	.010	.010	.010	.010	.010	.010	.010	.010	.010	.010	.010	.010	.010
10.76	4.17	-.006	-.008	-.010	-.013	-.018	-.031	-.041	-.035	-.027	-.018	-.010	-.001	.007	.015
9.72	4.17	-.004	-.005	-.013	-.021	-.026	-.026	-.017	-.004	.009	.019	.025	.022	-.017	-.090
8.68	4.17	-.010	-.004	-.015	-.017	-.005	.004	.006	-.049	-.099	-.105	-.106	-.106	-.106	-.105
7.63	4.17	-.003	.003	.011	.010	-.050	-.063	-.062	-.061	-.060	-.059	-.059	-.058	-.057	-.057
6.59	4.17	-.005	.005	-.030	-.028	-.024	-.017	-.016	-.016	-.014	-.011	-.009	-.007	-.006	-.006
5.55	4.17	-.076	-.076	-.057	.007	.023	.030	.036	.040	.044	.047	.050	.052	.055	.057
4.51	4.17	-.079	-.079	-.079	-.079	-.079	-.079	-.079	-.078	-.057	0	.059	.105	.133	.148
3.47	4.17	.006	.006	.006	.005	.005	.005	.004	.004	.004	.003	.003	.003	.002	.002
2.43	4.17	.010	.010	.010	.010	.010	.010	.010	.010	.010	.010	.010	.010	.010	.010
1.39	4.17	.010	.010	.010	.010	.010	.010	.010	.010	.010	.010	.010	.010	.010	.010
.35	4.17	.020	.020	.020	.020	.020	.020	.020	.020	.020	.020	.020	.020	.020	.020
10.76	6.94	.010	.009	.006	.004	.002	.001	.004	.022	.054	.069	.072	.073	.073	.072
9.72	6.94	.004	.005	-.004	-.008	.031	.045	.048	.049	.050	.050	.049	.048	.048	.046
8.68	6.94	0	.009	-.019	-.019	-.020	-.018	-.016	-.012	-.009	-.008	-.004	-.003	-.002	-.001
7.63	6.94	-.098	-.098	-.085	-.035	-.015	-.008	-.002	.005	.011	.016	.020	.023	.025	.027
6.59	6.94	-.070	-.070	-.070	-.070	-.070	-.070	-.070	-.070	-.057	-.028	-.010	.012	.012	.016
5.55	6.94	-.110	-.110	-.110	-.110	-.110	-.110	-.110	-.110	-.110	-.110	-.110	-.110	-.110	-.110
4.51	6.94	-.070	-.070	-.070	-.070	-.070	-.070	-.070	-.070	-.070	-.070	-.070	-.070	-.070	-.080
3.47	6.94	0	0	0	0	0	0	0	0	0	0	0	-.010	-.010	-.010
10.76	11.11	-.083	-.083	-.083	-.080	-.069	-.052	-.033	-.016	-.005	.001	.006	.009	.012	.014
9.72	11.11	-.058	-.058	-.058	-.058	-.058	-.058	-.058	-.057	-.051	-.040	-.028	-.012	.010	.027
8.68	11.11	-.042	-.042	-.042	-.042	-.042	-.042	-.042	-.042	-.041	-.040	-.039	-.038	-.037	-.036
7.63	11.11	-.040	-.040	-.040	-.040	-.040	-.040	-.040	-.040	-.040	-.040	-.040	-.040	-.040	-.040

TABLE II.- Continued

VALUES OF JET-ON PRESSURE COEFFICIENTS FOR ALL WING ORIFICE POSITIONS FOR TOTAL-PRESSURE RATIOS OF 2 TO 15

(d) Helium at test position II_b (sonic exit)

Orifice ordinates		Pressure coefficients for nacelle-exit total-pressure ratio H_j/p_o of –													
x/D_j	y/D_j	2	3	4	5	6	7	8	9	10	11	12	13	14	15
8.68	0.00	-0.022	-0.025	-0.026	-0.027	-0.026	-0.021	-0.016	-0.024	-0.037	-0.039	-0.035	-0.029	-0.019	-0.009
7.63	.00	.037	.035	.034	.033	.042	.029	.015	.016	.029	.043	.058	.073	.089	.104
6.59	.00	.060	.061	.063	.063	.042	.043	.060	.076	.090	.103	.112	.114	-.025	-.078
5.55	.00	.075	.075	.072	.059	.079	.095	.106	.089	-.065	-.071	-.072	-.073	-.073	-.073
4.51	.00	.083	.091	.101	.113	-.010	-.007	-.006	-.006	-.006	-.006	-.003	0	.002	.004
3.47	.00	.068	.082	.029	.036	.043	.052	.060	.064	.068	.074	.081	.086	.091	.095
2.43	.00	-.088	-.088	-.088	-.081	.014	.106	.143	.160	.173	.183	.193	.202	.211	.218
1.39	.00	-.128	-.126	-.124	-.127	-.125	-.126	-.125	-.124	-.124	-.124	-.123	-.122	-.120	-.119
.35	.00	-.020	-.020	-.020	-.020	-.020	-.020	-.020	-.020	-.020	-.020	-.020	-.020	-.020	-.020
-.69	.00	-.020	-.020	-.020	-.020	-.020	-.020	-.020	-.020	-.020	-.020	-.020	-.020	-.020	-.020
-1.73	.00	.005	.005	.005	.005	.005	.005	.005	.005	.005	.005	.005	.005	.005	.005
-2.77	.00	0	0	0	0	0	0	0	0	0	0	0	0	0	0
8.68	1.40	-.029	-.029	-.029	-.029	-.028	-.022	-.021	-.030	-.042	-.039	-.036	-.028	-.018	-.010
7.63	1.40	.025	.017	.017	.018	.025	.020	.001	.012	.021	.033	.045	.059	.070	.078
6.59	1.40	.046	.046	.047	.047	.030	.041	.056	.072	.084	.092	.103	.040	-.087	-.099
5.55	1.40	.074	.077	.068	.066	.086	.108	.095	-.030	-.055	-.059	-.060	-.060	-.059	-.058
4.51	1.40	.075	.072	.088	.085	-.001	-.004	-.003	-.002	-.001	0	.002	.008	.011	.012
3.47	1.40	.060	.069	.038	.047	.055	.062	.068	.074	.080	.086	.092	.098	.102	.106
2.43	1.40	-.099	-.099	-.099	-.099	-.095	-.046	.045	.117	.153	.170	.184	.196	.207	.215
1.39	1.40	-.104	-.104	-.104	-.104	-.104	-.104	-.104	-.104	-.104	-.104	-.104	-.104	-.104	-.104
.35	1.40	-.024	-.024	-.024	-.024	-.024	-.024	-.024	-.024	-.024	-.024	-.024	.024	-.024	-.024
-.69	1.40	0	0	0	0	0	0	0	0	0	0	0	0	0	0
-1.73	1.40	0	0	0	0	0	0	0	0	0	0	0	0	0	0
-2.77	1.40	0	0	0	0	0	0	0	0	0	0	0	0	0	0
8.68	4.17	-.028	-.028	-.028	-.020	-.023	-.028	.001	.003	.012	.017	.020	.016	.015	-.040
7.63	4.17	-.008	-.012	-.011	-.022	-.015	-.003	.008	0	-.193	-.074	-.110	-.117	-.117	-.116
6.59	4.17	-.008	-.010	-.009	.006	.003	-.048	-.075	-.080	-.079	-.078	-.077	-.076	-.075	-.073
5.55	4.17	.022	.018	.003	-.019	-.020	-.018	-.015	-.013	-.011	-.009	-.007	-.005	-.003	-.001
4.51	4.17	-.109	-.109	-.101	-.067	0	.030	.041	.048	.053	.057	.061	.065	.068	.070
3.47	4.17	-.123	-.125	-.126	-.126	-.126	-.125	-.125	-.125	-.115	-.087	-.037	-.022	-.023	-.075
2.43	4.17	-.026	-.026	-.026	-.026	-.026	-.026	-.026	-.026	-.026	-.026	-.026	-.026	-.026	-.026
1.39	4.17	.021	.021	.021	.021	.021	.021	.021	.021	.021	.021	.021	.021	.021	.021
.35	4.17	.010	.010	.010	.010	.010	.010	.010	.010	.010	.010	.010	.010	.010	.010
-.69	4.17	.020	.020	.020	.020	.020	.020	.020	.020	.020	.020	.020	.020	.020	.020
-1.73	4.17	-.010	-.010	-.010	-.010	-.010	-.010	-.010	-.010	-.010	-.010	-.010	-.010	-.010	-.010
8.68	6.94	.006	.006	.003	.003	-.011	-.026	-.036	-.035	-.034	.030	-.032	-.032	-.032	-.032
7.63	6.94	.011	.005	.005	.007	.007	.005	.003	.001	0	-.002	-.004	-.006	-.006	-.006
6.59	6.94	-.092	-.094	-.094	.085	-.057	-.021	.010	.026	..038	.044	.048	.051	.054	.053
5.55	6.94	-.096	-.097	-.099	-.100	-.100	-.099	-.098	-.097	-.095	-.083	-.066	-.043	-.019	.004
4.51	6.94	-.094	-.094	-.094	-.094	-.094	-.094	-.094	-.094	-.094	-.094	-.094	-.094	-.094	-.094
3.47	6.94	-.101	-.101	-.101	-.101	-.101	-.101	-.101	-.101	-.101	-.101	-.101	-.101	-.101	-.101
2.43	6.94	-.060	-.060	-.060	-.060	-.060	-.060	-.060	-.060	-.060	-.060	-.060	-.060	-.060	-.060
1.39	6.94	0	0	0	0	0	0	0	0	0	0	0	0	0	0
8.68	11.11	-.065	-.072	-.073	-.072	-.068	-.066	-.063	-.061	-.058	-.055	-.054	-.053	-.045	-.037
7.63	11.11	-.030	-.030	-.030	-.030	-.030	-.030	-.030	-.030	-.030	-.030	-.030	-.030	-.030	-.030
6.59	11.11	-.044	-.044	-.044	-.044	-.044	-.044	-.044	-.044	-.044	-.044	-.044	-.044	-.044	-.044
5.55	11.11	-.030	-.030	-.030	-.030	-.030	-.030	-.030	-.030	-.030	-.030	-.030	-.030	-.030	-.030

TABLE II.- Continued

VALUES OF JET-ON PRESSURE COEFFICIENTS FOR ALL WING ORIFICE POSITIONS FOR TOTAL-PRESSURE RATIOS OF 2 TO 15

(e) Helium at test position I_b (supersonic exit)

Orifice ordinates		Pressure coefficients for nacelle-exit total-pressure ratio H_j/p_o of —													
x/D_j	y/D_j	2	3	4	5	6	7	8	9	10	11	12	13	14	15
10.76	0.00	-0.037	-0.026	-0.026	-0.028	-0.026	-0.025	-0.026	-0.026	-0.024	-0.019	-0.017	-0.020	-0.029	-0.040
9.72	.00	.015	.025	.028	.026	.027	.025	.023	.022	.023	.020	.010	0	--.003	-.005
8.68	.00	.047	.055	.055	.054	.054	.050	.053	.053	.049	.040	.038	.040	.046	.055
7.63	.00	.076	.067	.064	.063	.063	.065	.060	.055	.056	.064	.075	.086	.097	.108
6.59	.00	.065	.066	.068	.071	.069	.059	.060	.070	.080	.088	.095	.100	.090	-.022
5.55	.00	.037	.044	.053	.044	.036	.041	.047	.049	.019	-.043	-.050	-.055	-.058	-.058
4.51	.00	.039	.054	.050	.051	.054	.053	-.002	-.006	-.008	-.007	-.006	-.005	-.005	-.003
3.47	.00	.050	.069	.092	.062	.022	.028	.036	.043	.050	.057	.063	.068	.072	.076
2.43	.00	-.079	-.079	-.079	-.079	-.079	-.058	.023	.080	.099	.113	.123	.131	.139	.146
1.39	.00	-.121	-.121	-.121	-.121	-.121	-.121	-.121	-.121	-.121	-.119	-.117	-.116	-.116	-.114
.35	.00	-.014	-.014	-.014	-.014	-.014	-.014	-.014	-.014	-.016	-.016	-.016	-.018	-.018	-.019
-.69	0	0	0	0	0	0	0	0	0	0	0	0	0	0	0
10.76	1.40	-.027	-.027	-.027	-.027	-.027	-.027	-.027	-.027	-.027	-.025	-.025	-.028	-.035	-.051
9.72	1.40	.009	.020	.019	.018	.018	.015	.015	.015	.013	.009	.004	-.006	-.007	-.006
8.68	1.40	.039	.043	.046	.045	.044	.043	.045	.044	.038	.033	.034	.040	.046	.054
7.63	1.40	.067	.060	.061	.060	.060	.061	.060	.050	.056	.068	.079	.090	.100	.105
6.59	1.40	.043	.045	.048	.052	.050	.040	.046	.052	.059	.067	.074	.053	-.016	-.055
5.55	1.40	.034	.041	.045	.031	.035	.039	.043	.036	-.030	-.039	-.043	-.045	-.046	-.046
4.51	1.40	.020	.034	.046	.054	.059	.038	.001	0	0	.001	.002	.004	.006	.008
3.47	1.40	.042	.061	.076	.010	.019	.030	.041	.050	.057	.063	.068	.073	.078	.083
2.43	1.40	-.095	-.095	-.095	-.095	-.095	-.095	-.091	-.062	-.003	.060	.105	.125	.137	.146
1.39	1.40	-.105	-.105	-.105	-.105	-.105	-.105	-.105	-.105	-.105	-.105	-.105	-.105	-.105	-.105
.35	1.40	0	0	0	0	0	0	0	0	0	0	0	0	0	0
-.69	1.40	0	0	0	0	0	0	0	0	0	0	0	0	0	0
10.76	4.17	-.029	-.010	-.011	-.017	-.016	-.021	-.023	-.026	-.026	-.028	-.032	.031	-.025	-.023
9.72	4.17	-.013	-.004	-.004	-.010	-.012	-.013	-.016	-.020	-.024	-.020	-.013	-.005	.002	.008
8.68	4.17	-.013	-.013	-.013	-.013	-.013	-.016	-.020	-.016	-.008	0	.007	.012	.013	.002
7.63	4.17	-.010	-.007	-.003	-.003	-.013	-.009	-.005	0	-.005	-.041	-.074	-.085	-.086	-.086
6.59	4.17	-.011	.001	-.015	-.003	.010	-.001	-.033	-.044	-.048	-.049	-.049	-.049	-.048	-.047
5.55	4.17	-.005	.003	.012	.019	-.008	-.020	-.018	-.016	-.014	-.012	-.010	-.008	-.006	-.003
4.51	4.17	-.060	-.060	-.060	-.057	-.022	.023	.046	.056	.064	.069	.074	.077	.081	.084
3.47	4.17	-.068	-.068	-.068	-.066	-.064	-.061	-.059	-.057	-.054	-.050	-.045	-.036	-.020	.005
2.43	4.17	0	0	0	0	0	0	0	0	0	0	0	0	0	0
1.39	4.17	.020	.020	.020	.020	.020	.020	.020	.020	.020	.020	.020	.020	.020	.020
.35	4.17	.010	.010	.010	.010	.010	.010	.010	.010	.010	.010	.010	.010	.010	.010
10.76	6.94	-.004	-.004	-.004	-.004	-.004	-.010	-.012	-.010	-.007	0	.006	.005	-.005	-.026
9.72	6.94	.003	-.005	-.002	.006	.006	.003	.001	.005	.023	.040	.052	.056	.057	.057
8.68	6.94	-.008	-.004	0	.002	.003	-.005	-.022	-.028	-.029	-.029	-.027	-.026	-.025	-.024
7.63	6.94	-.033	-.027	-.022	-.027	-.035	-.035	-.033	-.031	-.027	-.023	-.019	-.016	-.014	-.013
6.59	6.94	-.154	-.151	-.149	-.149	-.145	-.137	-.117	-.091	-.070	-.053	-.045	-.036	-.034	-.027
5.55	6.94	-.151	-.151	-.151	-.151	-.151	-.151	-.151	-.151	-.151	-.151	-.151	-.151	-.151	-.151
4.51	6.94	-.060	-.060	-.060	-.060	-.060	-.060	-.060	-.060	-.060	-.060	-.060	-.060	-.060	-.060
3.47	6.94	.010	.010	.010	.010	.010	.010	.010	.010	.010	.010	.010	.010	.010	.010
10.76	11.11	-.112	-.109	-.103	-.106	-.105	-.094	-.178	-.063	-.052	-.044	-.034	-.028	-.025	-.022
9.72	11.11	-.076	-.076	-.076	-.076	-.076	-.076	-.076	-.076	-.075	-.072	-.068	-.060	-.051	-.040
8.68	11.11	-.056	-.056	-.056	-.056	-.056	-.056	-.056	-.056	-.056	-.056	-.056	-.056	-.056	-.056
7.63	11.11	-.030	-.030	-.030	-.030	-.030	-.030	-.030	-.030	-.030	-.030	-.030	-.030	-.030	-.030

TABLE II.- Continued

VALUES OF JET-ON PRESSURE COEFFICIENTS FOR ALL WING ORIFICE POSITIONS FOR TOTAL-PRESSURE RATIOS OF 2 TO 15

(f) Air at test position I_b (sonic exit)

Orifice ordinates		Pressure coefficients for nacelle-exit total-pressure ratio H_j/p_o of —									
x/D_j	y/D_j	6	7	8	9	10	11	12	13	14	15
10.76	0.00	-0.018	-0.017	-0.018	-0.020	-0.022	-0.026	-0.030	-0.033	-0.035	-0.035
9.72	.00	.028	.024	.019	.015	.012	.010	.010	.013	.019	.028
8.68	.00	.050	.050	.047	.043	.043	.050	.059	.070	.083	.094
7.63	.00	.054	.053	.055	.063	.075	.091	.105	.116	.120	.101
6.59	.00	.052	.066	.082	.096	.098	-.065	-.123	-.131	-.137	-.142
5.55	.00	.058	.055	-.101	-.111	-.116	-.119	-.122	-.124	-.125	-.126
4.51	.00	-.058	-.059	-.058	-.058	-.057	-.056	-.052	-.053	-.050	-.049
3.47	.00	.038	.044	.050	.056	.062	.068	.073	.078	.082	.086
2.43	.00	.041	.128	.159	.177	.191	.204	.213	.222	.230	.237
1.39	.00	-.128	-.125	-.125	-.125	-.125	-.126	-.125	-.125	-.115	-.052
.35	.00	0	0	0	0	0	0	0	0	0	0
-.69	.00	0	0	0	0	0	0	0	0	0	0
10.76	1.40	-.021	-.018	-.026	-.026	-.026	-.027	-.034	-.034	-.034	-.034
9.72	1.40	.016	.017	.010	.005	.003	.004	.006	.009	.017	.027
8.68	1.40	.040	.040	.037	.033	.036	.045	.060	.066	.076	.087
7.63	1.40	.052	.048	.054	.065	.075	.090	.100	.102	.058	-.080
6.59	1.40	.045	.054	.065	.074	.010	-.111	-.116	-.119	-.121	-.122
5.55	1.40	.054	-.046	-.100	-.104	-.107	-.109	-.110	-.111	-.112	-.113
4.51	1.40	-.044	-.042	-.039	-.037	-.035	-.033	-.031	-.029	-.027	-.026
3.47	1.40	.050	.059	.067	.074	.079	.085	.090	.095	.099	.103
2.43	1.40	-.093	.003	.136	.172	.191	.206	.217	.227	.235	.242
1.39	1.40	-.095	-.095	-.095	-.095	-.095	-.095	-.095	-.095	-.095	-.094
.35	1.40	0	0	0	0	0	0	0	0	0	0
-.69	1.40	0	0	0	0	0	0	0	0	0	0
10.76	4.17	-.017	-.012	-.019	-.025	-.029	-.020	-.019	-.013	-.008	.003
9.72	4.17	-.013	-.013	-.013	-.012	-.009	-.004	.004	.009	.010	.002
8.68	4.17	-.020	-.013	-.007	-.002	-.001	-.035	-.113	-.164	-.176	-.182
7.63	4.17	.002	-.005	-.060	------	------	------	------	------	------	------
6.59	4.17	-.074	-.077	-.077	-.077	.078	-.077	-.076	.076	-.076	-.076
5.55	4.17	-.029	-.026	-.024	-.023	-.021	-.020	-.018	-.017	-.016	-.015
4.51	4.17	.065	.082	.078	.082	.086	.089	.091	.093	.095	.096
3.47	4.17	-.067	-.062	-.045	.005	.075	.145	.173	.189	.200	.207
2.43	4.17	.010	.010	.010	.010	.010	.010	.010	.010	.010	.010
1.39	4.17	.020	.020	.020	.020	.020	.020	.020	.020	.020	.020
.35	4.17	.010	.010	.010	.010	.010	.010	.010	.010	.010	.010
10.76	6.94	-.008	.001	.001	-.011	-.047	-.096	-.126	-.132	-.135	-.136
9.72	6.94	.010	.040	.076	.085	.087	.087	.087	.087	.087	.087
8.68	6.94	-.041	-.042	-.043	-.043	-.044	-.044	-.044	-.044	-.043	-.043
7.63	6.94	-.027	-.027	-.026	-.025	-.025	-.023	-.022	-.020	-.019	-.018
6.59	6.94	-.097	-.045	-.028	-.022	-.019	-.013	-.014	-.011	-.010	-.009
5.55	6.94	-.143	-.143	-.143	-.142	-.123	-.070	-.031	-.008	.004	.011
4.51	6.94	-.060	-.060	-.060	-.060	-.060	-.060	-.060	-.050	-.050	-.040
3.47	6.94	-.010	-.010	-.010	-.010	-.010	-.010	-.010	-.010	-.010	-.010
10.76	11.11	-.059	-.028	-.025	-.025	-.023	-.016	-.016	-.016	-.013	-.012
9.72	11.11	-.070	-.064	-.053	-.032	-.005	.014	.023	.029	.032	.034
8.68	11.11	-.051	-.051	-.051	-.051	-.051	-.046	-.039	-.025	-.004	.019
7.63	11.11	-.030	-.030	-.030	-.030	-.030	-.030	-.030	-.030	-.030	-.030

TABLE II.- Concluded

VALUES OF JET-ON PRESSURE COEFFICIENTS FOR ALL WING ORIFICE POSITIONS FOR TOTAL-PRESSURE RATIOS OF 2 TO 15

(g) Hydrogen and air at test position I_b (hot sonic exit)

Orifice ordinates		Pressure coefficients for nacelle-exit total-pressure ratio H_j/p_o of —				
x/D_j	y/D_j	6.50	6.75	7.00	7.25	7.50
10.76	0.00	-0.025	-0.027	-0.028	-0.023	-0.023
9.72	.00	.033	.032	.030	.038	.033
8.68	.00	.050	.051	.051	.053	.053
7.63	.00	.059	.053	.062	.062	.062
6.59	.00	.060	.063	.067	.071	.075
5.55	.00	.061	.064	.068	.070	.075
4.51	.00	-.061	-.060	-.060	-.061	-.060
3.47	.00	.033	.036	.039	.041	.043
2.43	.00	.121	.130	.139	.146	.152
1.39	.00	-.123	-.121	-.122	-.123	-.123
.35	.00	-.007	-.005	-.006	-.006	-.006
-.69	.00	0	0	0	0	0
10.76	1.40	-.028	-.031	-.032	-.024	-.025
9.72	1.40	.022	.020	.019	.025	.022
8.68	1.40	.039	.045	.037	.044	.044
7.63	1.40	.057	.059	.057	.056	.055
6.59	1.40	.043	.044	.049	.056	.050
5.55	1.40	.061	.064	.065	.065	.054
4.51	1.40	-.044	-.043	-.043	-.041	-.041
3.47	1.40	.050	.052	.054	.058	.059
2.43	1.40	.008	.021	.073	.102	.128
1.39	1.40	-.107	-.106	-.109	-.104	-.107
.35	1.40	0	0	0	0	0
-.69	1.40	0	0	0	0	0
10.76	4.17	-.019	-.027	-.032	-.015	-.022
9.72	4.17	-.012	-.016	-.018	-.010	-.013
8.68	4.17	-.016	-.017	-.019	-.017	-.015
7.63	4.17	.004	.004	.008	.008	.010
6.59	4.17	-.069	-.071	-.071	-.083	-.077
5.55	4.17	-.028	-.027	-.026	-.025	-.024
4.51	4.17	.068	.069	.073	.075	.077
3.47	4.17	-.067	-.066	-.065	-.062	-.058
2.43	4.17	.010	.010	.010	.010	.010
1.39	4.17	.020	.020	.020	.020	.020
.35	4.17	.010	.020	.020	.020	.020
10.76	6.94	-.011	-.016	-.018	-.005	-.010
9.72	6.94	.001	.002	0	0	.005
8.68	6.94	-.041	-.044	-.049	-.044	-.045
7.63	6.94	-.033	-.036	-.039	-.029	-.032
6.59	6.94	-.063	-.059	-.048	-.036	-.034
5.55	6.94	-.148	-.148	-.148	-.148	-.148
4.51	6.94	-.060	-.060	-.060	-.060	-.060
3.47	6.94	-.010	-.010	-.010	-.010	-.010
10.76	11.11	-.049	-.050	-.047	-.035	-.034
9.72	11.11	-.078	-.074	-.072	-.066	-.053
8.68	11.11	-.054	-.056	-.056	-.051	-.054
7.63	11.11	-.030	-.030	-.030	-.030	-.030

TABLE III

VALUES OF INCREMENTAL PRESSURE COEFFICIENTS FOR ALL WING ORIFICE POSITIONS FOR TOTAL-PRESSURE RATIOS OF 2 TO 15

(a) Helium at test position I_a (sonic exit)

Orifice ordinates		Pressure coefficients for nacelle-exit total-pressure ratio H_j/p_o of –													
x/D_j	y/D_j	2	3	4	5	6	7	8	9	10	11	12	13	14	15
10.76	0.00	-0.016	-0.014	-0.013	-0.011	-0.009	-0.008	-0.007	-0.010	-0.012	-0.007	-0.002	0.003	0.008	0.012
9.72	.00	-.018	-.016	-.015	-.011	-.005	-.009	-.018	-.011	-.009	-.007	.003	.005	.007	.003
8.68	.00	-.020	-.016	-.013	-.011	-.009	-.008	-.011	-.005	.004	.009	.009	-.002	.030	-.046
7.63	.00	-.016	-.015	-.014	-.014	-.012	-.009	-.004	-.005	-.019	-.046	-.057	-.053	-.042	-.031
6.59	.00	-.019	-.019	-.019	-.019	-.017	-.010	-.024	-.054	-.050	-.040	-.027	-.009	.013	.033
5.55	.00	-.025	-.025	-.024	-.022	-.040	-.049	-.039	-.021	.001	.023	.046	.068	.080	.081
4.51	.00	-.045	-.039	-.036	-.047	-.051	-.022	.005	.027	.039	.023	-.165	-.258	-.275	-.287
3.47	.00	-.052	-.038	-.052	-.027	-.007	0	-.208	-.220	.227	-.231	-.235	-.237	-.239	-.239
2.43	.00	.105	.116	.125	-.003	-.015	-.008	-.002	.004	.010	.017	.024	.033	.043	.052
1.39	.00	.202	.173	.197	.023	.242	.263	.281	.299	.316	.334	.351	.367	.382	.394
.35	.00	0	0	0	0	.001	-.007	.066	.160	.221	.251	.291	.311	.336	.355
-.69	.00	0	0	0	0	0	0	0	0	0	0	0	0	0	0
10.76	1.40	-.019	-.016	-.014	-.012	-.008	-.009	-.009	-.014	-.013	0	-.004	-.001	.002	.006
9.72	1.40	-.020	-.016	-.013	-.011	-.007	-.012	-.017	-.012	-.007	-.006	.004	.007	.004	-.004
8.68	1.40	-.013	-.012	-.011	-.010	-.009	-.008	-.006	0	.003	.003	-.005	-.028	-.044	-.043
7.63	1.40	-.011	-.011	-.010	-.009	-.007	-.004	-.002	-.007	-.031	-.047	-.046	-.038	-.024	-.012
6.59	1.40	-.014	-.010	-.014	-.010	-.006	-.008	-.038	-.037	-.029	-.030	-.003	.012	.031	.052
5.55	1.40	-.032	-.031	-.030	-.029	-.048	-.047	-.025	-.003	.017	.034	.048	.054	.039	-.056
4.51	1.40	-.049	-.046	-.049	-.060	-.041	-.020	-.004	.005	-.127	-.234	-.247	-.254	-.258	-.260
3.47	1.40	-.021	-.024	-.011	.001	.002	-.152	-.164	-.163	-.162	-.163	-.162	.160	-.157	-.155
2.43	1.40	.189	.216	.107	.104	.114	.119	.127	.138	.145	.149	.157	.167	.172	.182
1.39	1.40	0	.017	.139	.186	.216	.239	.258	.274	.282	.289	.302	.318	.332	.344
.35	1.40	0	0	0	0	0	.010	.020	.030	.080	.110	.160	.210	.250	.280
-.69	1.40	0	0	0	0	0	0	0	0	0	0	0	0	0	0
10.76	4.17	-.018	-.011	-.020	-.019	-.010	-.017	-.019	-.016	-.013	-.011	-.016	-.025	-.033	-.035
9.72	4.17	-.023	-.025	-.026	-.025	-.018	-.026	-.025	-.027	-.039	-.042	-.044	-.044	-.040	-.029
8.68	4.17	-.015	-.015	-.015	-.015	-.015	-.017	-.030	-.033	-.030	-.023	-.015	-.008	-.003	0
7.63	4.17	-.018	-.018	-.018	.018	-.026	-.028	-.018	-.009	-.003	.001	.001	-.005	.035	-.075
6.59	4.17	-.026	-.023	-.028	-.033	-.022	-.012	-.029	-.060	-.107	-.127	.132	-.034	-.135	-.135
5.55	4.17	.038	.036	.037	.040	.008	-.027	-.036	-.036	-.036	-.035	-.035	-.034	-.033	-.032
4.51	4.17	.120	.126	.101	.087	.087	.089	.092	.094	.095	.097	.098	.100	.101	.102
3.47	4.17	.003	.012	.039	.081	.115	.132	.143	.150	.154	.158	.161	.164	.167	.170
2.43	4.17	0	0	0	0	0	.020	.040	.070	.120	.160	.190	.210	.220	.220
1.39	4.17	0	0	0	0	0	0	0	0	0	0	0	0	0	0
.35	4.17	0	0	0	0	0	0	0	0	0	0	0	0	0	0
10.76	6.94	-.022	-.025	-.024	-.020	-.021	-.027	-.033	-.038	-.024	-.021	-.019	-.019	-.022	-.020
9.72	6.94	.016	.015	.015	.018	.023	.019	.015	.015	.030	.045	.060	.074	.086	.097
8.68	6.94	0	0	0	.001	.004	-.015	-.041	-.050	-.053	-.054	-.053	-.053	-.052	-.051
7.63	6.94	.071	.074	.071	.061	.052	.046	.043	.043	.045	.046	.048	.050	.051	.053
6.59	6.94	.017	.021	.040	.058	.074	.078	.080	.082	.084	.085	.087	.056	.050	.056
5.55	6.94	0	0	0	0	.008	.029	.071	.100	.113	.116	.123	.128	.131	.135
4.51	6.94	0	0	0	0	.010	.010	.010	.020	.030	.040	.050	.070	.090	.100
3.47	6.94	0	0	0	0	0	0	0	0	0	0	0	0	0	0
10.76	11.11	-.003	-.003	.014	.032	.052	.058	.063	.066	.069	.070	.072	.073	.074	.076
9.72	11.11	0	0	0	0	.006	.017	.033	.053	.067	.075	.080	.083	.086	.087
8.68	11.11	0	0	0	.002	.005	.003	-.002	.002	.006	.013	.029	.042	.059	.043
7.63	11.11	0	0	0	0	0	0	0	0	0	0	0	0	0	.010

TABLE III.- Continued

VALUES OF INCREMENTAL PRESSURE COEFFICIENTS FOR ALL WING ORIFICE POSITIONS FOR TOTAL-PRESSURE RATIOS OF 2 TO 15

(b) Helium at test position I_b (sonic exit)

Orifice ordinates		Pressure coefficients for nacelle-exit total-pressure ratio H_j/p_o of –													
x/D_j	y/D_j	2	3	4	5	6	7	8	9	10	11	12	13	14	15
10.76	0.00	-0.014	-0.011	-0.007	-0.010	-0.008	-0.004	-0.007	-0.005	0.001	0.004	-0.004	-0.004	-0.031	-0.032
9.72	.00	-.019	-.014	-.011	-.011	-.012	-.016	-.015	-.013	-.018	-.028	-.044	-.046	-.045	-.041
8.68	.00	-.014	-.014	-.009	-.014	-.014	-.013	-.014	-.025	-.040	-.037	-.031	-.022	-.013	-.002
7.63	.00	-.016	-.021	-.020	-.021	-.019	-.033	-.046	-.032	-.026	-.011	.004	.018	.032	.044
6.59	.00	-.030	-.030	-.030	-.030	-.045	-.031	-.015	0	.018	.035	.032	-.093	-.106	-.195
5.55	.00	-.035	-.030	-.040	-.030	-.010	.002	-.045	-.166	-.173	-.174	-.175	-.175	-.176	.015
4.51	.00	.035	.039	.058	.030	-.054	-.054	-.053	-.051	-.049	-.045	-.043	-.039	-.038	-.035
3.47	.00	.143	.164	.112	.120	.124	.137	.144	.151	.158	.158	.169	.176	.181	.185
2.43	.00	-.002	-.002	-.002	-.001	.045	.148	.214	.239	.258	.273	.284	.299	.301	.309
1.39	.00	0	0	0	0	0	0	.004	.007	.010	.012	.013	.013	.014	.013
.35	.00	0	0	-.001	0	0	-.004	0	-.005	0	0	0	-.005	0	-.003
-.69	.00	0	0	0	0	0	0	0	0	0	0	0	0	0	0
10.76	1.40	-.016	-.011	-.009	-.008	-.007	-.009	-.007	-.009	-.003	-.003	-.004	-.015	-.039	-.035
9.72	1.40	-.016	-.011	-.009	-.009	-.015	-.016	-.015	-.013	-.018	-.039	-.044	-.043	-.039	-.036
8.68	1.40	-.012	-.012	-.011	-.012	-.012	-.010	-.012	-.028	-.034	-.027	-.021	-.013	-.003	.005
7.63	1.40	-.021	-.021	-.022	-.021	-.021	-.023	-.040	-.028	-.012	.001	.013	.018	.037	-.055
6.59	1.40	-.030	-.026	-.024	-.041	-.039	-.024	-.009	.008	.019	.016	-.077	-.158	-.173	-.175
5.55	1.40	-.034	-.036	-.046	-.024	-.007	-.006	-.147	-.157	-.159	-.160	-.160	-.159	-.159	-.159
4.51	1.40	.088	.126	.161	.065	.060	.062	.065	.067	.070	.073	.076	.079	.081	.084
3.47	1.40	.129	.127	.116	.128	.139	.147	.154	.159	.167	.173	.179	.185	.190	.195
2.43	1.40	-.001	-.002	-.002	-.002	0	.021	.115	.200	.254	.281	.288	.314	.320	.327
1.39	1.40	0	0	0	0	0	0	0	0	0	0	0	0	0	0
.35	1.40	0	0	0	0	0	0	0	0	0	0	0	0	0	0
-.69	1.40	0	0	0	0	0	0	0	0	0	0	0	0	0	0
10.76	4.17	-.019	-.010	-.007	-.009	-.020	-.021	-.021	-.022	-.032	-.040	-.039	-.030	-.024	-.014
9.72	4.17	-.015	-.016	-.014	-.008	-.020	-.024	-.036	-.039	-.035	-.026	-.020	-.008	-.001	.010
8.68	4.17	-.024	-.021	-.018	-.018	-.032	-.033	-.024	-.013	-.004	.005	.011	.010	-.010	-.067
7.63	4.17	-.025	-.020	-.025	-.030	-.019	-.009	-.005	-.052	-.111	-.120	-.120	-.120	-.119	-.119
6.59	4.17	.041	.046	.056	.056	-.007	-.024	-.025	-.024	-.024	-.022	-.022	-.021	-.020	-.018
5.55	4.17	.102	.115	.075	.071	.074	.076	.079	.081	.084	.086	.088	.089	.091	.092
4.51	4.17	-.003	-.004	.018	.092	.117	.126	.131	.134	.139	.142	.146	.149	.151	.154
3.47	4.17	0	0	0	0	.001	.001	.005	.018	.052	.107	.166	.207	.235	.250
2.43	4.17	0	0	0	0	0	0	0	0	0	0	0	0	0	0
1.39	4.17	0	0	0	0	0	0	0	0	0	0	0	0	0	0
.35	4.17	0	0	0	0	0	0	0	0	0	0	0	0	0	0
10.76	6.94	-.023	-.018	-.013	-.017	-.030	-.031	-.024	-.017	-.013	-.012	-.017	-.046	-.061	-.084
9.72	6.94	.013	.017	.016	.013	.007	.007	.032	.060	.075	.082	.085	.086	.085	.084
8.68	6.94	.068	.070	.072	.057	.032	.027	.027	.027	.025	.027	.029	.030	.032	.033
7.63	6.94	.057	.059	.062	.062	.063	.064	.067	.068	.070	.072	.075	.077	.081	.083
6.59	6.94	-.003	-.001	.001	.012	.045	.083	.111	.121	.127	.133	.134	.139	.140	.143
5.55	6.94	-.005	-.005	-.003	-.004	-.004	-.003	-.004	-.003	.004	.012	.035	.070	.102	.119
4.51	6.94	0	0	0	0	0	0	0	0	0	0	0	0	0	0
3.47	6.94	0	0	0	0	0	0	0	0	0	0	0	0	0	0
10.76	11.11	-.001	.007	.010	.028	.048	.067	.074	.081	.084	.087	.089	.094	.096	.101
9.72	11.11	-.003	-.003	-.003	-.003	-.003	-.003	.005	.017	.034	.059	.077	.087	.097	.128
8.68	11.11	-.004	-.004	-.004	-.004	-.004	-.004	-.004	-.004	-.004	-.004	-.004	.004	.008	.019
7.63	11.11	0	0	0	0	0	0	0	0	0	0	0	0	0	0

TABLE III.- Continued

VALUES OF INCREMENTAL PRESSURE COEFFICIENTS FOR ALL WING ORIFICE POSITIONS FOR TOTAL-PRESSURE RATIOS OF 2 TO 15

(c) Helium at test position I_c (sonic exit)

Orifice ordinates		Pressure coefficients for nacelle-exit total-pressure ratio H_j/p_o of —													
x/D_j	y/D_j	2	3	4	5	6	7	8	9	10	11	12	13	14	15
10.76	0.00	-0.015	-0.013	-0.012	-0.012	-0.014	-0.015	-0.011	-0.011	-0.016	-0.026	-0.030	-0.028	-0.024	-0.020
9.72	.00	-.019	-.019	-.019	-.019	-.019	-.019	-.025	-.040	-.039	-.031	-.023	-.014	-.006	.002
8.68	.00	-.021	-.019	-.024	-.018	-.026	-.042	-.033	-.026	-.010	.001	.015	.022	-.029	.030
7.63	.00	-.030	-.025	-.023	-.048	-.032	-.019	-.007	.003	.009	-.085	-.156	-.160	-.161	-.160
6.59	.00	-.030	-.026	-.020	-.013	-.003	-.107	-.125	-.125	-.135	-.125	-.125	-.125	-.125	-.124
5.55	.00	.116	.134	.102	.066	.070	.073	.075	.077	.079	.081	.083	.085	.087	.089
4.51	.00	.017	.081	.096	.104	.113	.119	.125	.129	.135	.141	.145	.147	.152	.155
3.47	.00	0	.234	.002	.003	.003	.010	.077	.152	.229	.270	.287	.297	.312	.317
2.43	.00	0	0	-.001	-.001	-.001	-.001	-.002	-.003	-.004	-.005	-.005	-.005	-.006	-.006
1.39	.00	0	0	0	0	0	0	0	0	0	0	0	0	0	0
.35	.00	0	0	0	0	0	0	0	0	0	0	0	0	0	0
-.69	.00	0	0	0	0	0	0	0	0	0	0	0	0	0	0
10.76	1.40	-.023	-.020	-.013	-.016	-.017	-.016	-.012	-.011	-.021	-.030	-.030	-.026	-.020	-.015
9.72	1.40	-.014	-.013	-.017	-.018	-.017	-.017	-.030	-.038	-.032	-.024	-.019	-.009	.002	.011
8.68	1.40	-.018	-.018	-.021	-.016	-.029	-.037	-.026	-.014	-.003	.007	.017	.026	.032	0
7.63	1.40	-.030	-.026	-.027	-.045	-.028	-.011	.001	.008	-.048	-.139	-.148	-.150	-.151	-.150
6.59	1.40	-.032	-.027	-.020	-.009	-.009	-.106	-.109	-.109	-.109	-.108	-.108	-.108	-.107	-.106
5.55	1.40	.117	.137	.076	.074	.078	.081	.062	.086	.058	.090	.092	.094	.096	.099
4.51	1.40	0	.008	.096	.108	.117	.124	.131	.137	.142	.148	.152	.156	.159	.162
3.47	1.40	0	0	0	0	0	0	.001	.024	.104	.194	.249	.269	.298	.309
2.43	1.40	0	0	0	0	0	-.001	-.003	-.003	-.003	-.003	-.005	-.006	-.007	-.007
1.39	1.40	0	0	0	0	0	0	0	0	0	0	0	0	0	0
.35	1.40	0	0	0	0	0	0	0	0	0	0	0	0	0	0
-.69	1.40	0	0	0	0	0	0	0	0	0	0	0	0	0	0
10.76	4.17	-.012	-.014	-.016	-.019	-.024	-.037	-.047	-.041	-.033	-.024	-.016	-.007	.001	.009
9.72	4.17	-.024	-.025	-.033	-.041	-.046	-.046	-.037	-.024	-.011	-.001	.005	.002	-.037	-.110
8.68	4.17	-.025	-.019	-.030	-.031	-.020	-.011	-.009	-.064	-.114	-.120	-.121	-.121	-.121	-.120
7.63	4.17	.047	.053	.061	.060	0	-.013	-.012	-.011	-.010	-.009	-.009	-.008	-.007	-.007
6.59	4.17	.094	.104	.069	.071	.075	.082	.083	.083	.085	.088	.090	.092	.093	.093
5.55	4.17	-.004	-.004	.015	.079	.095	.102	.108	.112	.116	.119	.129	.131	.134	.136
4.51	4.17	0	0	0	0	0	0	0	.001	.022	.079	.138	.184	.212	.227
3.47	4.17	.001	.001	.001	0	0	0	-.001	-.001	-.001	-.002	-.002	-.002	-.003	-.003
2.43	4.17	0	0	0	0	0	0	0	0	0	0	0	0	0	0
1.39	4.17	0	0	0	0	0	0	0	0	0	0	0	0	0	0
.35	4.17	0	0	0	0	0	0	0	0	0	0	0	0	0	0
10.76	6.94	-.020	-.021	-.024	-.026	-.028	-.029	-.026	-.008	.024	.039	.042	.043	.043	.042
9.72	6.94	-.043	-.042	-.051	-.055	-.016	-.002	.001	.002	.003	.003	.002	.001	.001	-.001
8.68	6.94	.064	.073	.045	.045	.044	.046	.048	.052	.055	.056	.060	.061	.062	.063
7.63	6.94	0	0	.013	.063	.083	.090	.096	.093	.087	.114	.118	.075	.123	.125
6.59	6.94	0	0	0	0	0	0	0	0	.013	.042	.060	.082	.082	.086
5.55	6.94	0	0	0	0	0	0	0	0	0	0	0	0	0	0
4.51	6.94	0	0	0	0	0	0	0	0	0	0	0	0	0	-.01
3.47	6.94	0	0	0	0	0	0	0	0	0	0	0	-.01	-.01	-.01
10.76	11.11	0	0	0	.003	.014	.031	.050	.067	.078	.084	.089	.092	.095	.097
9.72	11.11	0	0	0	0	0	0	0	-.001	.007	.018	.030	.046	.068	.085
8.68	11.11	0	0	0	0	0	0	0	0	.001	.002	.003	.004	.005	.006
7.63	11.11	0	0	0	0	0	0	0	0	0	0	0	0	0	0

TABLE III.- Continued

VALUES OF INCREMENTAL PRESSURE COEFFICIENTS FOR ALL WING ORIFICE POSITIONS FOR TOTAL-PRESSURE RATIOS OF 2 TO 15

(d) Helium at test position II_b (sonic exit)

Orifice ordinates		Pressure coefficients for nacelle-exit total-pressure ratio H_j/p_o of –													
x/D_j	y/D_j	2	3	4	5	6	7	8	9	10	11	12	13	14	15
8.68	0.00	-0.010	-0.013	-0.014	-0.015	-0.014	-0.009	-0.004	-0.012	-0.025	-0.027	-0.023	-0.017	-0.007	0.003
7.63	.00	-.019	-.021	-.035	-.033	-.014	-.027	-.041	-.040	-.027	-.013	.002	.017	.033	.048
6.59	.00	-.021	-.020	-.018	-.018	-.039	-.038	-.021	.005	.009	.022	.031	.033	-.106	-.159
5.55	.00	-.031	-.031	-.034	-.047	-.027	-.011	0	-.017	-.171	-.177	-.178	-.179	-.179	-.179
4.51	.00	.013	.021	.031	.043	-.080	-.077	-.076	-.076	-.076	-.076	-.073	-.070	-.072	-.074
3.47	.00	.141	.155	.102	.109	.116	.125	.133	.137	.141	.147	.154	.159	.164	.168
2.43	.00	-.002	-.002	-.002	.005	.100	.192	.229	.246	.259	.269	.107	.288	.297	.304
1.39	.00	0	.004	.006	.003	.005	.004	.005	.006	.006	.006	.007	.008	.010	.011
.35	.00	0	0	0	0	0	0	0	0	0	0	0	0	0	0
-.69	.00	0	0	0	0	0	0	0	0	0	0	0	0	0	0
-1.73	.00	0	0	0	0	0	0	0	0	0	0	0	0	0	0
-2.77	.00	0	0	0	0	0	0	0	0	0	0	0	0	0	0
8.68	1.40	-.011	-.011	-.011	-.011	-.010	-.004	-.003	-.012	-.024	-.021	-.018	-.010	0	.008
7.63	1.40	-.033	-.041	-.041	-.040	-.033	-.038	-.057	-.046	-.037	-.025	-.013	.001	.012	.020
6.59	1.40	-.023	-.023	-.022	-.022	-.039	-.028	-.013	.003	.015	.023	.033	-.029	-.156	-.168
5.55	1.40	-.029	-.026	-.035	-.037	-.017	.005	-.008	-.133	-.158	.162	-.163	-.163	.162	-.161
4.51	1.40	.099	.096	.112	.109	.023	.020	.021	.022	.023	.024	.026	.016	.035	.036
3.47	1.40	.134	.145	.112	.121	.129	.136	.142	.148	.154	.160	.166	.172	.176	.180
2.43	1.40	.002	.002	.002	.002	.006	.055	.146	.218	.254	.271	.285	.297	.308	.316
1.39	1.40	0	0	0	0	0	0	0	0	0	0	0	0	0	0
.35	1.40	0	0	0	0	0	0	0	0	0	0	0	0	0	0
-.69	1.40	0	0	0	0	0	0	0	0	0	0	0	0	0	0
-1.73	1.40	0	0	0	0	0	0	0	0	0	0	0	0	0	0
-2.77	1.40	0	0	0	0	0	0	0	0	0	0	0	0	0	0
8.68	4.17	-.029	-.029	-.029	-.021	-.024	-.029	0	.002	.011	.016	.019	.015	.014	-.041
7.63	4.17	-.018	-.022	-.021	-.032	-.025	-.013	-.002	-.010	-.203	-.084	-.120	-.127	-.127	-.126
6.59	4.17	-.001	-.003	-.002	.013	.010	-.041	-.068	-.073	-.072	-.071	-.070	-.069	-.068	.066
5.55	4.17	.110	.106	.110	.069	.060	.070	.073	.075	.077	.079	.081	.083	.085	.087
4.51	4.17	-.001	-.001	-.001	.041	.108	.138	.149	.156	.161	.165	.169	.173	.176	.178
3.47	4.17	.005	.003	.002	.002	.002	.003	.003	.003	.013	.041	.091	.006	.105	.053
2.43	4.17	0	0	0	0	0	0	0	0	0	0	0	0	0	0
1.39	4.17	0	0	0	0	0	0	0	0	0	0	0	0	0	0
.35	4.17	0	0	0	0	0	0	0	0	0	0	0	0	0	0
-.69	4.17	0	0	0	0	0	0	0	0	0	0	0	0	0	0
-1.73	4.17	0	0	0	0	0	0	0	0	0	0	0	0	0	0
8.68	6.94	.055	.055	.052	.052	.038	.023	.013	.014	.015	.019	.017	.017	.017	.017
7.63	6.94	.071	.065	.065	.067	.067	.065	.063	.061	.060	.058	.056	.054	.054	.054
6.59	6.94	.002	0	0	.009	.037	.073	.104	.120	.056	.138	.142	.145	.148	.147
5.55	6.94	0	-.001	-.003	-.004	-.004	-.003	-.002	-.001	.001	.013	.030	.053	.077	.100
4.51	6.94	0	0	0	0	0	0	0	0	0	0	0	0	0	0
3.47	6.94	0	0	0	0	0	0	0	0	0	0	0	0	0	0
2.43	6.94	0	0	0	0	0	0	0	0	0	0	0	0	0	0
1.39	6.94	0	0	0	0	0	0	0	0	0	0	0	0	0	0
8.68	11.11	.002	-.005	-.006	-.005	-.001	.001	.004	.006	.009	.012	.013	.014	.022	.030
7.63	11.11	0	0	0	0	0	0	0	0	0	0	0	0	0	0
6.59	11.11	0	0	0	0	0	0	0	0	0	0	0	0	0	0
5.55	11.11	0	0	0	0	0	0	0	0	0	0	0	0	0	0

TABLE III.- Continued

VALUES OF INCREMENTAL PRESSURE COEFFICIENTS FOR ALL WING ORIFICE POSITIONS FOR TOTAL-PRESSURE RATIOS OF 2 TO 15

(e) Helium at test position I_b (supersonic exit)

Orifice ordinates		Pressure coefficients for nacelle-exit total-pressure ratio H_j/p_o of –													
x/D_j	y/D_j	2	3	4	5	6	7	8	9	10	11	12	13	14	15
10.76	0.00	-0.012	-0.001	-0.001	-0.003	-0.001	0	-0.001	-0.001	0.001	0.006	0.008	0.005	-0.004	-0.015
9.72	.00	.017	-.007	-.004	-.006	-.005	-.007	-.009	-.010	-.009	-.012	-.022	-.132	-.035	-.037
8.68	.00	-.015	-.007	-.007	-.008	-.008	-.012	-.009	-.009	-.013	-.022	-.024	-.022	-.016	-.007
7.63	.00	-.004	-.013	-.016	-.017	-.017	-.015	-.020	-.025	-.024	-.016	-.005	.006	.017	.028
6.59	.00	-.028	-.027	-.025	-.022	-.024	-.034	-.033	-.023	-.013	-.005	.002	.007	-.003	-.115
5.55	.00	-.038	-.031	-.022	-.031	-.039	-.034	-.028	-.026	-.056	-.118	-.025	-.130	-.133	-.133
4.51	.00	.029	.044	.040	.041	.044	-.043	-.012	-.016	-.018	-.017	-.004	-.015	-.015	-.013
3.47	.00	.135	.154	.177	.147	.107	.113	.121	.128	.135	.142	.148	-.153	.157	.161
2.43	.00	0	0	0	0	0	.021	.102	.159	.178	.192	.202	.210	.218	.225
1.39	.00	0	0	0	0	0	0	0	0	0	.002	.004	.005	.005	.007
.35	.00	0	0	0	0	0	0	0	0	-.002	-.002	-.002	-.004	-.004	-.005
-.69	.00	0	0	0	0	0	0	0	0	0	0	0	0	0	0
10.76	1.40	0	0	0	0	0	0	0	0	0	.002	.002	-.001	-.008	-.024
9.72	1.40	-.013	-.002	-.003	-.004	-.004	-.007	-.007	-.007	-.009	-.013	-.018	-.028	-.029	-.028
8.68	1.40	-.015	-.011	-.008	-.009	-.010	-.011	-.009	-.010	-.016	-.021	-.020	-.014	-.008	0
7.63	1.40	-.012	-.019	-.018	-.019	-.019	-.018	-.019	-.029	-.023	-.011	0	.011	.021	.026
6.59	1.40	-.029	-.027	-.024	-.020	-.022	-.032	-.026	-.020	-.013	-.005	.002	-.019	-.088	-.127
5.55	1.40	-.038	-.031	-.027	-.041	-.037	-.033	-.029	-.036	-.042	-.111	-.115	-.117	-.118	-.118
4.51	1.40	.105	.119	.131	.139	.144	.123	.086	.085	.085	.086	.087	.089	.091	.093
3.47	1.40	.130	.149	.164	.099	.107	.118	.129	.138	.145	.151	.156	.161	.166	.171
2.43	1.40	0	0	0	0	0	0	.004	.033	.092	.155	.200	.220	.232	.241
1.39	1.40	0	0	0	0	0	0	0	0	0	0	0	0	0	0
.35	1.40	0	0	0	0	0	0	0	0	0	0	0	0	0	0
-.69	1.40	0	0	0	0	0	0	0	0	0	0	0	0	0	0
10.76	4.17	-.007	.012	.011	.005	.006	.001	-.001	-.004	-.004	-.006	-.010	.009	-.003	-.001
9.72	4.17	-.008	.001	.001	-.005	-.007	-.008	-.011	-.015	-.019	-.015	-.008	0	.003	.013
8.68	4.17	-.011	-.015	-.015	-.015	-.015	-.018	-.022	-.018	-.010	-.002	.005	.010	.001	0
7.63	4.17	-.028	-.025	.021	-.021	-.031	-.027	-.023	-.018	-.023	-.059	-.092	.103	-.104	-.104
6.59	4.17	.035	.047	.031	.043	.056	.045	.013	.002	-.002	-.003	-.003	-.003	-.002	-.001
5.55	4.17	-.096	.104	.113	.120	.093	.081	.083	.085	-.087	.089	.111	.093	.095	.098
4.51	4.17	0	0	0	.003	.038	.083	.106	.116	.124	.129	.134	.017	.141	.144
3.47	4.17	0	0	0	.002	.004	.007	.009	.011	.014	.018	.023	.032	.048	.073
2.43	4.17	0	0	0	0	0	0	0	0	0	0	0	0	0	0
1.39	4.17	0	0	0	0	0	0	0	0	0	0	0	0	0	0
.35	4.17	0	0	0	0	0	0	0	0	0	0	0	0	0	0
10.76	6.94	0	0	0	0	0	.006	-.008	-.006	-.003	.004	.010	.009	-.001	-.022
9.72	6.94	.013	.005	.008	.016	.016	.013	.011	.015	.033	.050	.062	.066	.067	.067
8.68	6.94	.072	.076	.080	.082	.083	.075	.058	.052	.051	.051	.053	.054	.055	.056
7.63	6.94	.069	.075	.080	.075	.067	.067	.069	.071	.075	.079	.083	.086	.088	.089
6.59	6.94	0	.003	.005	.005	.009	.017	.037	.063	.084	.101	.192	.118	.120	.127
5.55	6.94	0	0	0	0	0	0	0	0	0	0	0	0	0	0
4.51	6.94	0	0	0	0	0	0	0	0	0	0	0	0	0	0
3.47	6.94	0	0	0	0	0	0	0	0	0	0	0	0	0	0
10.76	11.11	.009	.012	.018	.015	.016	.027	-.057	.058	.069	.077	.087	.093	.096	.099
9.72	11.11	0	0	0	0	0	0	0	0	.001	.004	.008	.016	.025	.036
8.68	11.11	0	0	0	0	0	0	0	0	0	0	0	0	0	0
7.63	11.11	0	0	0	0	0	0	0	0	0	0	0	0	0	0

TABLE III.- Continued

VALUES OF INCREMENTAL PRESSURE COEFFICIENTS FOR ALL WING ORIFICE POSITIONS FOR TOTAL-PRESSURE RATIOS OF 2 TO 15

(f) Air at test position I_b (sonic exit)

Orifice ordinates		Pressure coefficients for nacelle-exit total-pressure ratio H_j/p_o of –									
x/D_j	y/D_j	6	7	8	9	10	11	12	13	14	15
10.76	0.00	-0.001	0	-0.001	-0.003	-0.005	-0.009	-0.013	-0.016	-0.018	-0.018
9.72	.00	-.009	-.013	-.016	-.022	-.025	-.027	-.027	-.024	-.016	-.009
8.68	.00	-.017	-.017	-.020	-.024	-.024	-.017	-.008	.003	.016	.027
7.63	.00	-.031	-.032	-.030	-.022	-.010	.006	.020	.031	.045	.016
6.59	.00	-.043	-.029	-.013	.001	.003	-.160	-.218	-.226	-.232	-.237
5.55	.00	-.020	-.023	-.179	-.189	-.198	-.197	-.200	-.202	-.203	-.204
4.51	.00	-.068	-.069	-.068	-.068	-.067	-.066	-.062	-.063	-.060	-.059
3.47	.00	.124	.130	.136	.142	.148	.154	.159	.164	.168	.172
2.43	.00	.124	.211	.242	.260	.274	.287	.296	.305	.313	.320
1.39	.00	0	.003	.003	.003	.003	.002	.003	.003	.013	.076
.35	.00	0	0	0	0	0	0	0	0	0	0
-.69	.00	0	0	0	0	0	0	0	0	0	0
10.76	1.40	0	.003	-.005	-.005	-.005	-.006	-.013	-.013	-.013	-.013
9.72	1.40	-.012	.011	-.018	-.023	-.025	-.024	-.022	-.019	-.011	-.001
8.68	1.40	-.015	-.015	-.018	-.022	-.019	-.010	.005	.011	.021	.032
7.63	1.40	-.024	-.028	-.022	-.011	-.001	.014	.024	.026	-.018	-.156
6.59	1.40	-.029	-.020	-.009	0	-.064	-.185	-.190	-.193	-.195	-.196
5.55	1.40	-.019	-.119	-.173	-.177	-.180	-.182	-.183	-.184	-.185	-.186
4.51	1.40	.046	.048	.051	.053	.055	.057	.059	.061	.063	.064
3.47	1.40	.137	.146	.154	.161	.166	.002	.177	.182	.186	.190
2.43	1.40	.008	.104	.237	.273	.292	.307	.318	.328	.336	.343
1.39	1.40	0	0	0	0	0	0	0	0	0	.001
.35	1.40	0	0	0	0	0	0	0	0	0	0
-.69	1.40	0	0	0	0	0	0	0	0	0	0
10.76	4.17	-.005	0	-.007	-.013	-.017	-.018	-.007	-.001	.004	.015
9.72	4.17	-.013	-.013	-.013	-.012	-.009	-.004	.004	.009	.010	.002
8.68	4.17	-.026	-.019	-.013	-.008	-.007	-.041	-.119	-.170	-.182	-.188
7.63	4.17	-.018	-.025	-.080	------	------	------	------	------	------	------
6.59	4.17	-.027	-.030	-.030	-.030	-.031	-.030	-.029	-.029	-.029	-.029
5.55	4.17	.072	.075	.077	.078	.080	.081	.083	.084	.085	.086
4.51	4.17	.130	.147	.143	.147	.151	.154	.156	.158	.160	.161
3.47	4.17	.004	.009	.026	.076	.146	.116	.244	.260	.271	.278
2.43	4.17	0	0	0	0	0	0	0	0	0	0
1.39	4.17	0	0	0	0	0	0	0	0	0	0
.35	4.17	0	0	0	0	0	0	0	0	0	0
10.76	6.94	-.014	-.005	-.005	-.017	-.053	-.102	-.132	-.138	-.141	-.142
9.72	6.94	.019	.049	.085	.094	.096	.096	.096	.096	.096	.096
8.68	6.94	.034	.033	.032	.032	.031	.031	.031	.031	.032	.032
7.63	6.94	.075	.075	.076	.077	.077	.079	.080	.082	.083	.084
6.59	6.94	.059	.111	.128	.134	.137	.143	.142	.145	.146	.147
5.55	6.94	0	0	0	.001	.020	.073	.112	.135	.147	.154
4.51	6.94	0	0	0	0	0	0	0	.010	.010	.020
3.47	6.94	0	0	0	0	0	0	0	0	0	0
10.76	11.11	.061	.092	.095	.095	.097	.104	.104	.104	.107	.108
9.72	11.11	.003	.009	.020	.041	.068	.087	.096	.102	.105	.107
8.68	11.11	0	0	0	0	0	.005	.012	.026	.047	.070
7.63	11.11	0	0	0	0	0	0	0	0	0	0

TABLE III.- Concluded

VALUES OF INCREMENTAL PRESSURE COEFFICIENTS FOR ALL WING ORIFICE POSITIONS FOR TOTAL-PRESSURE RATIOS OF 2 TO 15

(g) Hydrogen and air at test position I_b (hot sonic exit)

Orifice ordinates		Pressure coefficients for nacelle-exit total-pressure ratio H_j/p_o of —				
x/D_j	y/D_j	6.50	6.75	7.00	7.25	7.50
10.76	0.00	-0.008	-0.010	-0.011	-0.006	-0.006
9.72	.00	-.004	-.005	-.007	.001	-.004
8.68	.00	-.017	-.016	-.016	-.014	-.014
7.63	.00	-.026	-.032	-.023	-.023	-.023
6.59	.00	-.035	-.032	-.028	-.024	-.020
5.55	.00	-.017	-.014	-.010	-.008	-.003
4.51	.00	-.071	-.070	-.070	-.071	-.070
3.47	.00	.119	.122	.125	.127	.129
2.43	.00	.204	.213	.222	.229	.235
1.39	.00	.005	.007	.006	.005	.005
.35	.00	-.007	-.005	-.006	-.006	-.006
-.69	.00	0	0	0	0	0
10.76	1.40	-.007	-.010	-.011	-.003	-.004
9.72	1.40	-.006	-.008	-.009	-.003	-.006
8.68	1.40	-.016	-.010	-.018	-.001	-.011
7.63	1.40	-.019	-.017	-.019	-.020	-.021
6.59	1.40	-.031	-.030	-.025	-.018	-.024
5.55	1.40	-.012	-.009	-.008	-.008	-.019
4.51	1.40	.046	.047	.047	.049	.049
3.47	1.40	.037	.139	.141	.145	.146
2.43	1.40	.093	.122	.174	.203	.229
1.39	1.40	-.012	-.011	-.014	-.009	-.012
.35	1.40	0	0	0	0	0
-.69	1.40	0	0	0	0	0
10.76	4.17	-.007	-.015	-.020	-.003	-.010
9.72	4.17	-.012	-.016	-.018	-.010	-.013
8.68	4.17	-.022	-.023	-.025	-.023	-.021
7.63	4.17	-.016	-.016	-.012	-.012	-.010
6.59	4.17	-.022	.024	-.024	-.036	-.030
5.55	4.17	.073	.074	.075	.076	.077
4.51	4.17	.133	.134	.138	.140	.142
3.47	4.17	.004	.005	.006	.009	.013
2.43	4.17	0	0	0	0	0
1.39	4.17	0	0	0	0	0
.35	4.17	0	0	0	0	0
10.76	6.94	-.017	-.022	-.024	-.011	-.016
9.72	6.94	.010	.011	.009	.009	.014
8.68	6.94	.034	.031	.026	.031	.030
7.63	6.94	.069	.066	.063	.073	.070
6.59	6.94	.093	.097	.108	.120	.122
5.55	6.94	-.005	-.005	-.005	-.005	-.005
4.51	6.94	0	0	0	0	0
3.47	6.94	0	0	0	0	0
10.76	11.11	.071	.070	.073	.085	.086
9.72	11.11	-.005	-.001	.001	.007	.020
8.68	11.11	-.003	-.005	-.005	0	-.003
7.63	11.11	0	0	0	0	0

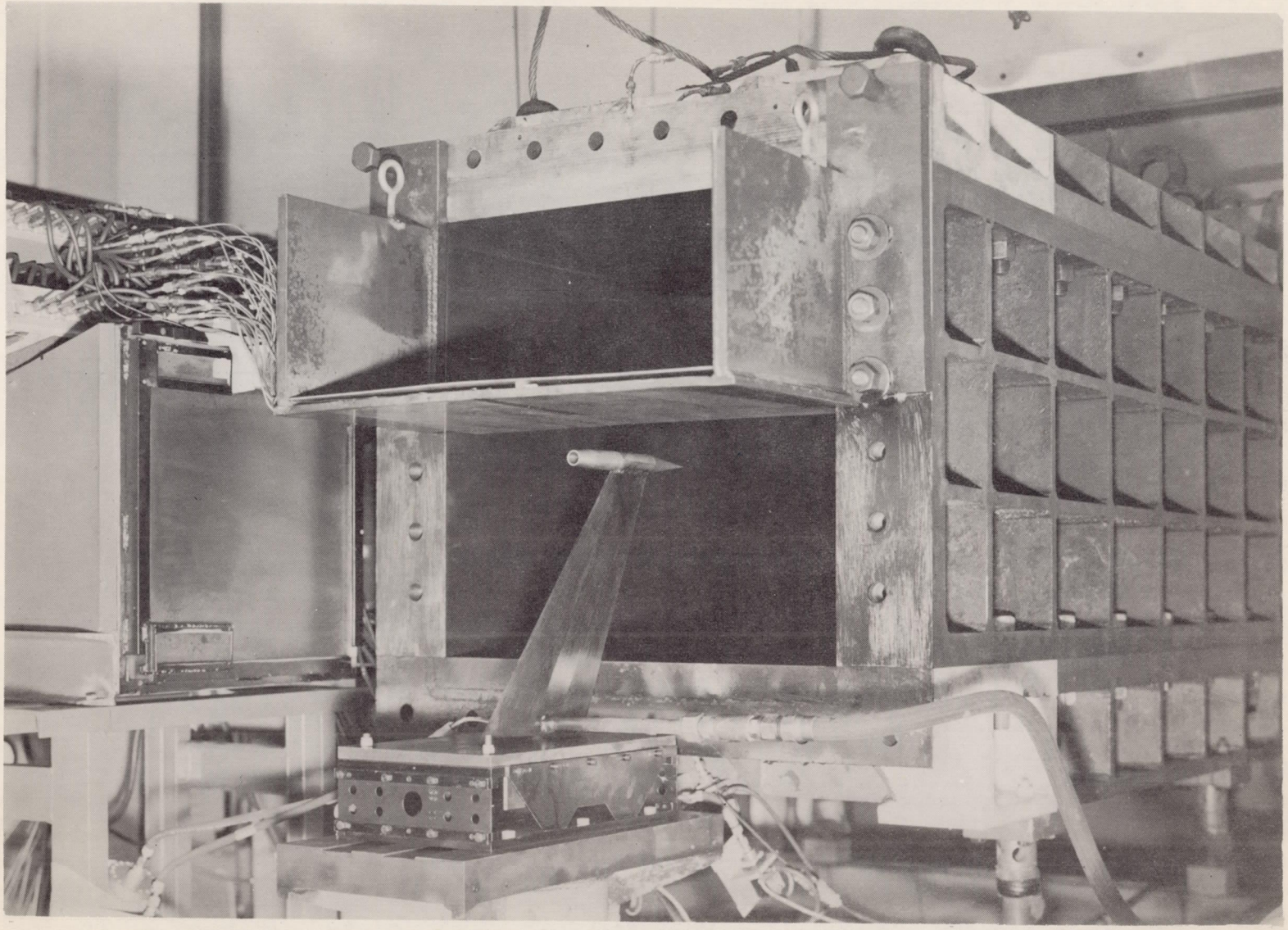
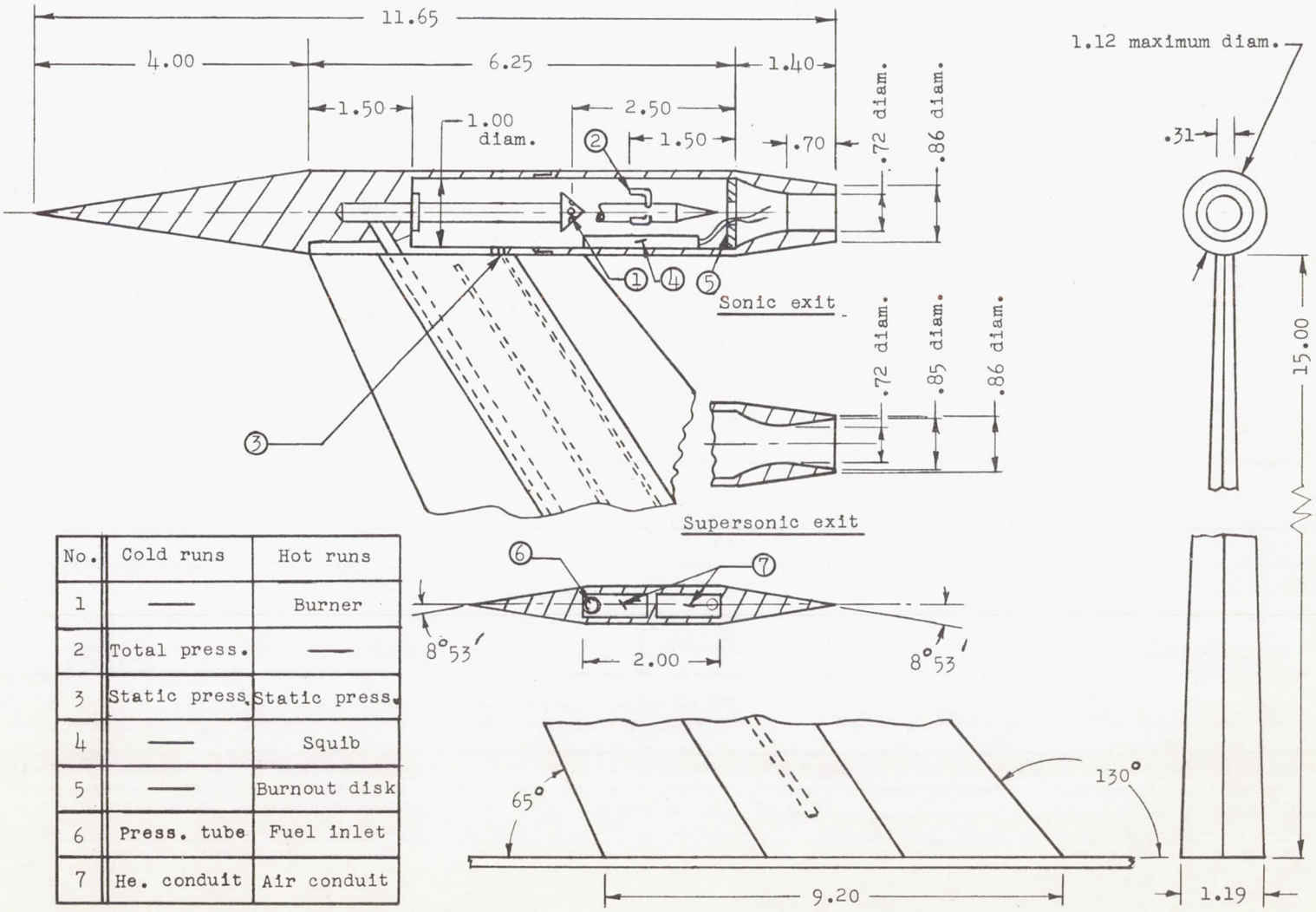


Figure 1.- Photograph of the nacelle mounted beneath the flat-surface wing in the 27- by 27-inch preflight-jet nozzle. L-86661



No.	Cold runs	Hot runs
1	—	Burner
2	Total press.	—
3	Static press.	Static press.
4	—	Squib
5	—	Burnout disk
6	Press. tube	Fuel inlet
7	He. conduit	Air conduit

Figure 2.- Schematic diagram of nacelle. All dimensions are in inches.

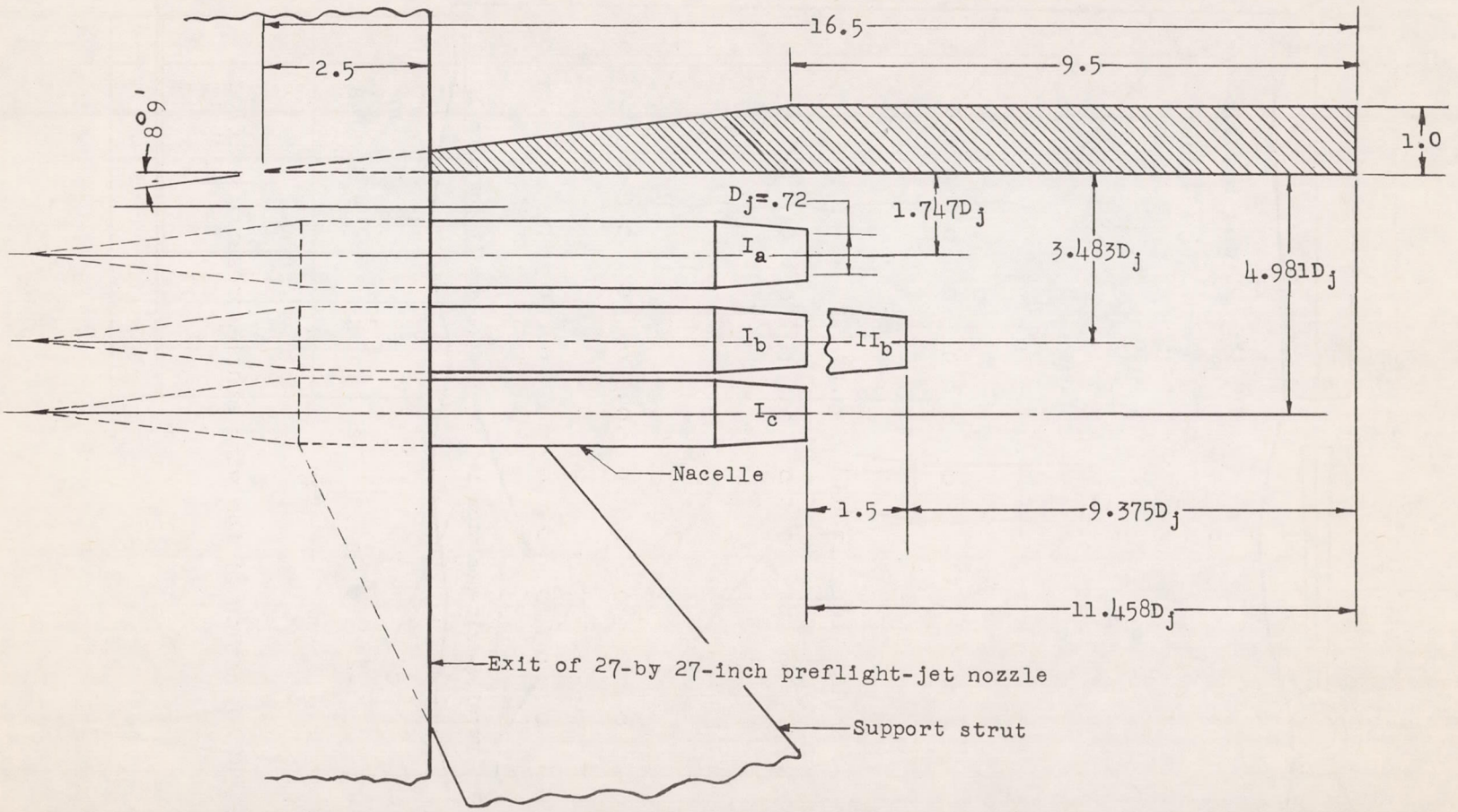


Figure 3.- Arrangement of the nacelle relative to the exit of the 27- by 27-inch preflight-jet nozzle and wing for the four test positions. Dimensions are in inches except as otherwise noted.

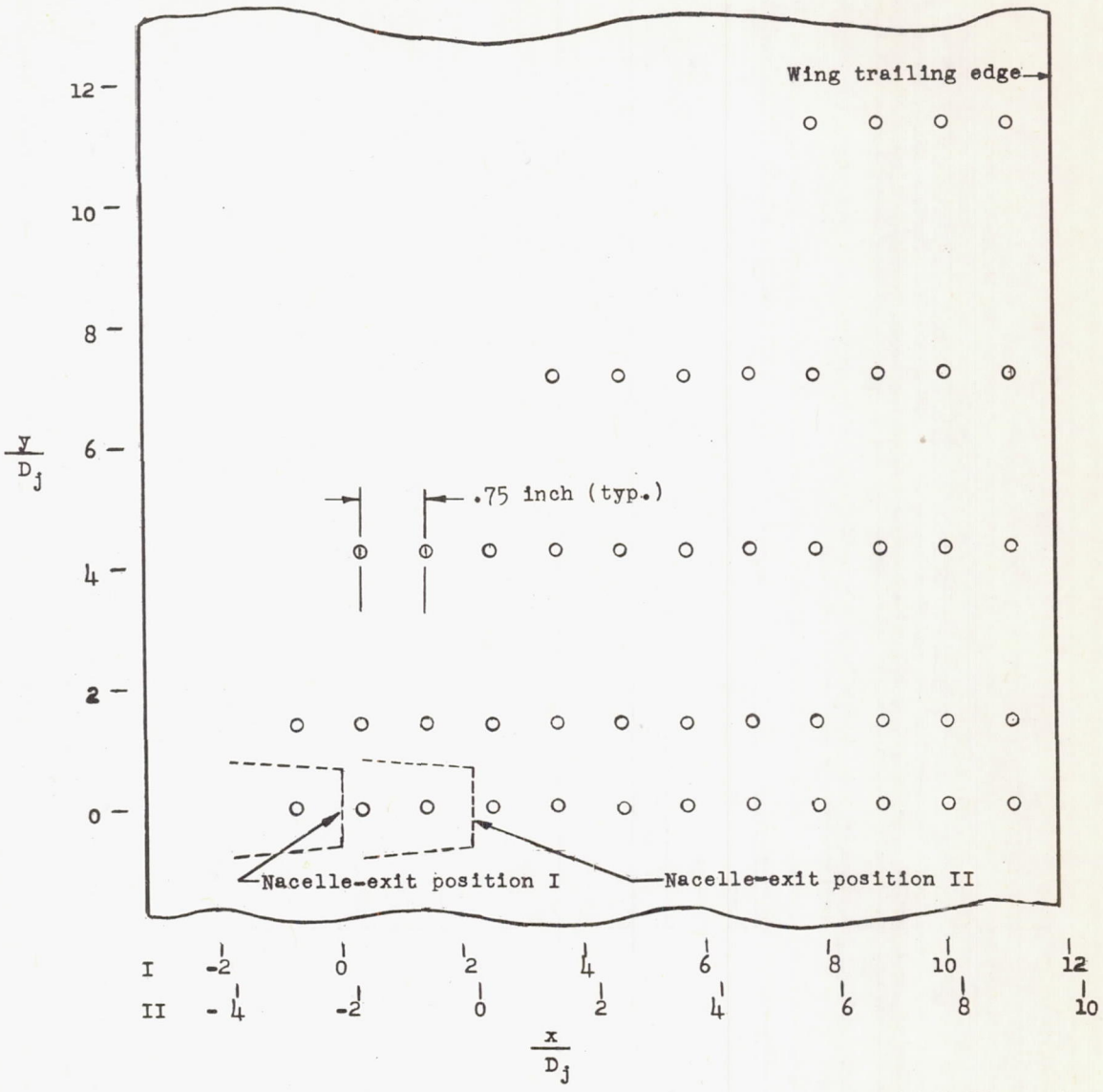


Figure 4.- Location of the wing static-pressure orifices.

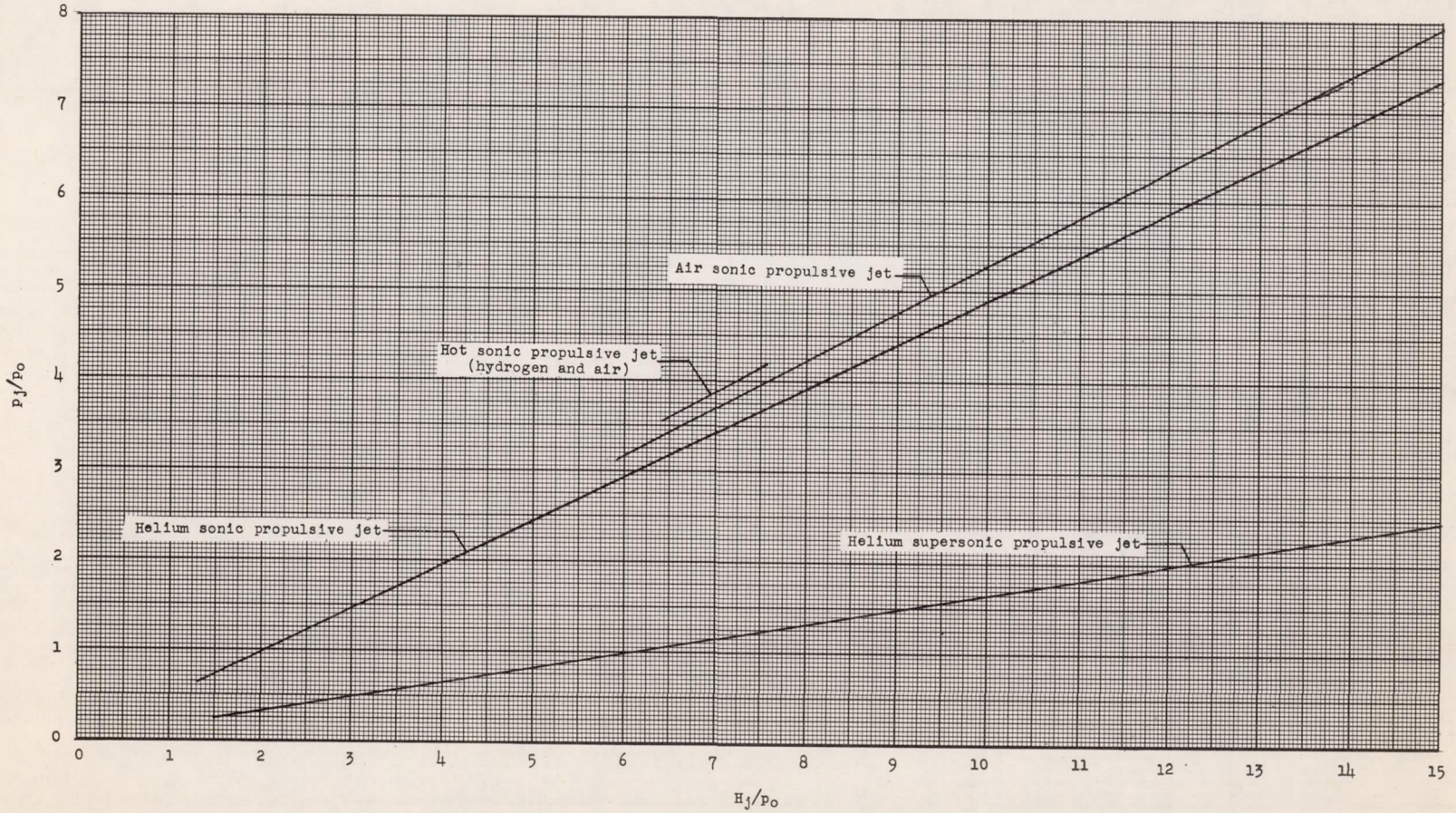
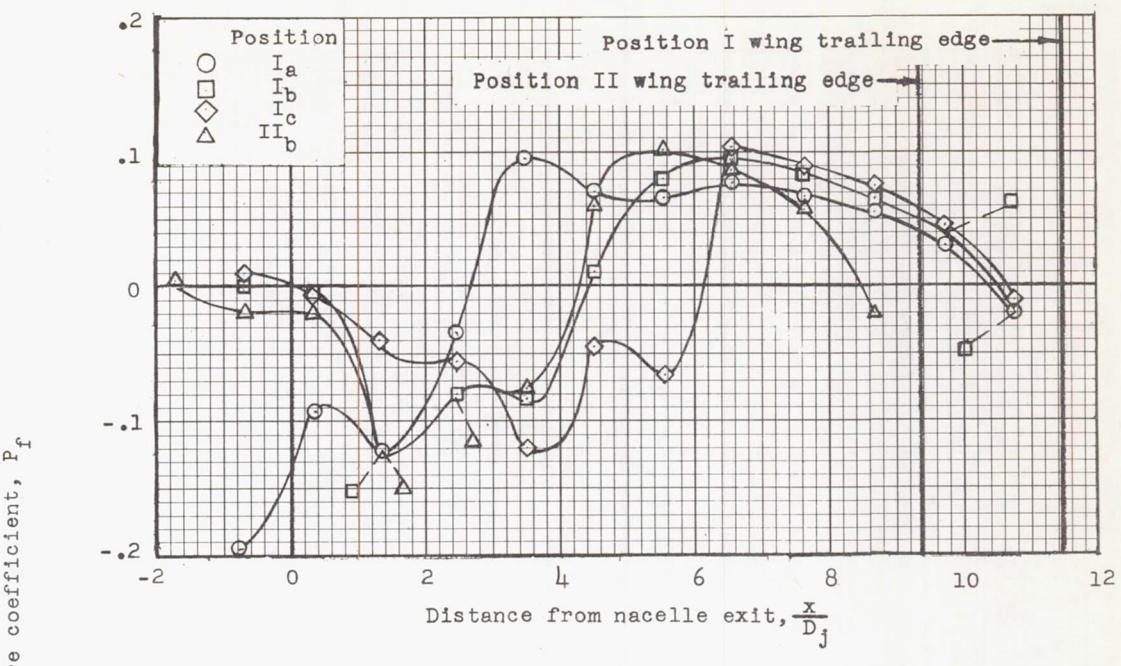
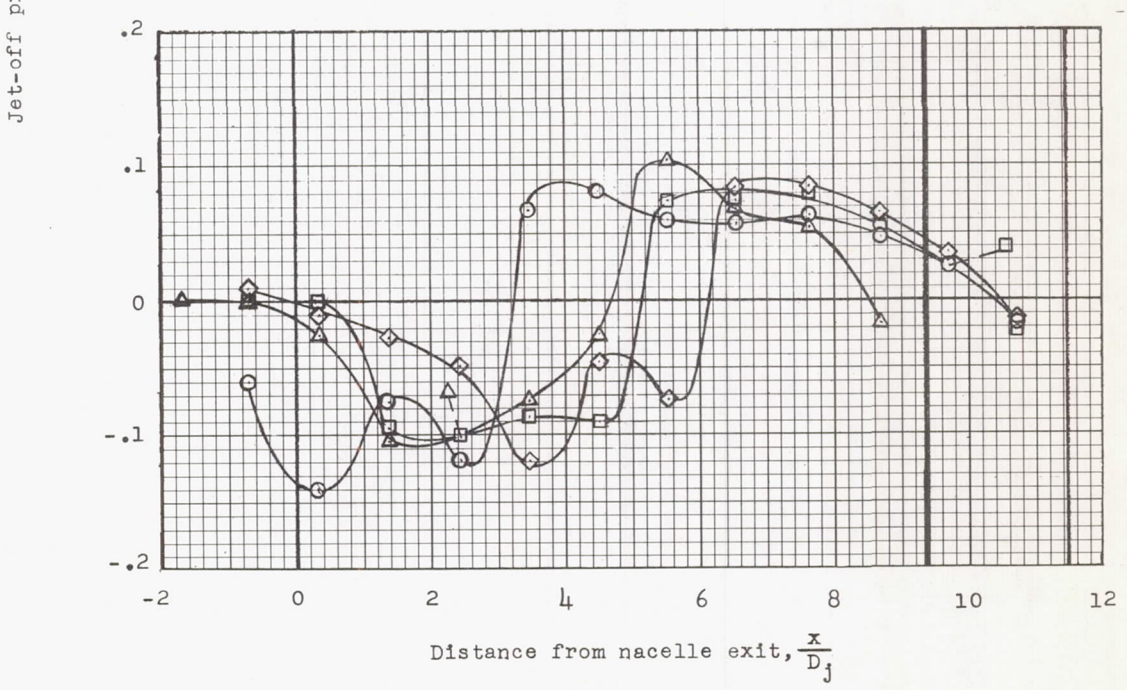


Figure 5.- Variation of static-pressure ratio with total-pressure ratio for all propulsive jets tested.

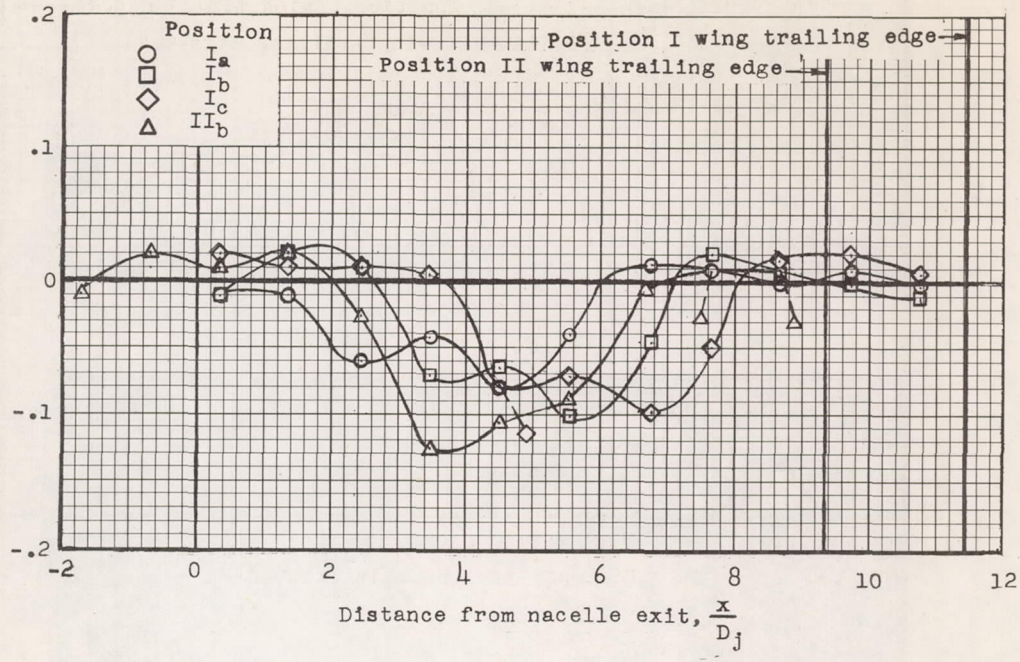


(a) Along nacelle center line.

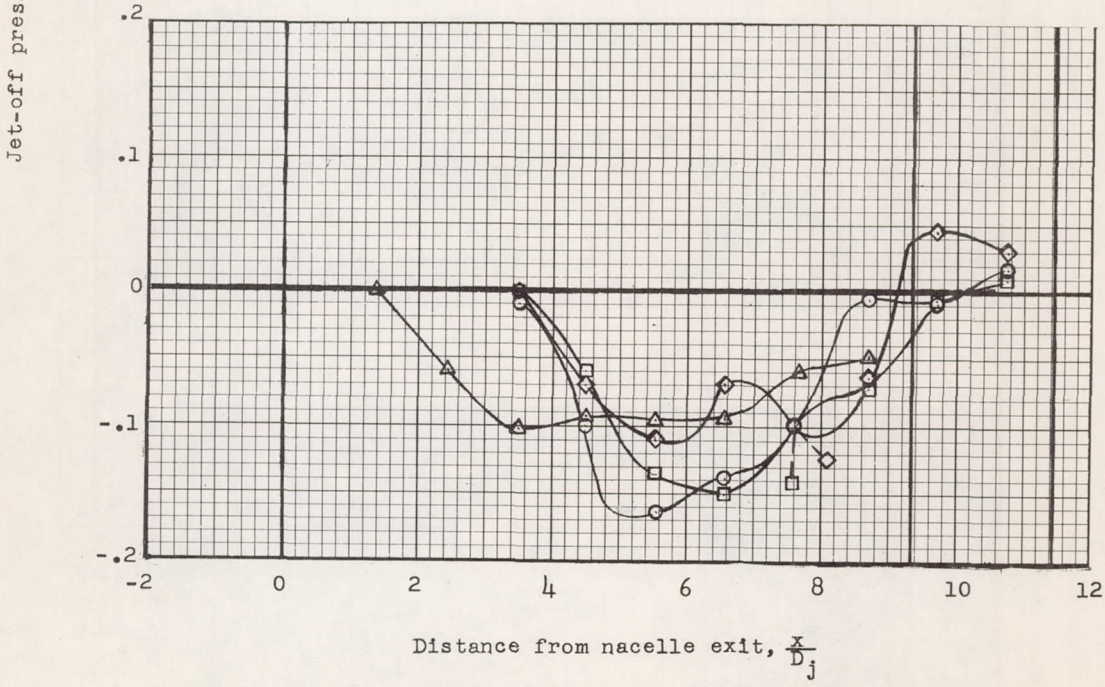


(b) $1.40D_j$ spanwise from nacelle center line.

Figure 6.- Chordwise variation of jet-off pressure coefficients for all test positions.

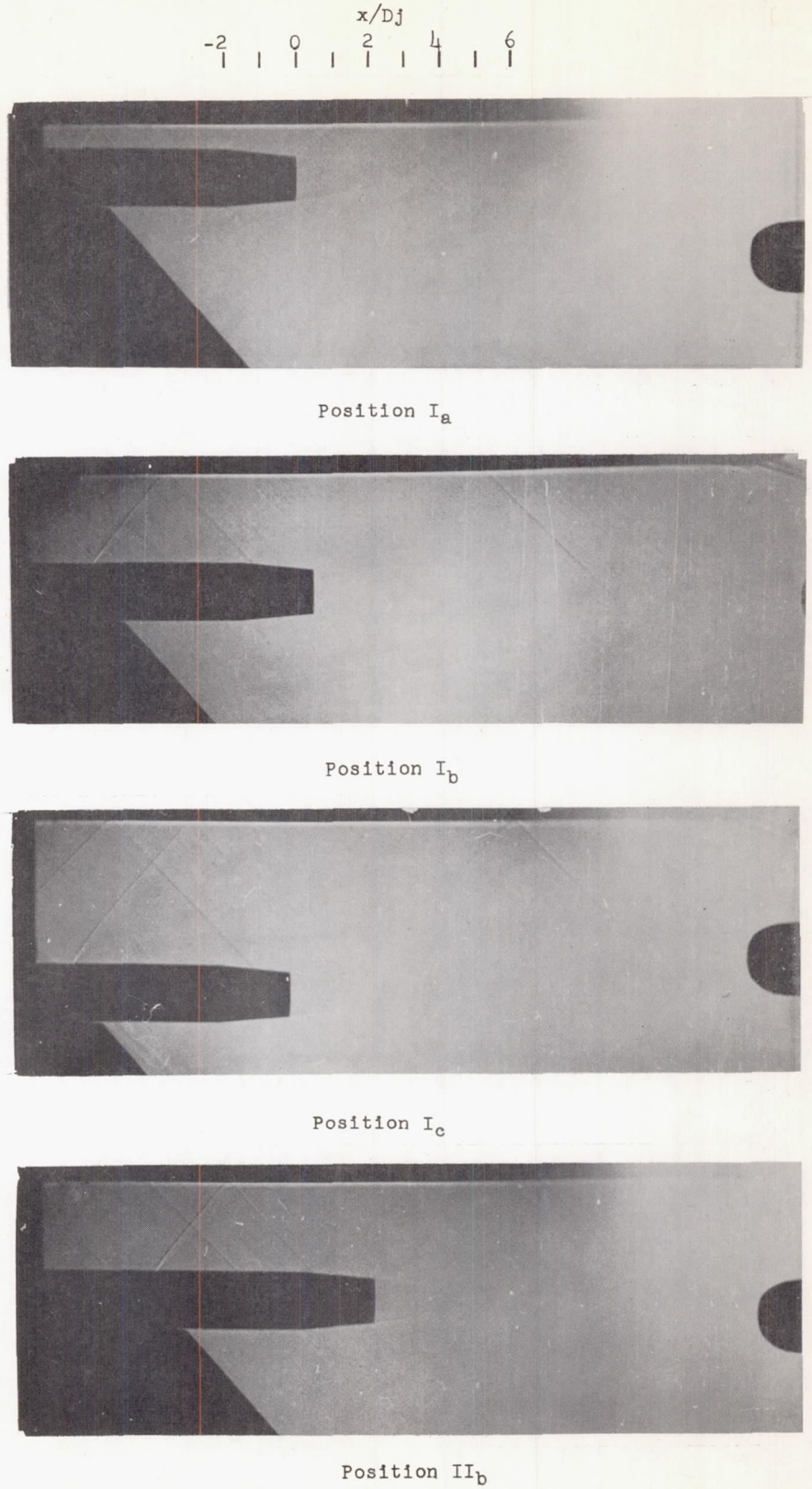


(c) $4.17D_j$ spanwise from nacelle center line.



(d) $6.94D_j$ spanwise from nacelle center line.

Figure 6.- Concluded.



L-91682

Figure 7.- Shadowgraph pictures of the flow field about the nacelle exit with jet off for test positions I_a, I_b, I_c, and II_b.

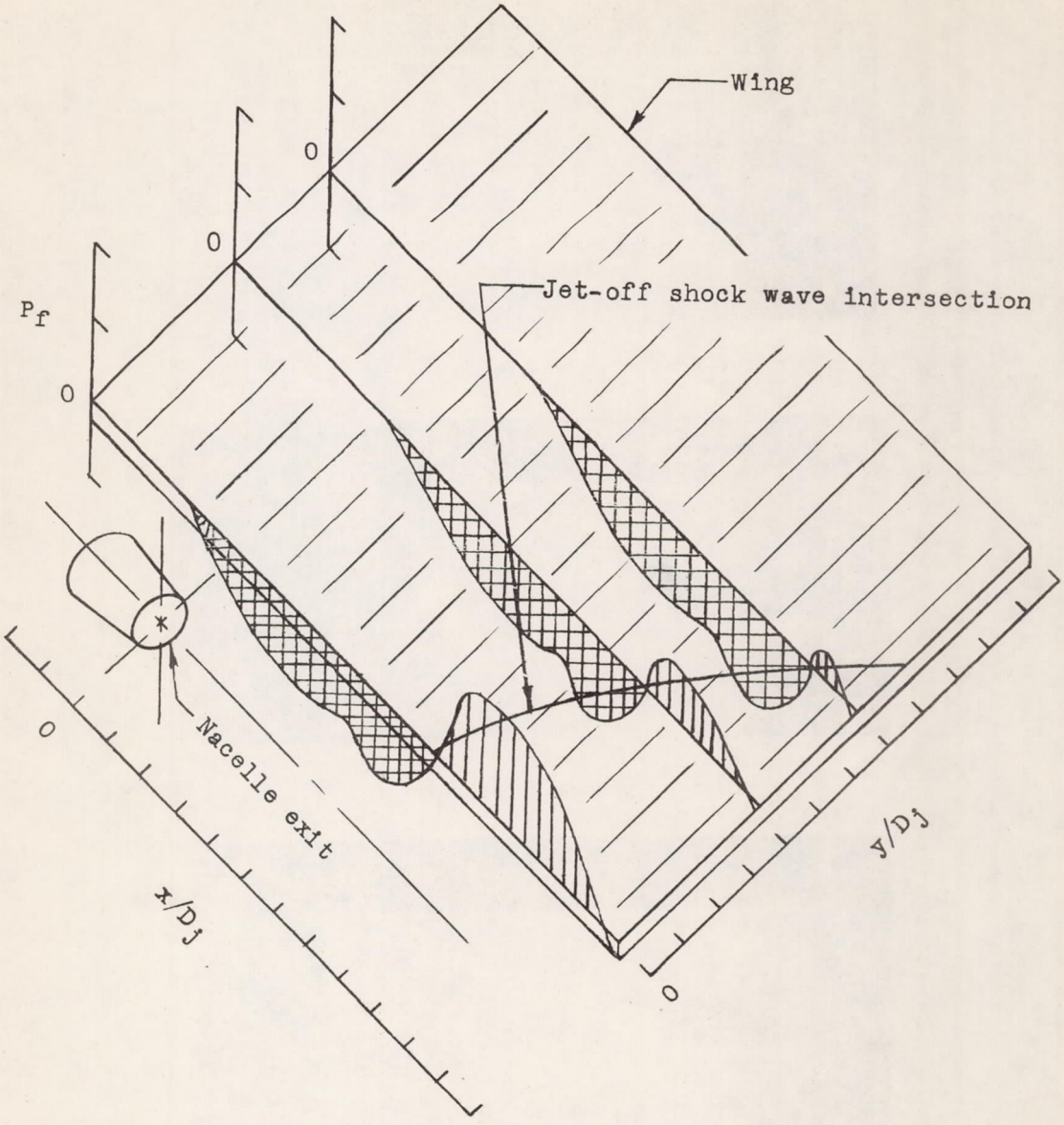
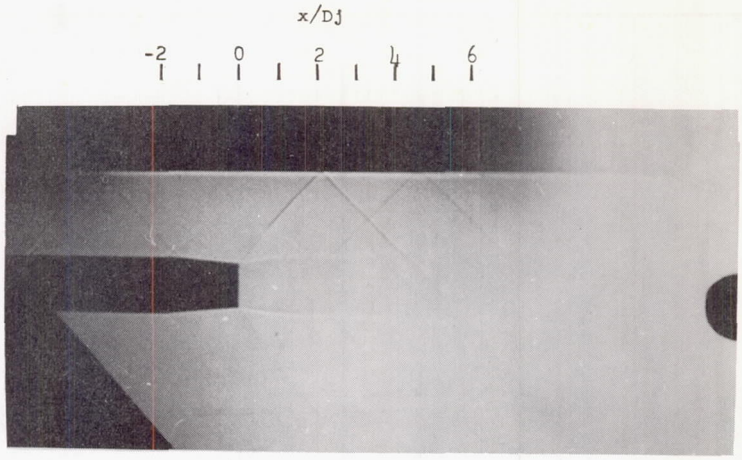
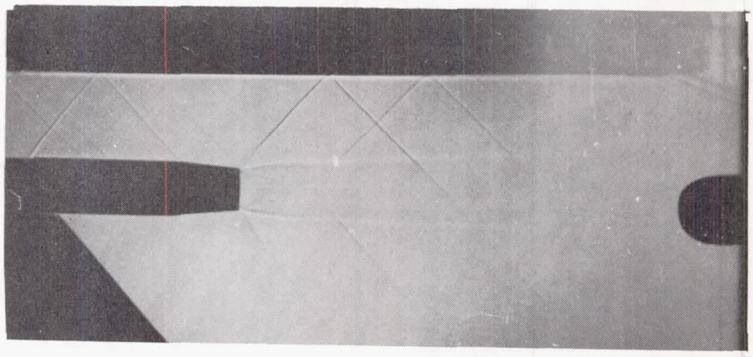


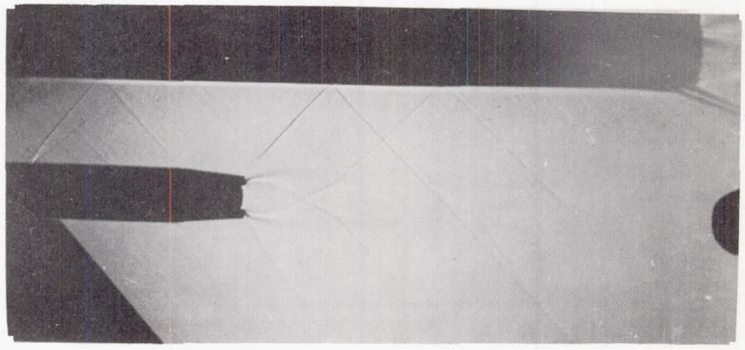
Figure 8.- Typical jet-off pressure field on the wing.



(a) Hot propulsive jet, $p_j/p_o = 3.87$



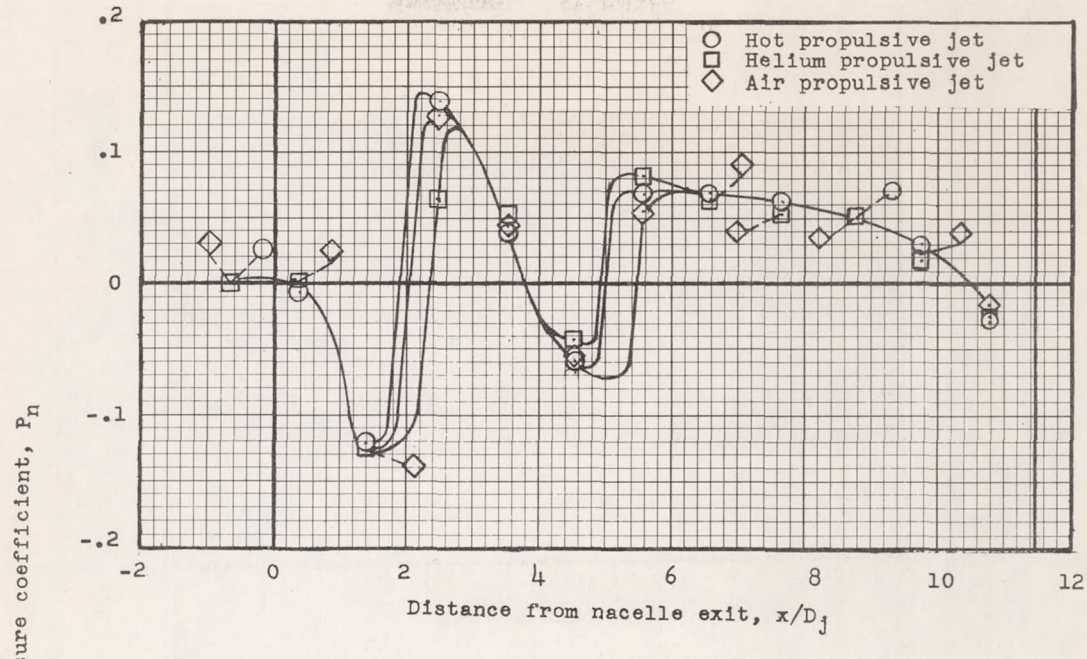
(b) Helium propulsive jet, $p_j/p_o = 3.42$



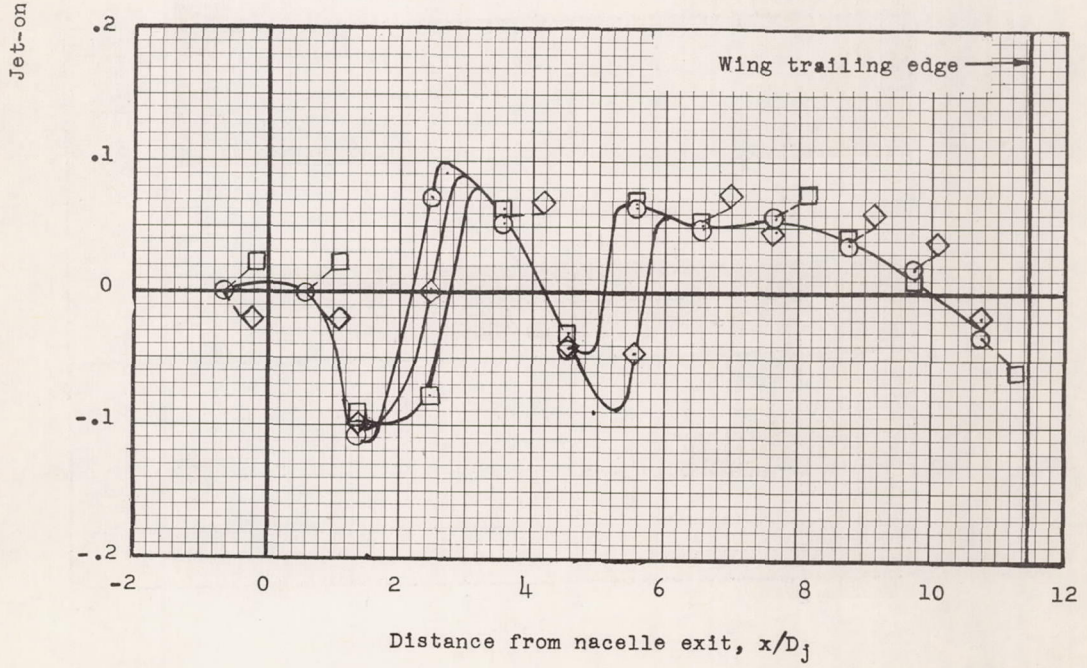
(c) Air propulsive jet, $p_j/p_o = 3.69$

L-91683

Figure 9.- Shadowgraph pictures of the flow field about the nacelle exit for a total-pressure ratio of 7 at test position I_b.

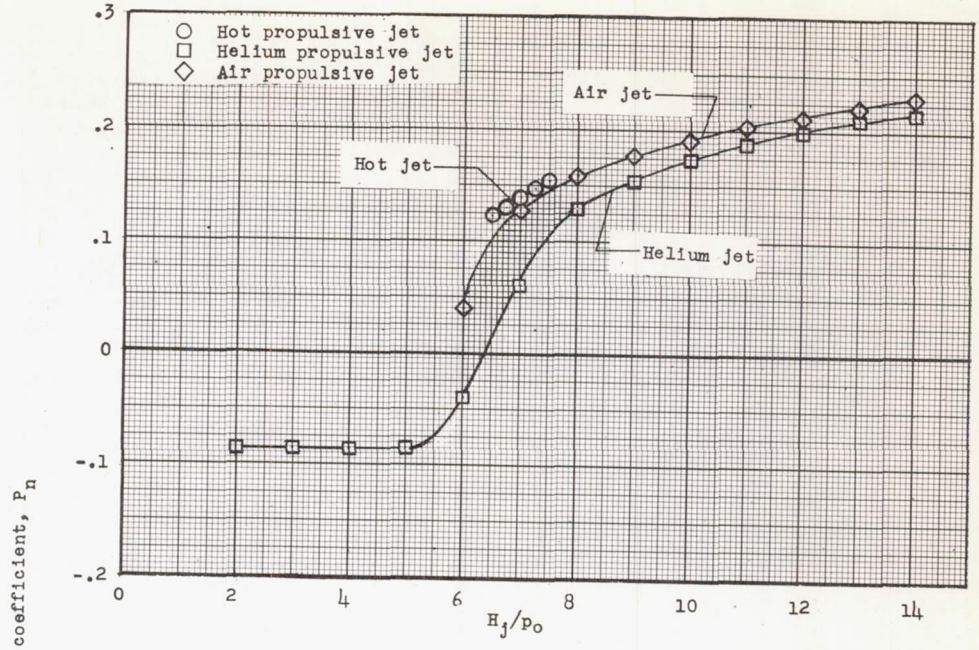


(a) Along nacelle center line.

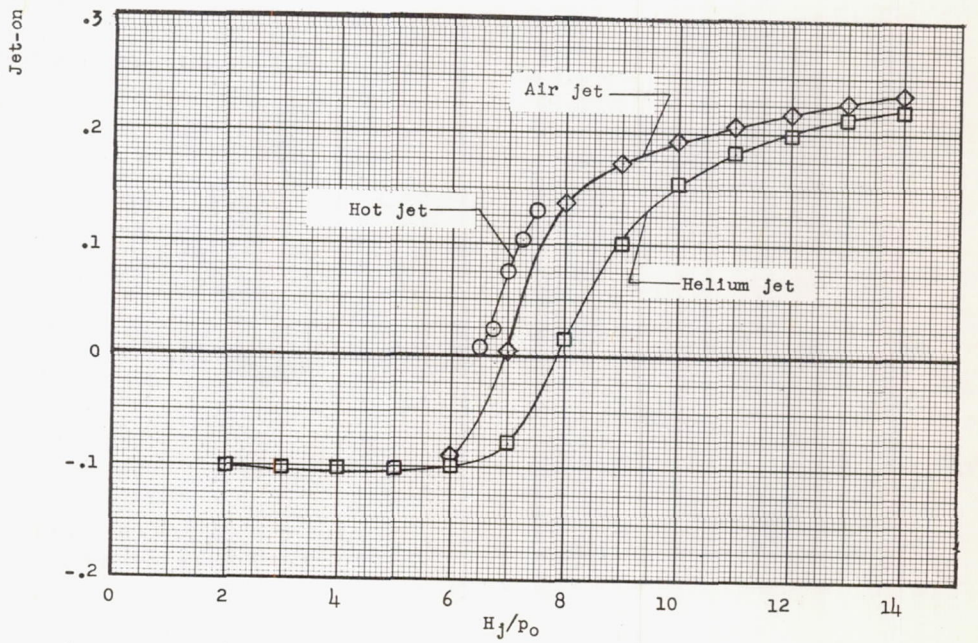


(b) $1.40D_j$ spanwise from nacelle center line.

Figure 10.- Chordwise variation of jet-on pressure coefficients at test position I_b for two wing spanwise positions from both hot and cold propulsive jets at a nacelle-exit total-pressure ratio of 7.

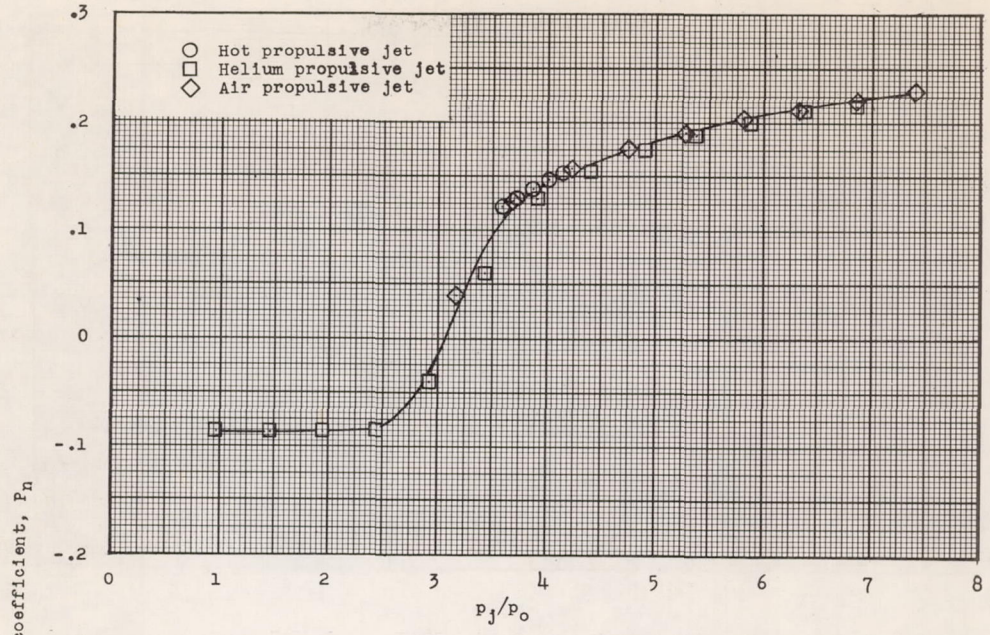


(a) At nacelle center line.

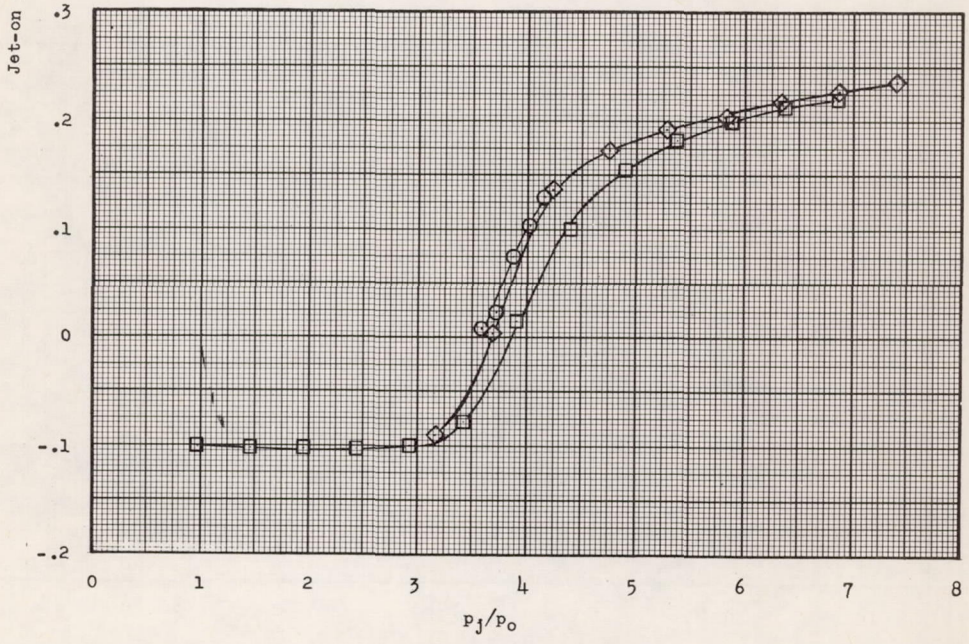


(b) At $1.40D_j$ spanwise from nacelle center line.

Figure 11.- Variation of jet-on pressure coefficient with nacelle-exit total-pressure ratio for the orifices located 2.43 jet diameters behind the exit at test position I_b from both hot and cold propulsive jets.

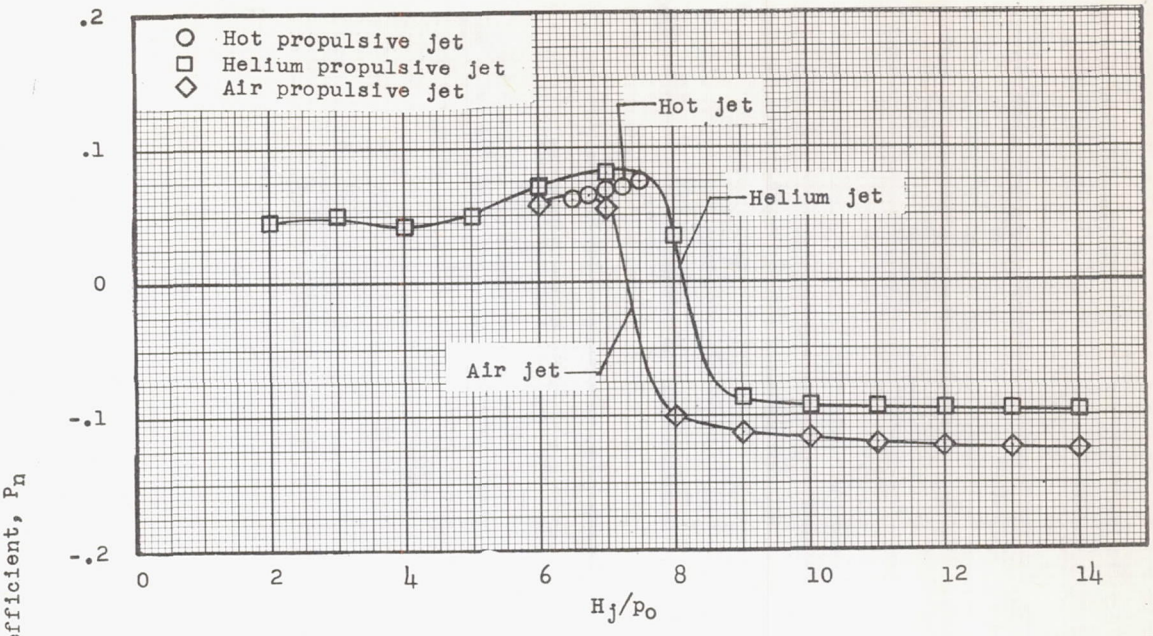


(a) At nacelle center line.

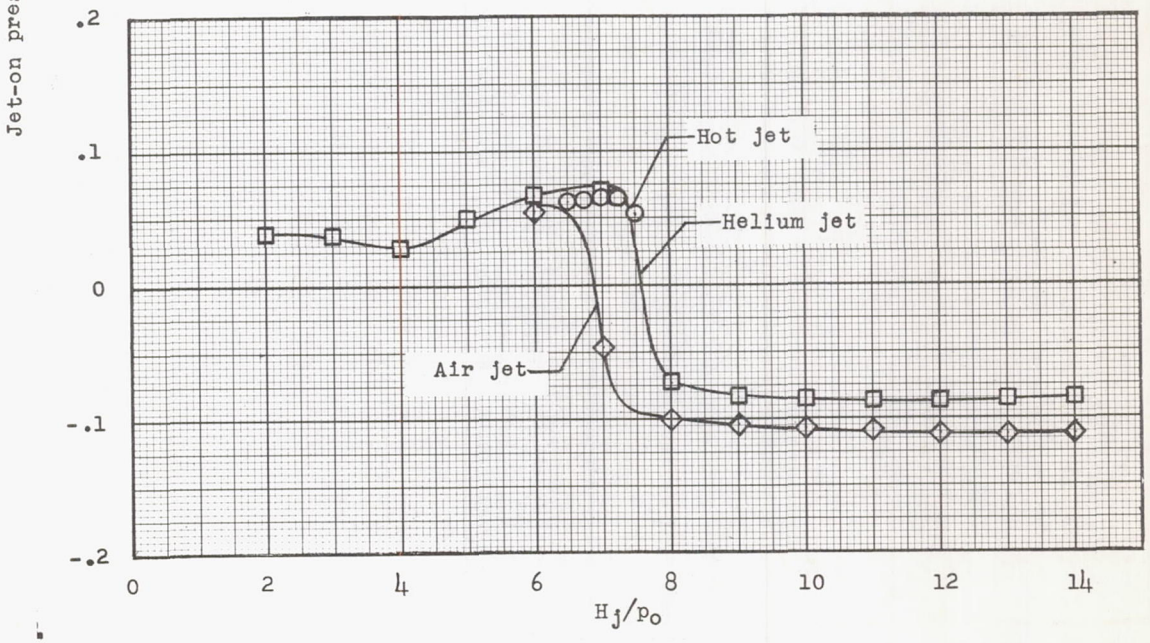


(b) At $1.40D_j$ spanwise from nacelle center line.

Figure 12.- Variation of jet-on pressure coefficient with nacelle-exit static-pressure ratio for the orifices located 2.43 jet diameters behind the exit at test position I_b from both hot and cold propulsive jets.



(a) At nacelle center line.



(b) At $1.40D_j$ spanwise from nacelle center line.

Figure 13.- Variation of jet-on pressure coefficient with nacelle-exit total-pressure ratio for the orifices located 5.55 jet diameters behind the exit at test position I_b from both hot and cold propulsive jets.

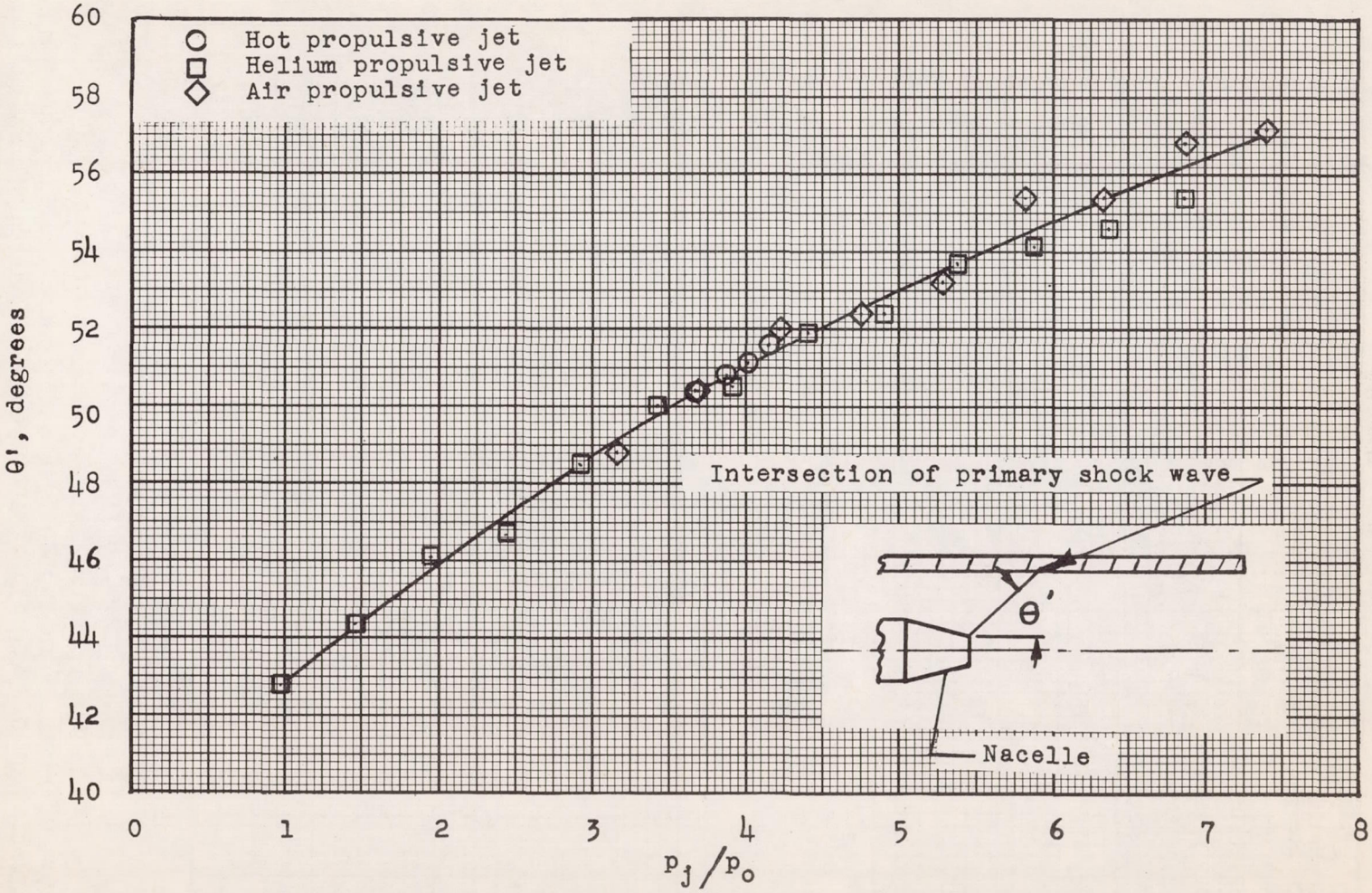
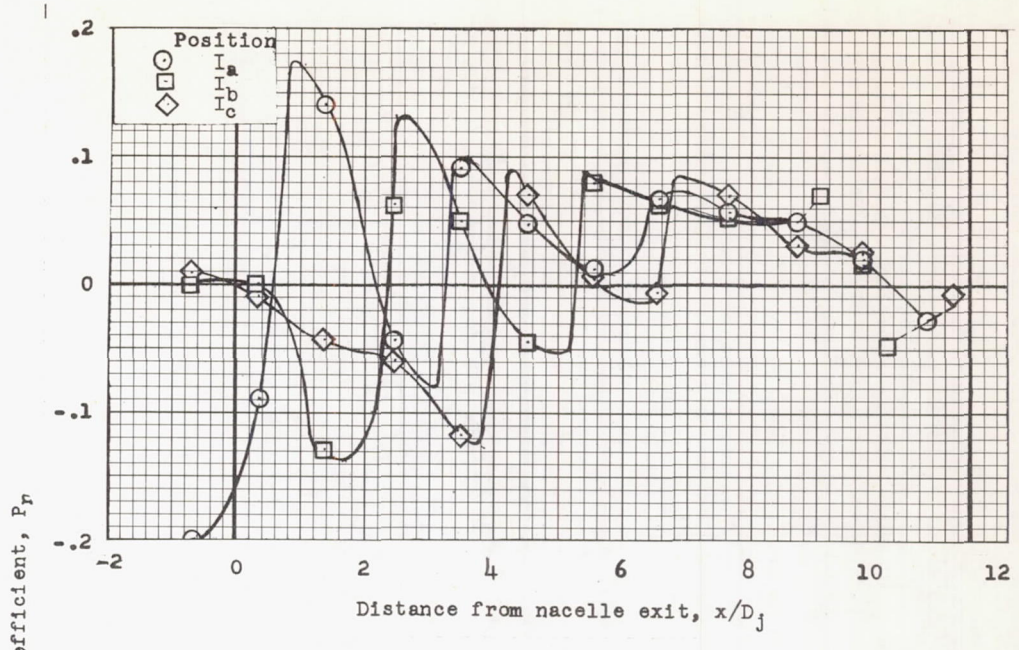
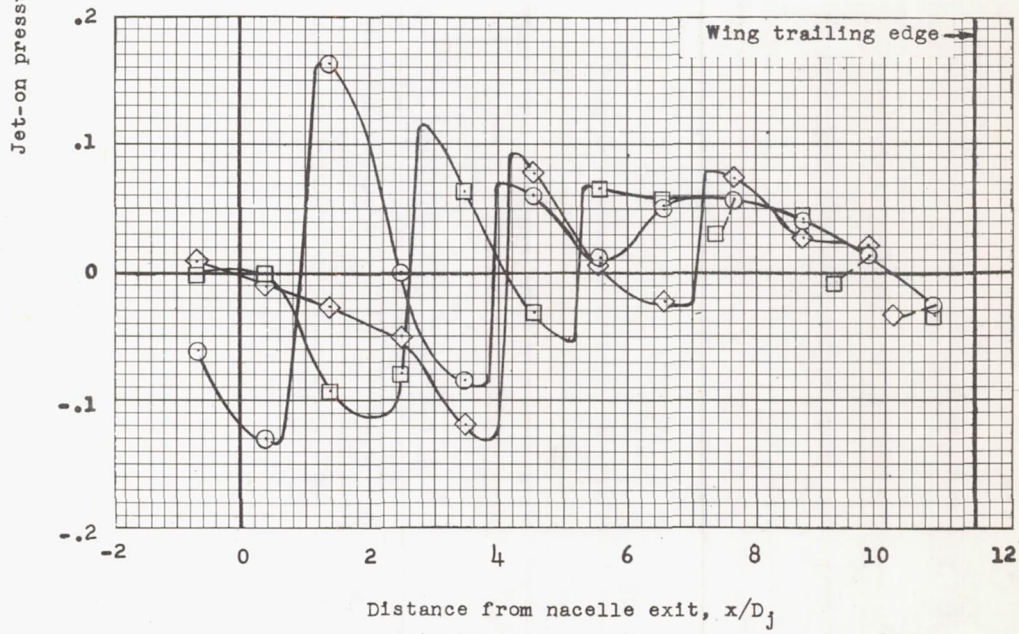


Figure 14.- Variation of the angle between the point of intersection on the wing of the primary shock wave and the nacelle exit with nacelle-exit static-pressure ratio for the three types of propulsive jets tested.

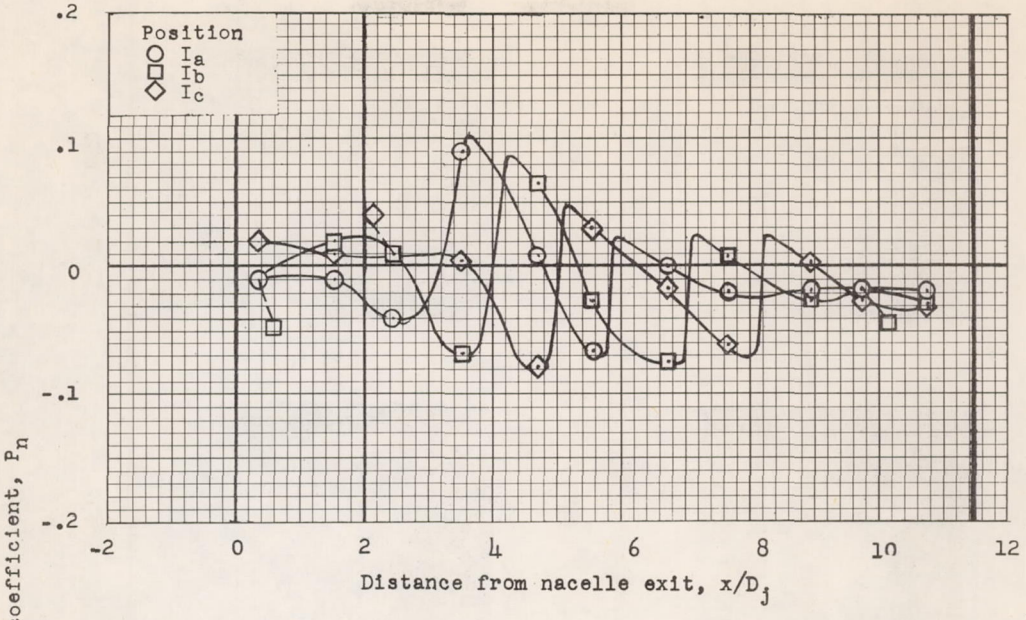


(a) Along nacelle center line.

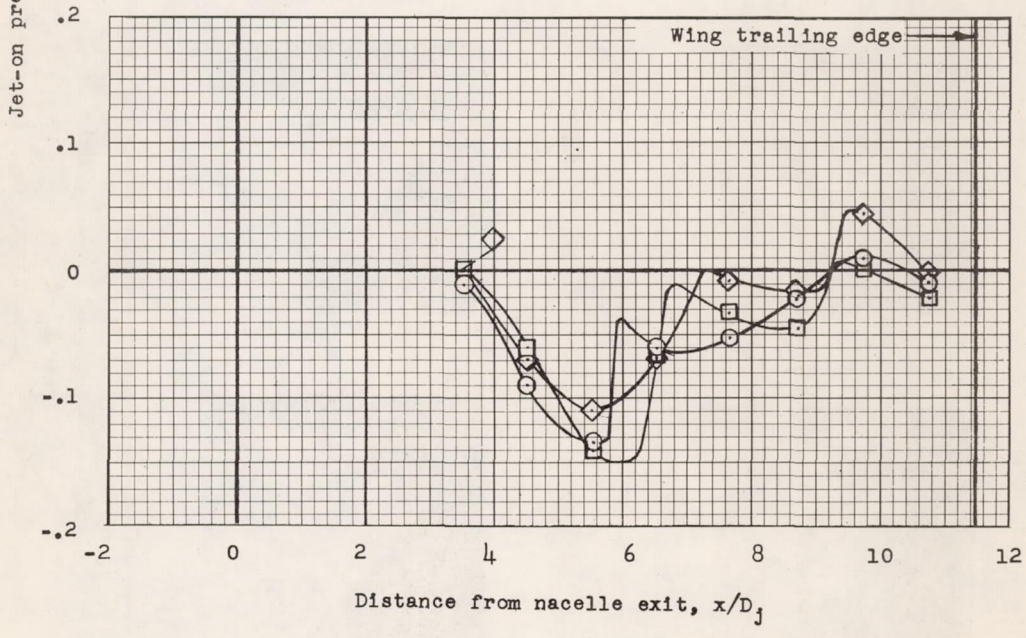


(b) $1.40D_j$ spanwise from nacelle center line.

Figure 15.- Chordwise variation of jet-on pressure coefficients for test positions I_a, I_b, and I_c using a cold helium propulsive jet at a nacelle-exit total-pressure ratio of 7.

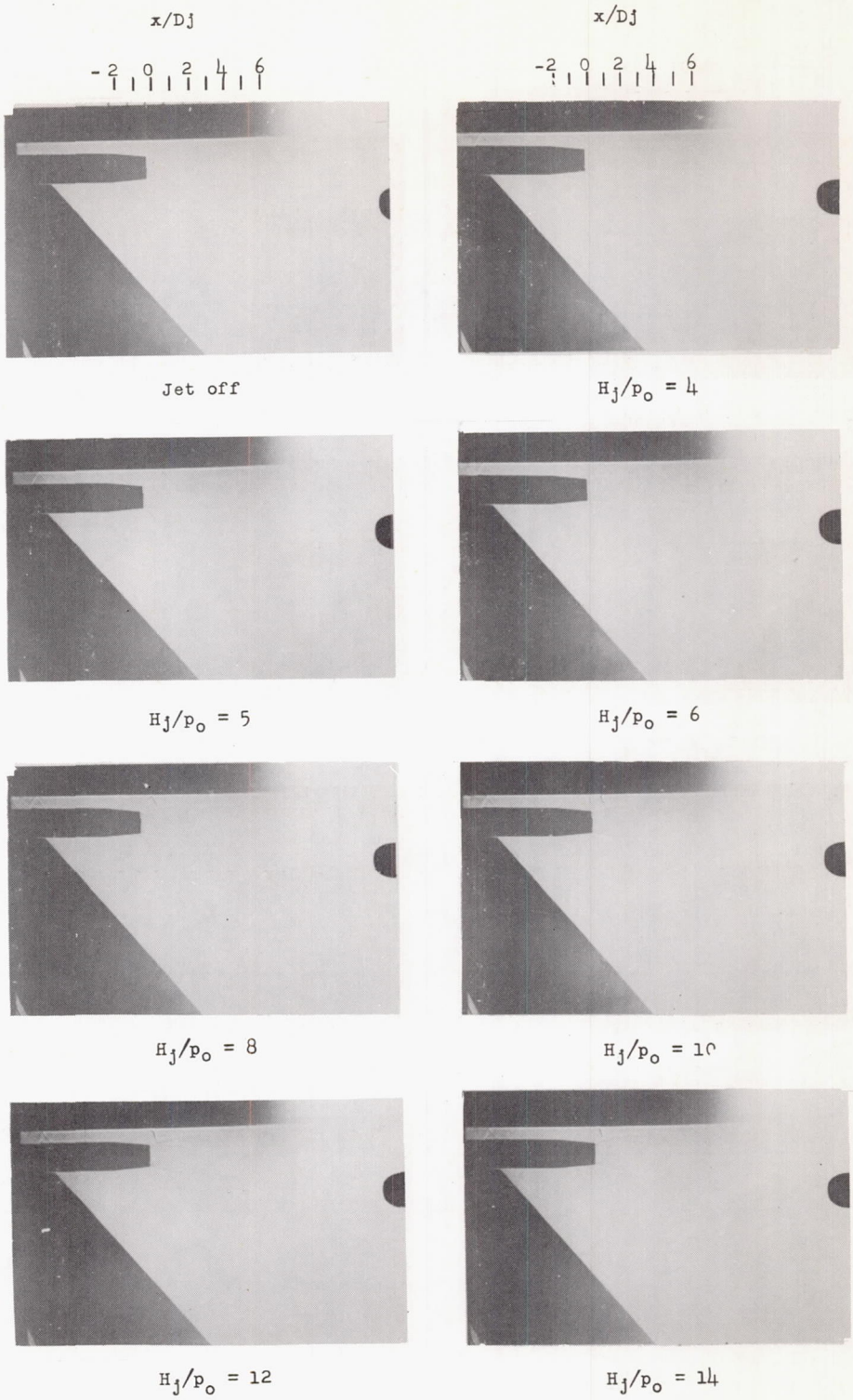


(c) $4.17D_j$ spanwise from nacelle center line.



(d) $6.94D_j$ spanwise from nacelle center line.

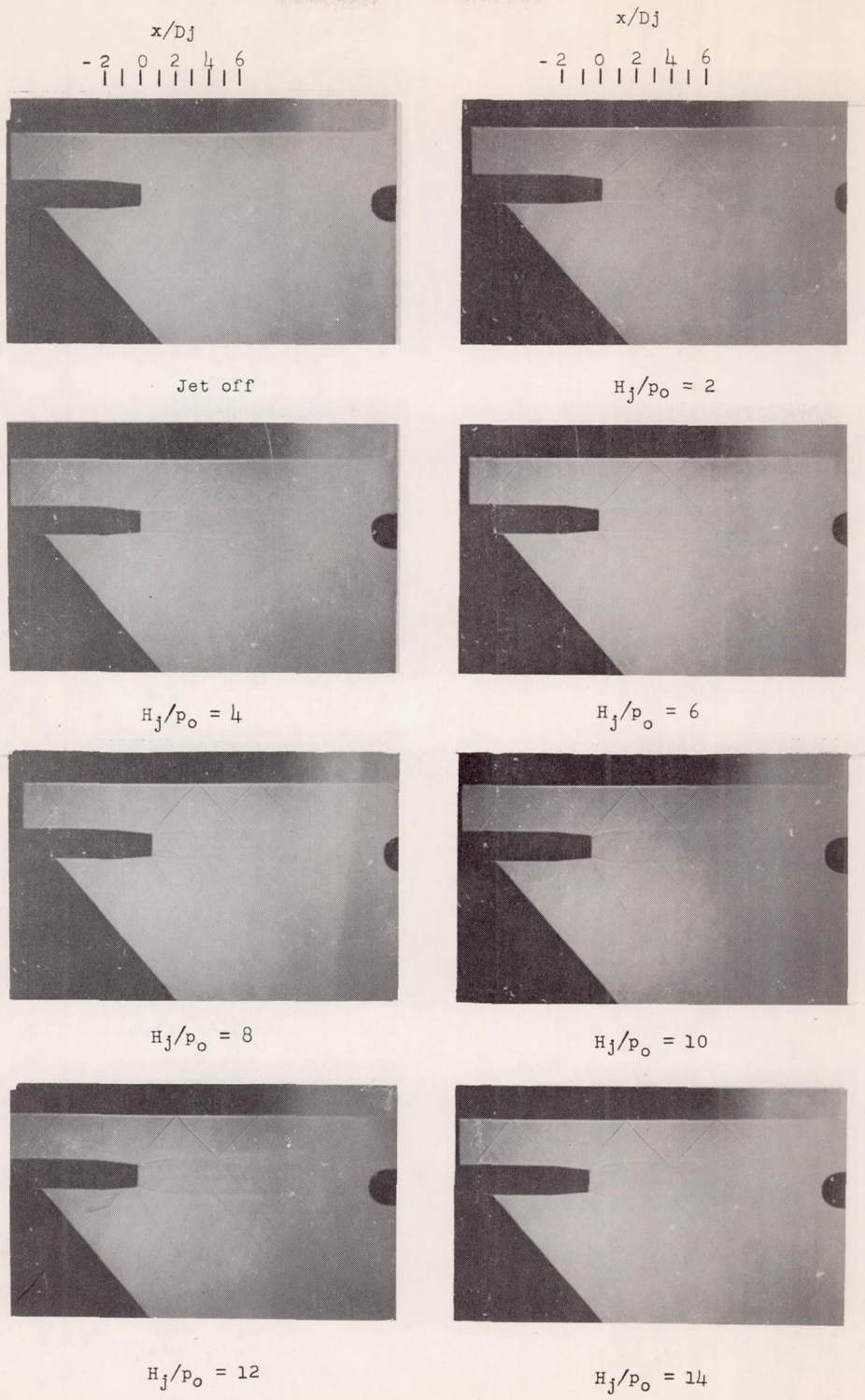
Figure 15.- Concluded.



(a) Position I_a.

L-91684

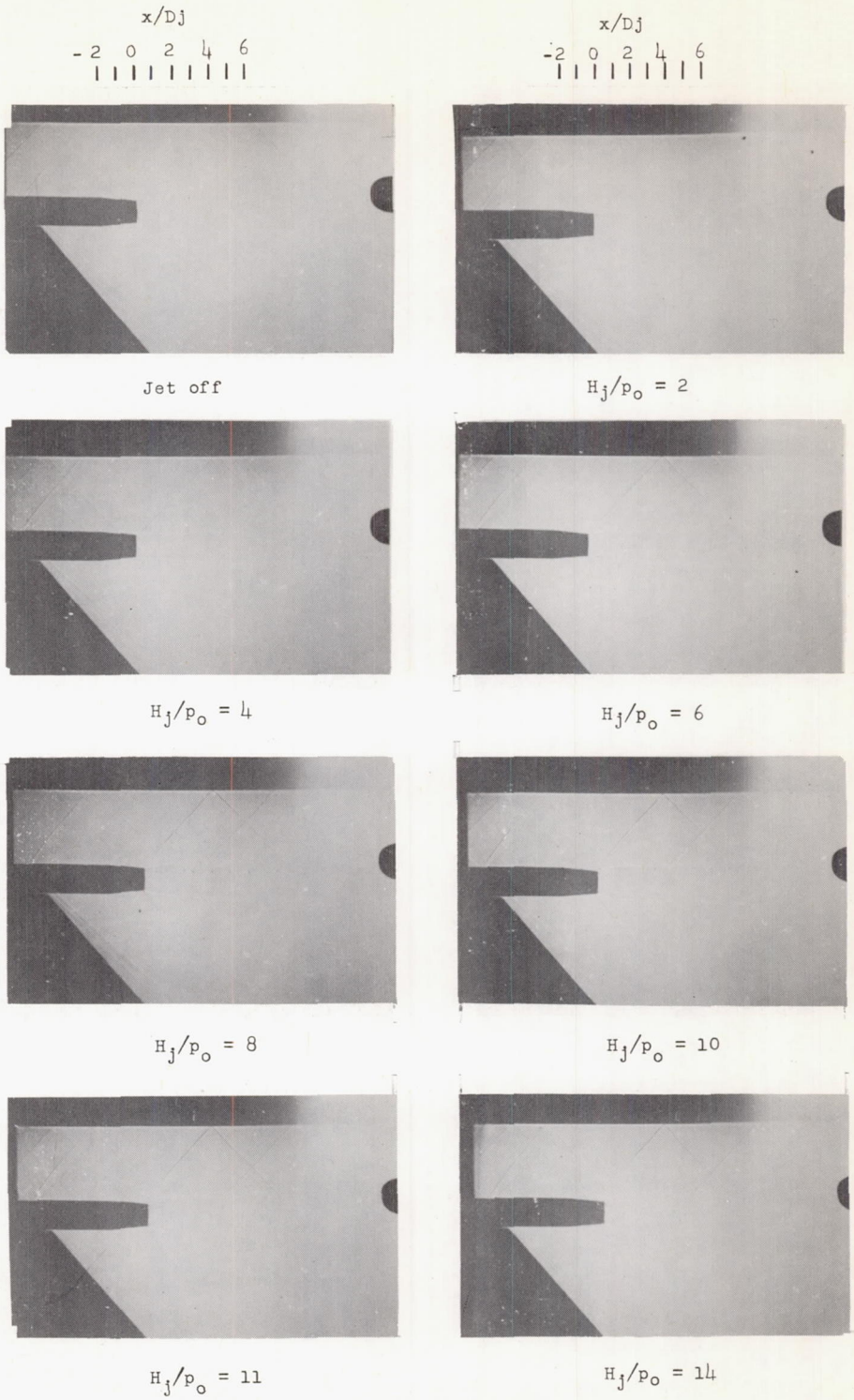
Figure 16.- Shadowgraph pictures of the flow field about the nacelle exit with jet on and jet off for test positions I_a, I_b, I_c, and II_b.



(b) Position I_b.

L-91685

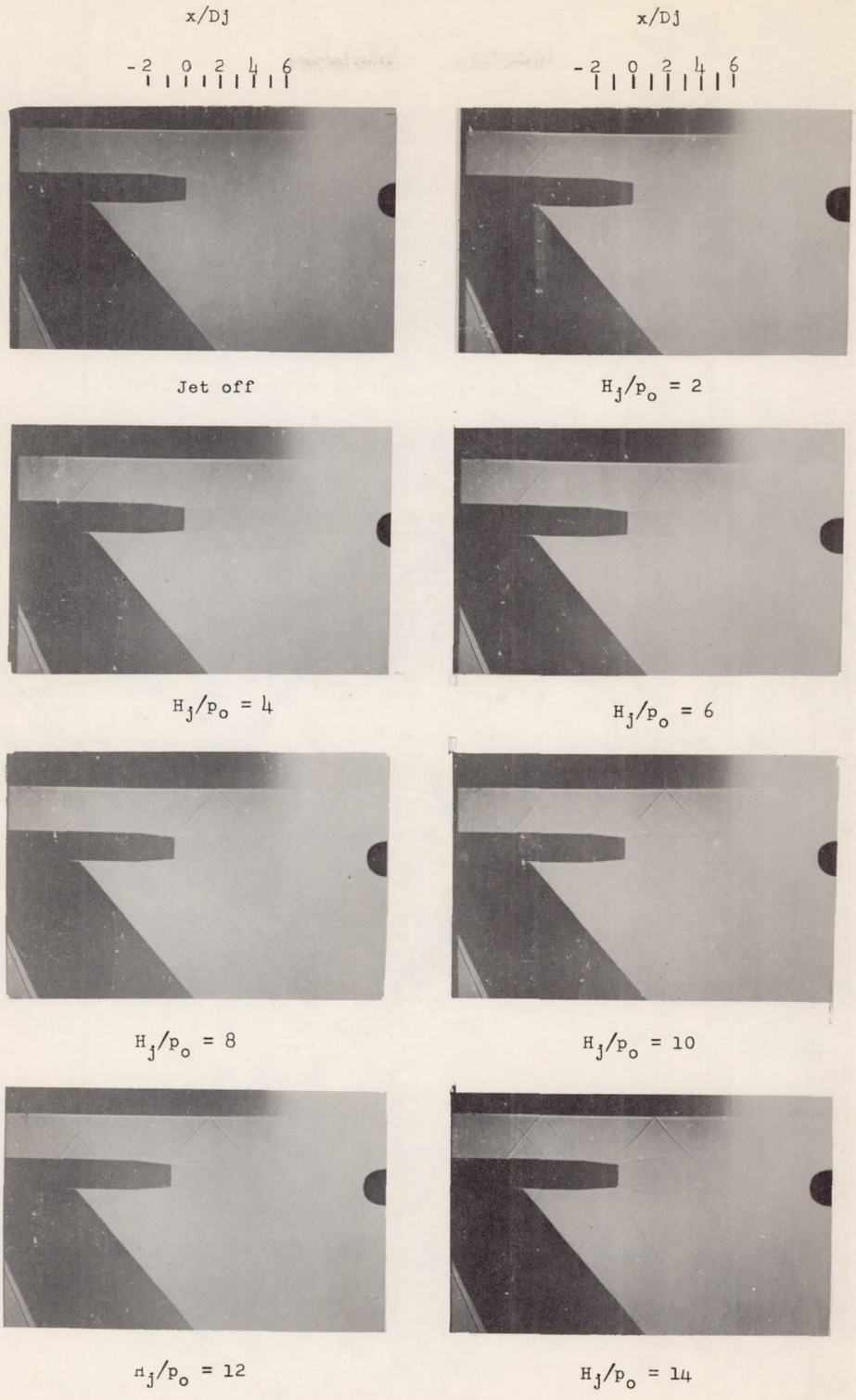
Figure 16.- Continued.



(c) Position I_c.

L-91686

Figure 16.- Continued.



(d) Position II_b.

L-91687

Figure 16.- Concluded.

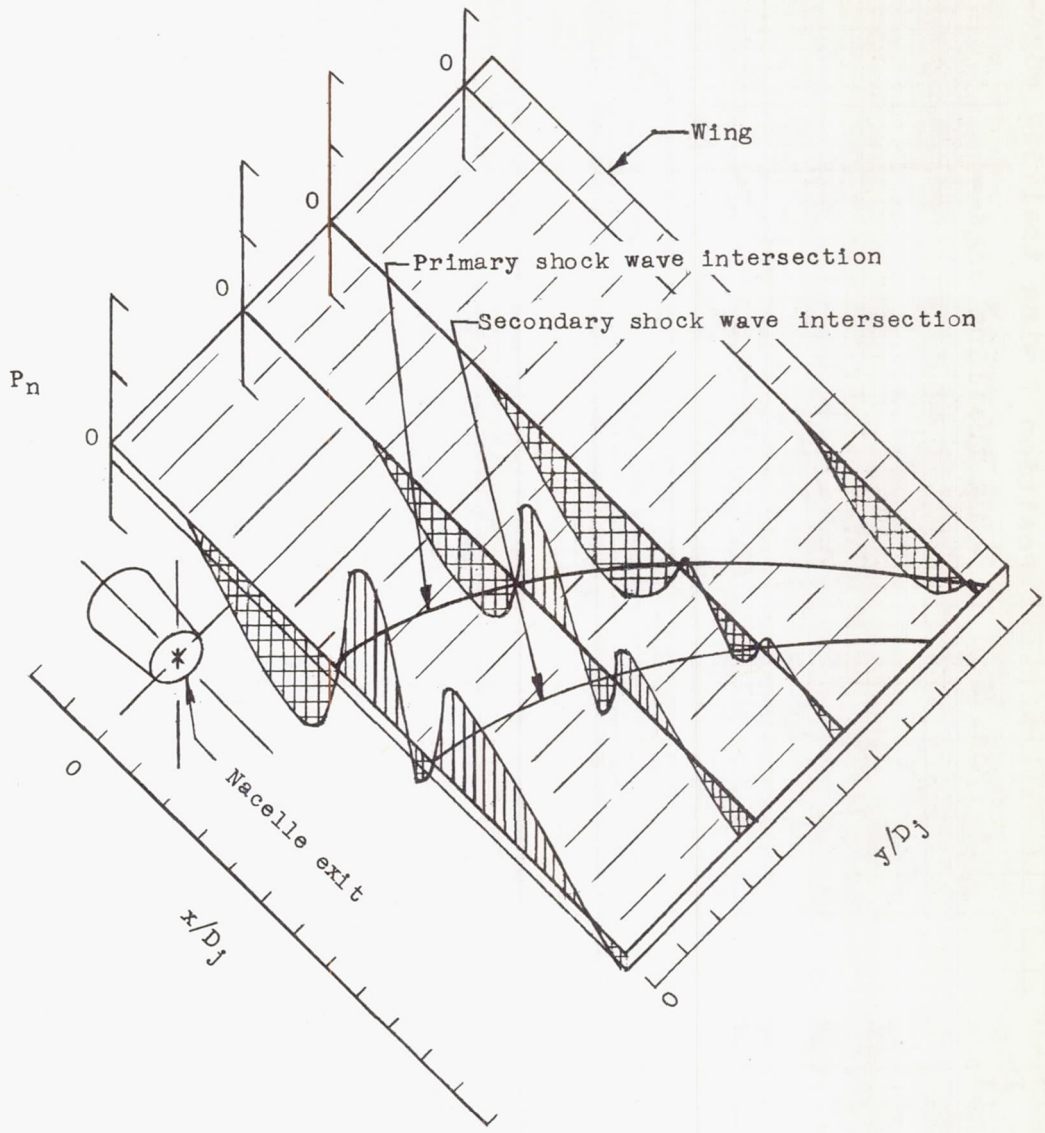


Figure 17.- Typical jet-on pressure field on the wing.

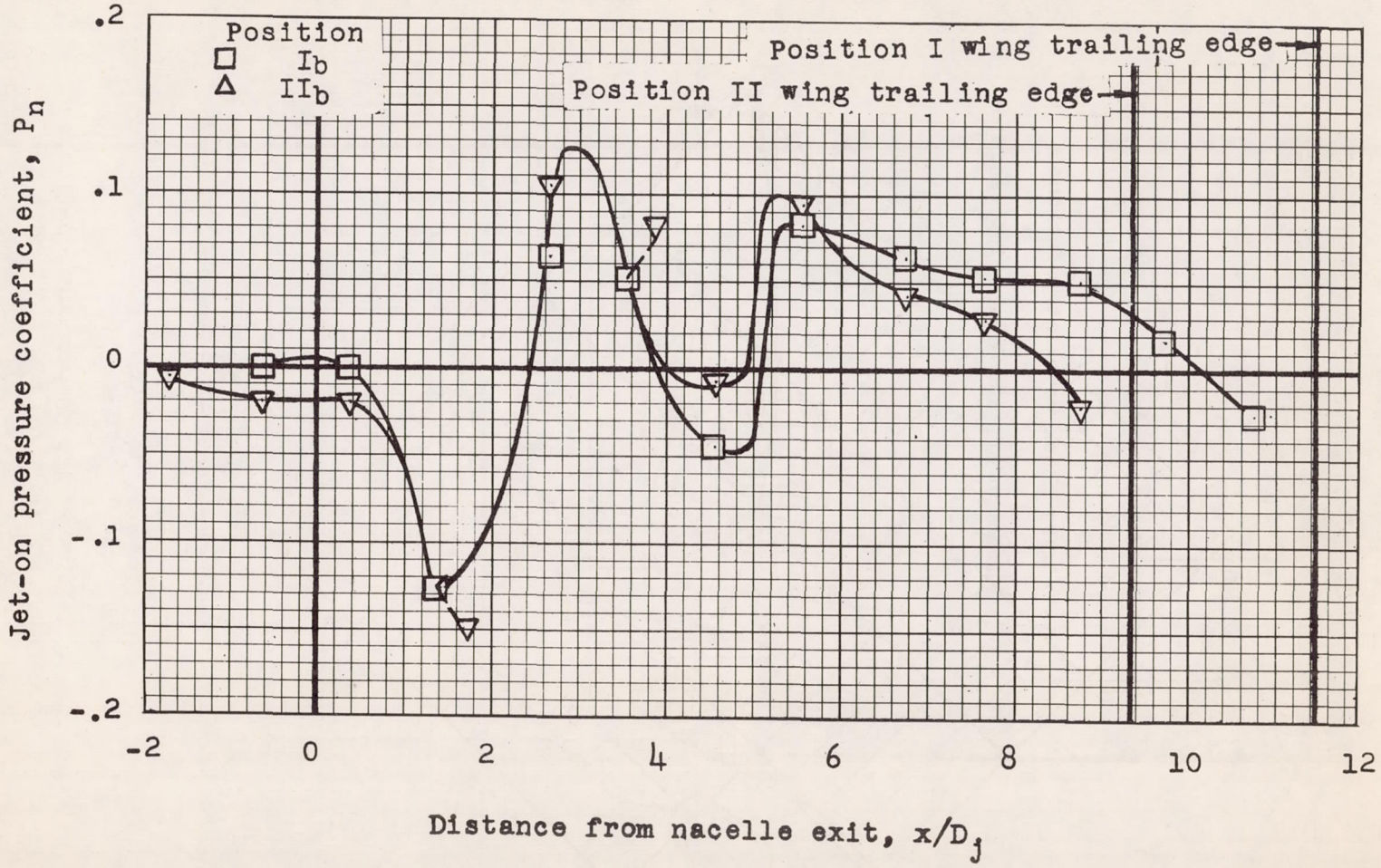
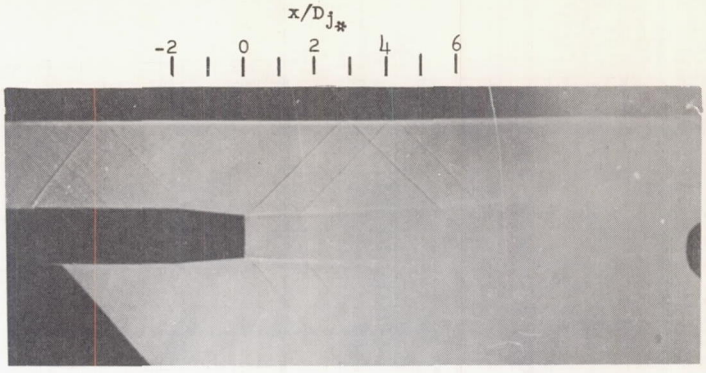
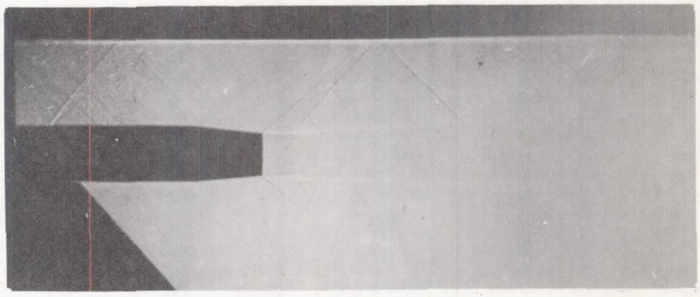


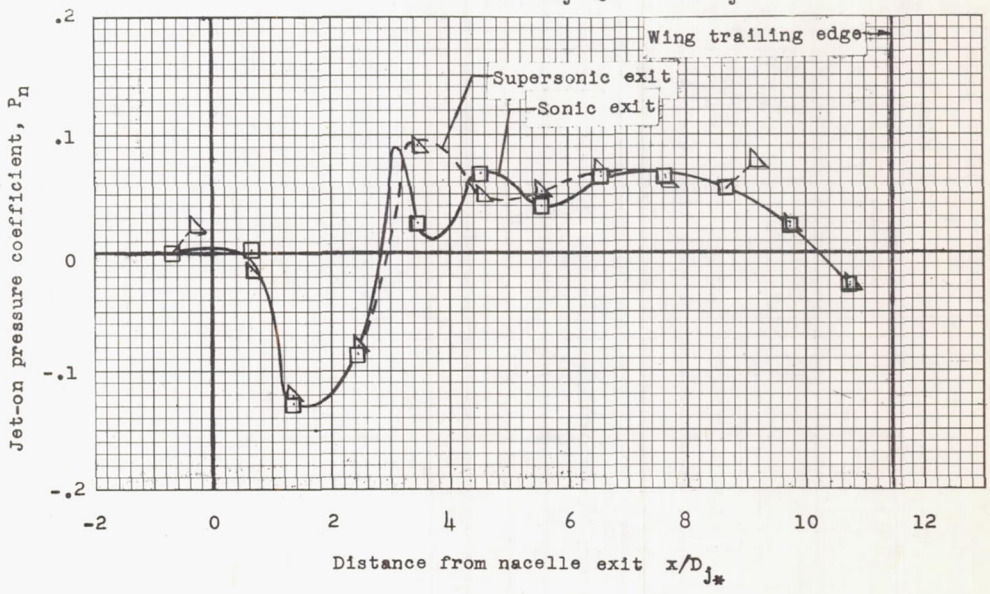
Figure 18.- Chordwise variation of jet-on pressure coefficient for test positions I_b and II_b at a nacelle-exit total-pressure ratio of 7 along the nacelle center line.



Sonic nacelle exit, $p_j/p_o = 1.96$, $M_j = 1.0$

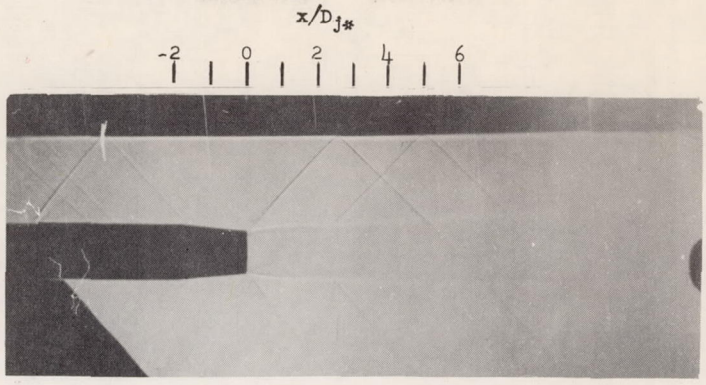


Supersonic nacelle exit, $p_j/p_o = 0.65$, $M_j = 1.79$ L-91688

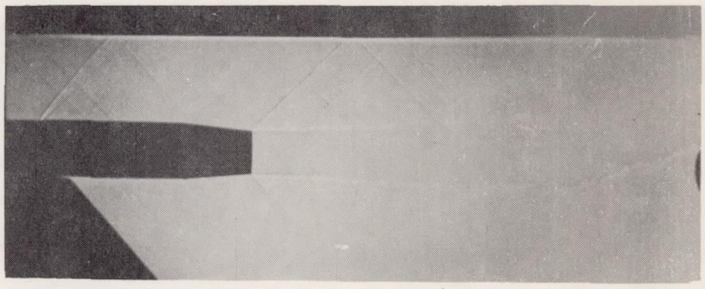


(a) $H_j/p_o = 4$.

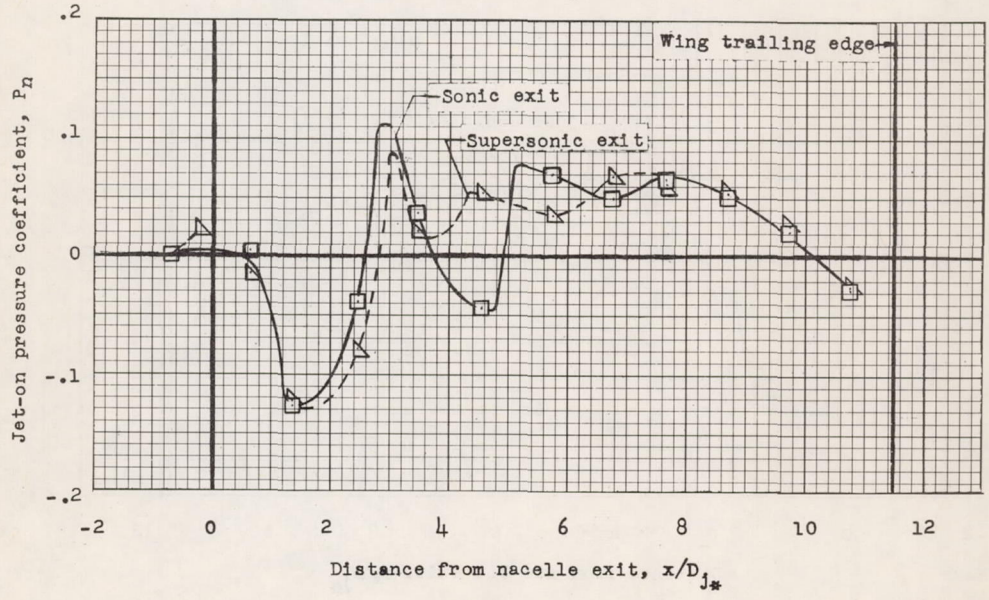
Figure 19.- Chordwise variation of jet-on pressure coefficients with shadowgraph pictures at test positions I_b for both sonic and supersonic nacelle exits at nacelle-exit total-pressure ratios of 4, 6, 8, 10, and 12 for the helium propulsive jet.



Sonic nacelle exit, $p_j/p_o = 2.94$, $M_j = 1.0$

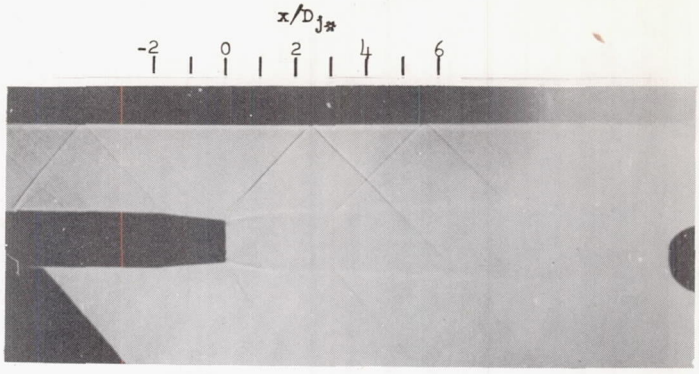


Supersonic nacelle exit, $p_j/p_o = 0.98$, $M_j = 1.79$ L-91689

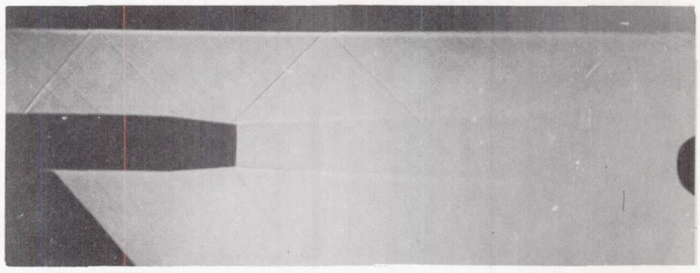


(b) $H_j/p_o = 6$.

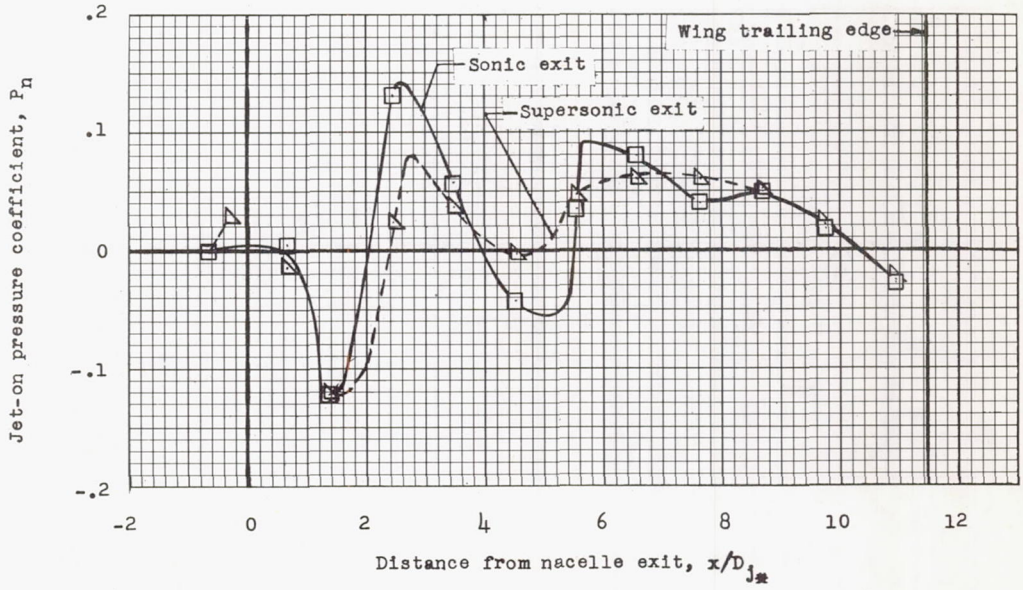
Figure 19.- Continued.



Sonic nacelle exit, p_j/p_o = 3.93, M_j = 1.0

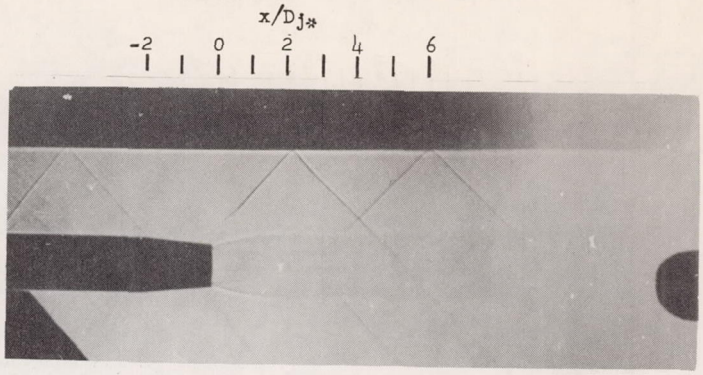


Supersonic nacelle exit, p_j/p_o = 1.30, M_j = 1.79 L-91700

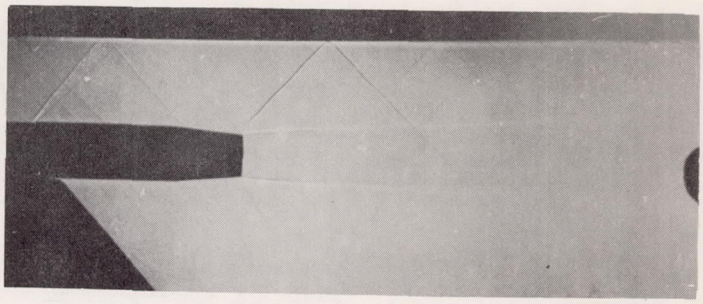


(c) H_j/p_o = 8.

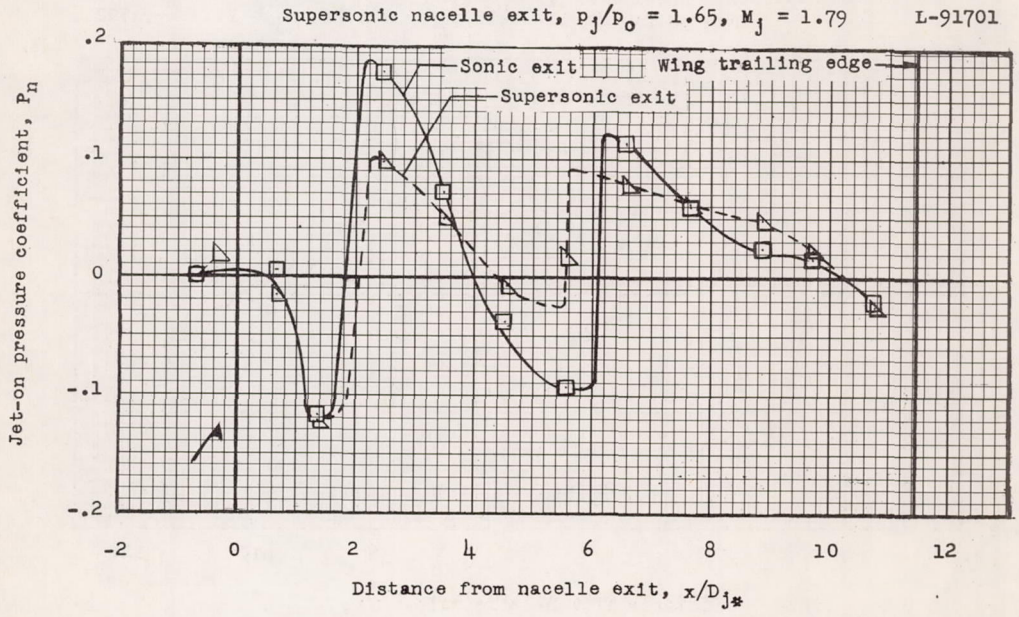
Figure 19.- Continued.



Sonic nacelle exit, $p_j/p_o = 4.90$, $M_j = 1.0$

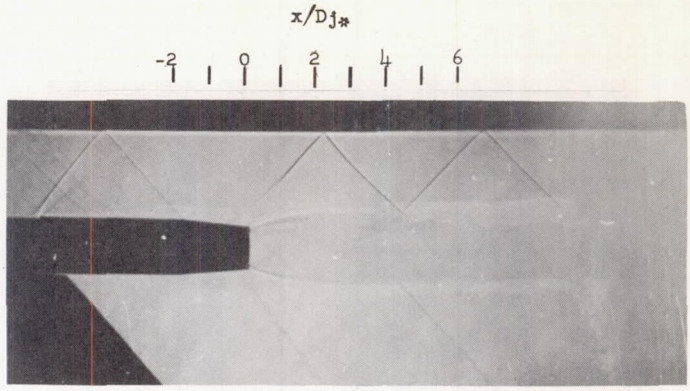


Supersonic nacelle exit, $p_j/p_o = 1.65$, $M_j = 1.79$ L-91701

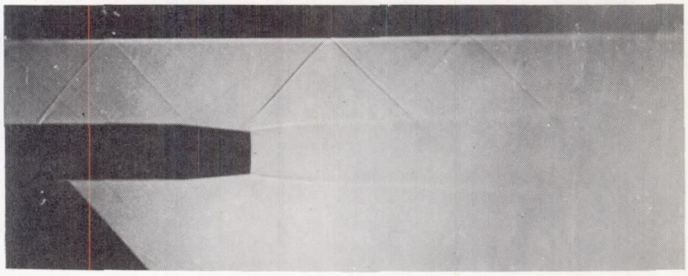


(d) $H_j/p_o = 10$.

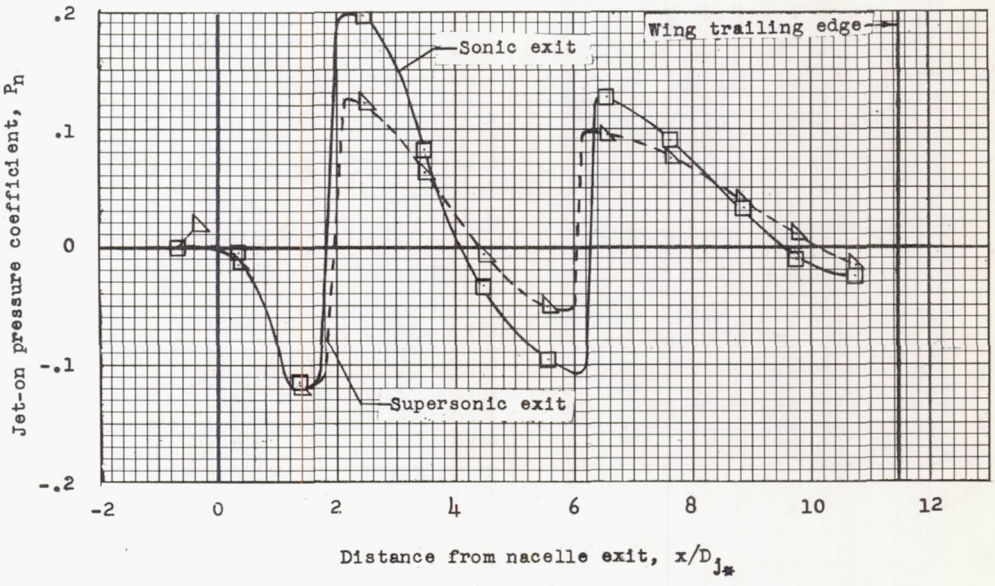
Figure 19.- Continued.



Sonic nacelle exit, $p_j/p_o = 5.87$, $M_j = 1.0$



Supersonic nacelle exit, $p_j/p_o = 1.96$, $M_j = 1.79$ L-91702



(e) $H_j/p_o = 12.$

Figure 19.- Concluded.

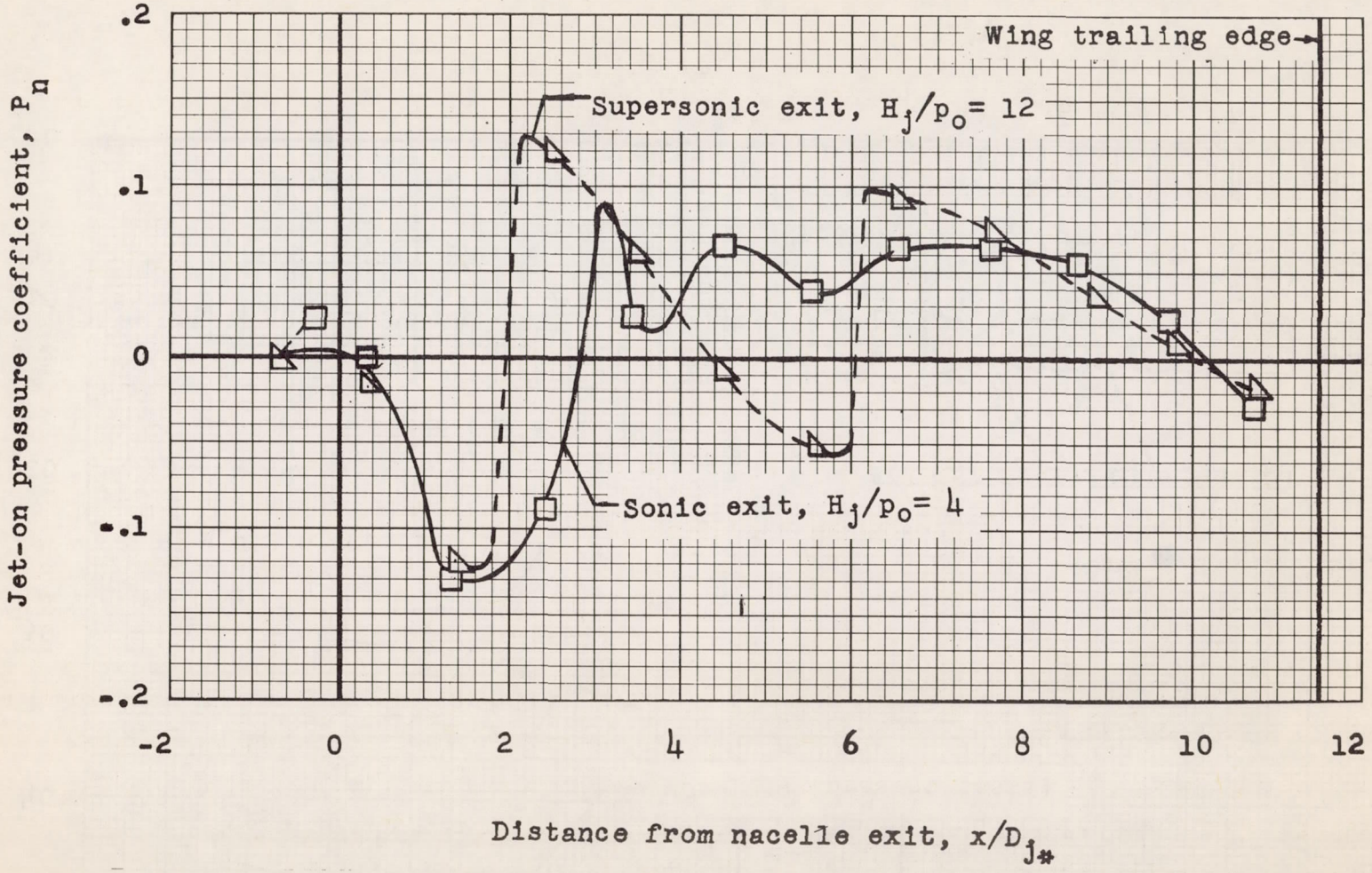


Figure 20.- Chordwise variation of jet-on pressure coefficients along the wing center line at test position I_b for both sonic and supersonic nacelle exits at a nacelle-exit static pressure ratio of 1.96.

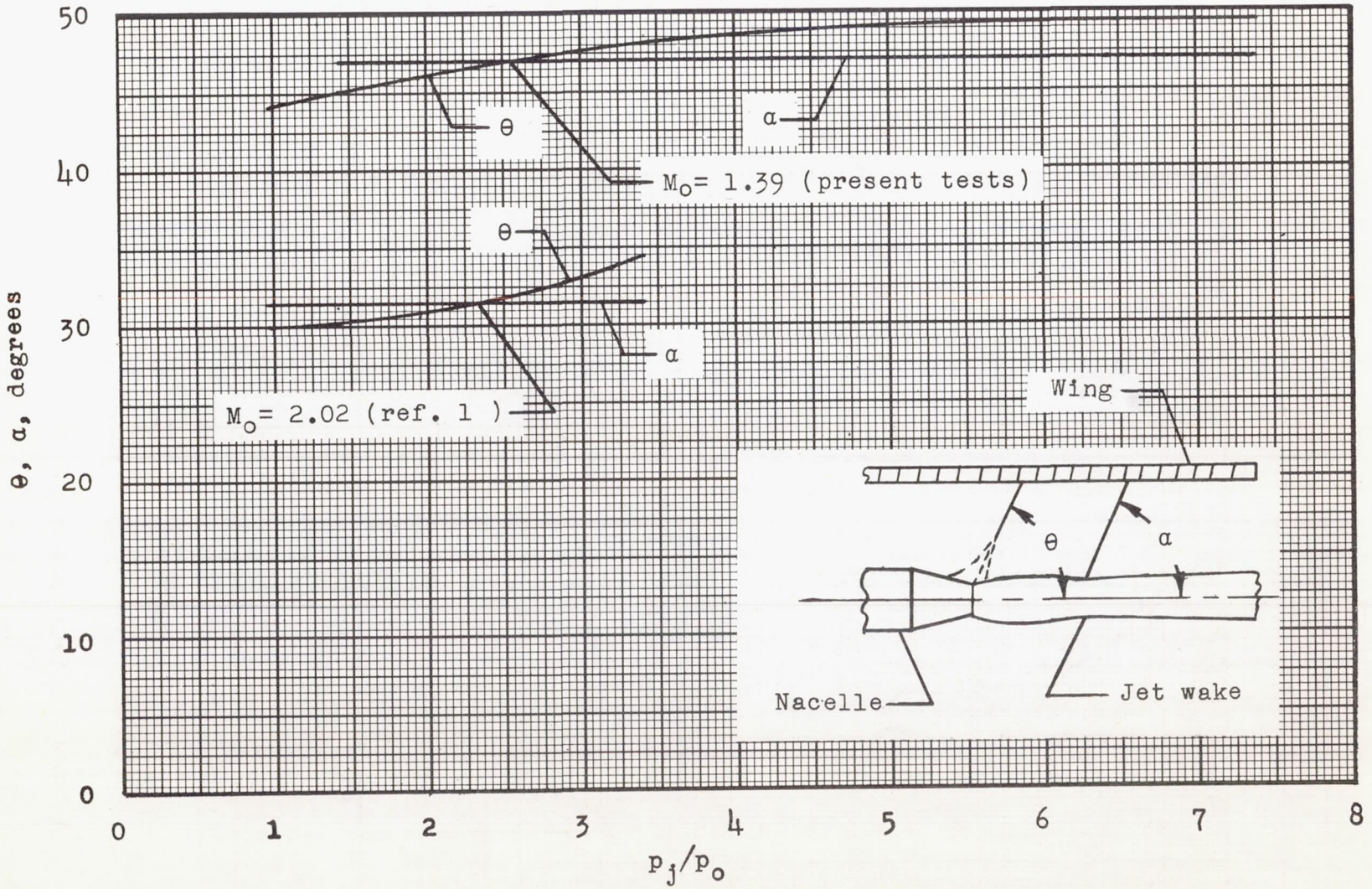


Figure 21.- Variation of primary and secondary jet-on shock wave angles with nacelle-exit static-pressure ratio for a sonic exit.

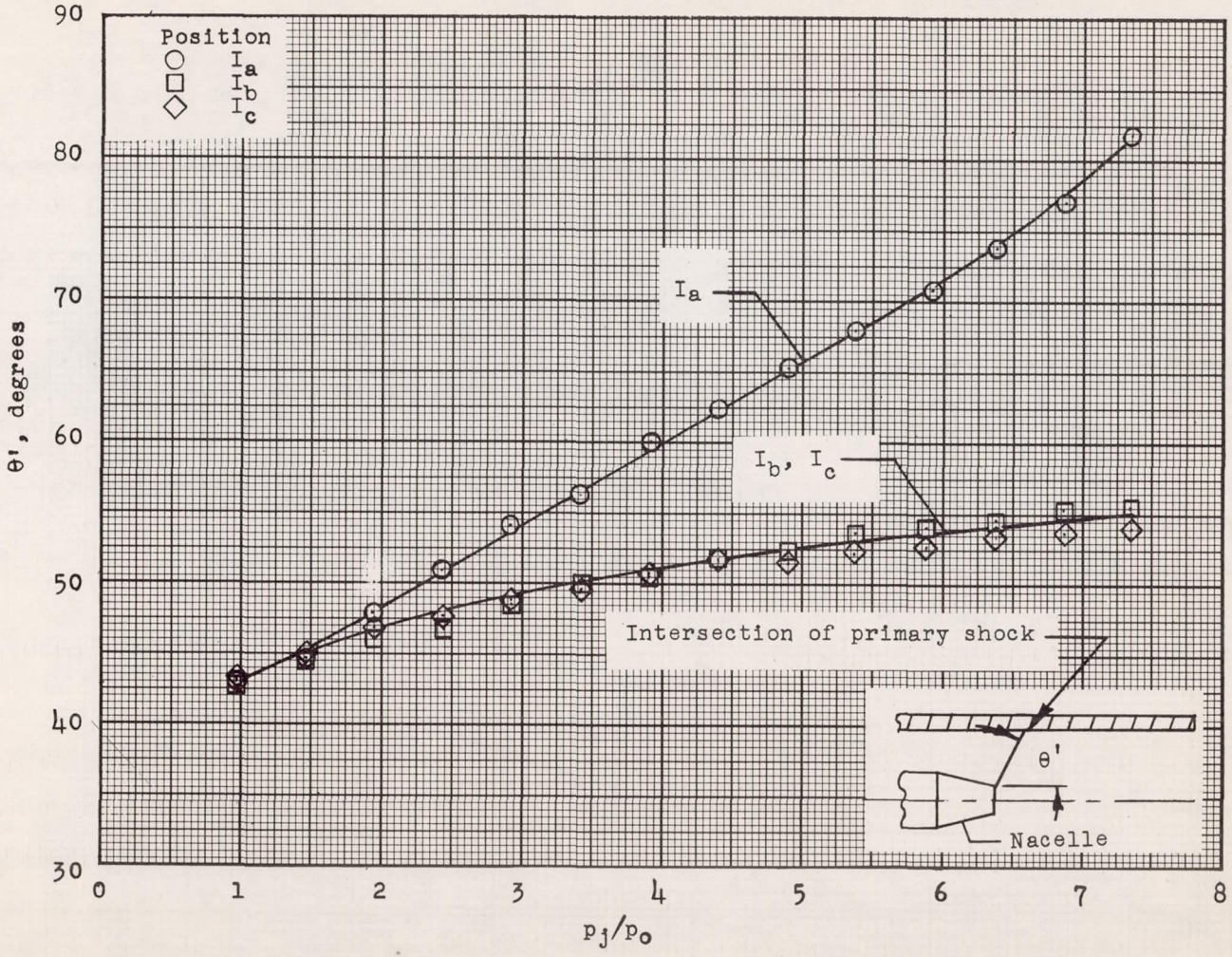


Figure 22.- Variation of the angle between the point of intersection on the wing of the primary shock wave and the nacelle exit with nacelle-exit static-pressure ratio for the three vertical positions tested.

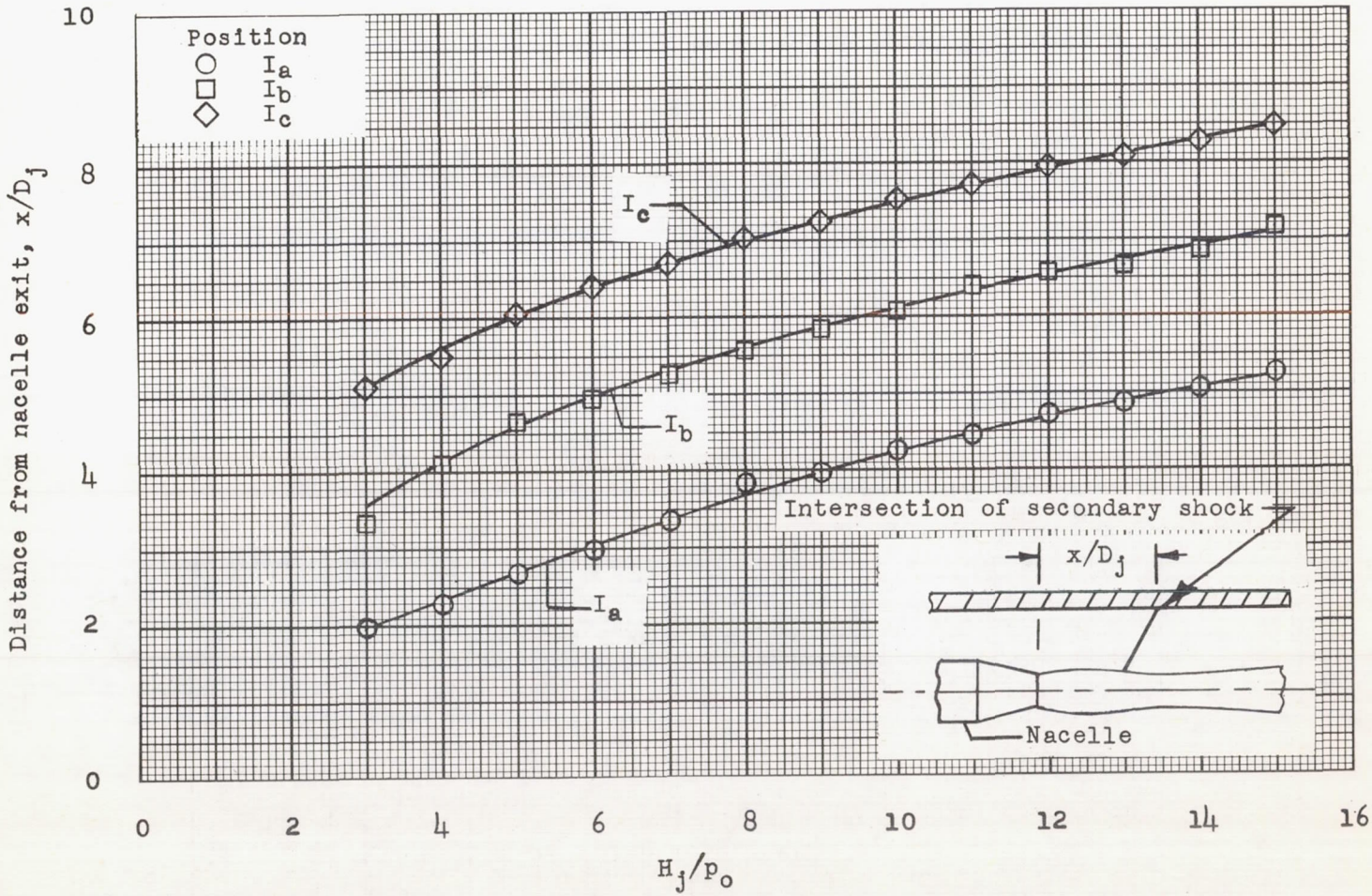


Figure 23.- Variation of the point of intersection on the center line of the wing of the secondary shock wave with nacelle-exit total-pressure ratio at test positions I_a, I_b, and I_c as measured from the shadowgraph pictures.

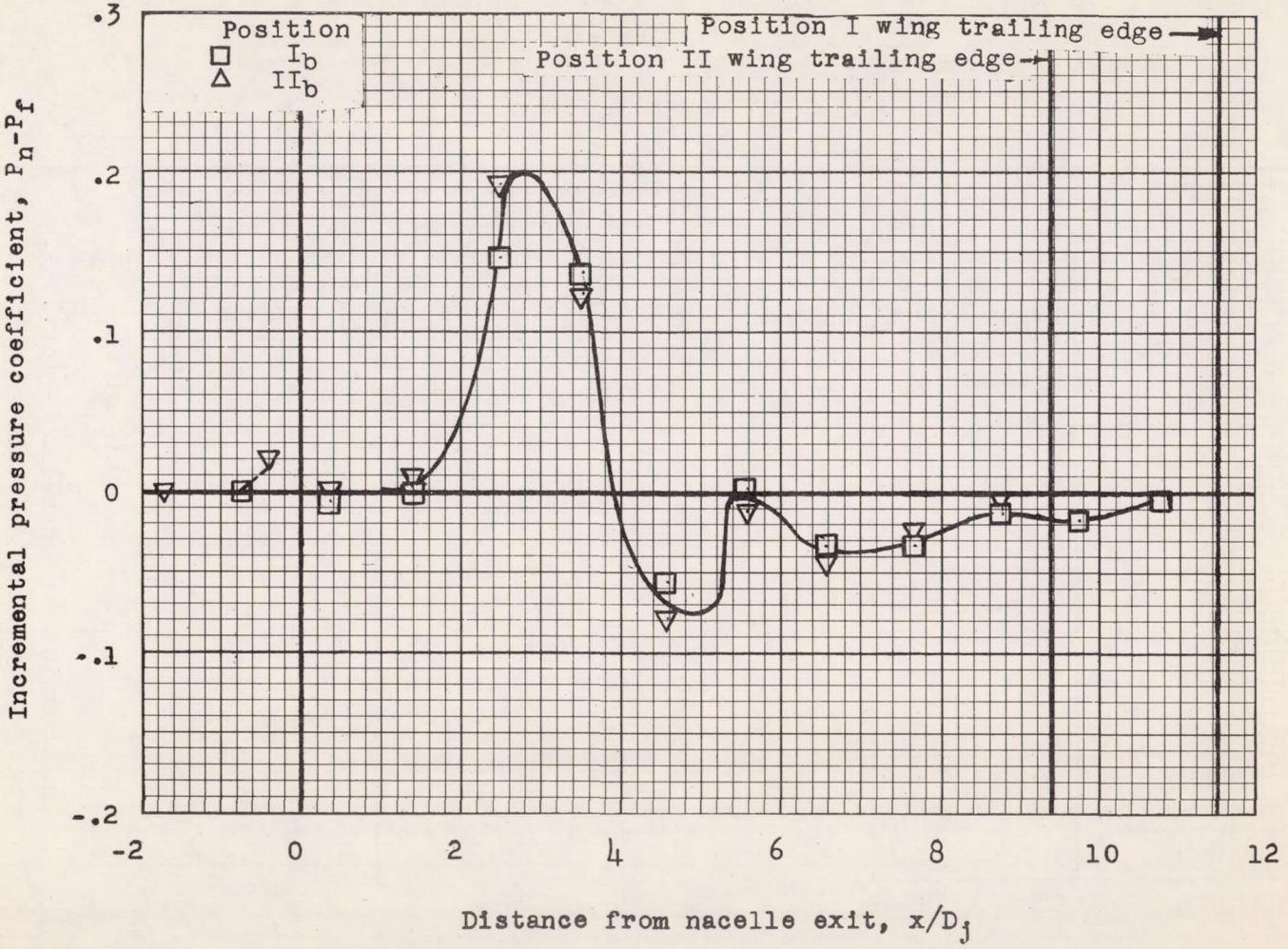
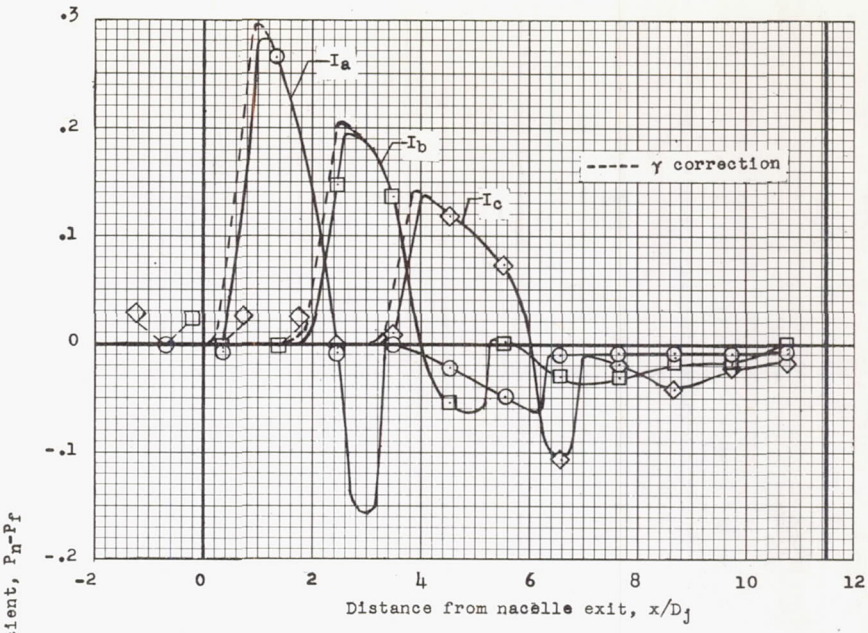
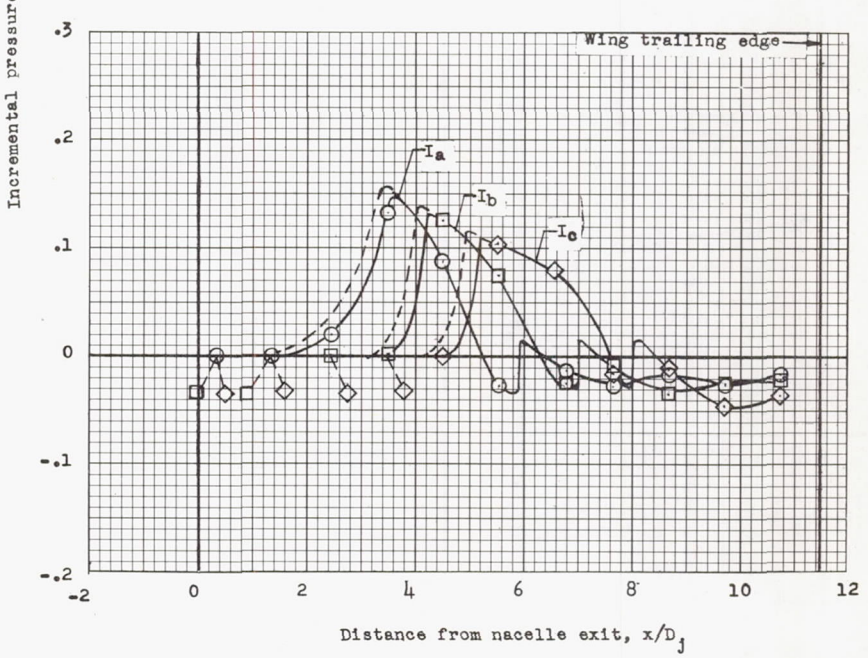


Figure 24.- Chordwise variation of incremental pressure coefficient for test positions I_b and II_b at a nacelle-exit total-pressure ratio of 7 along the nacelle center line.



(a) Along nacelle center line.



(b) $4.17D_j$ spanwise from nacelle center line.

Figure 25.- Chordwise variation of incremental pressure coefficient $P_n - P_f$ at two spanwise stations for positions I_a, I_b, and I_c at a nacelle-exit total-pressure ratio of 7.

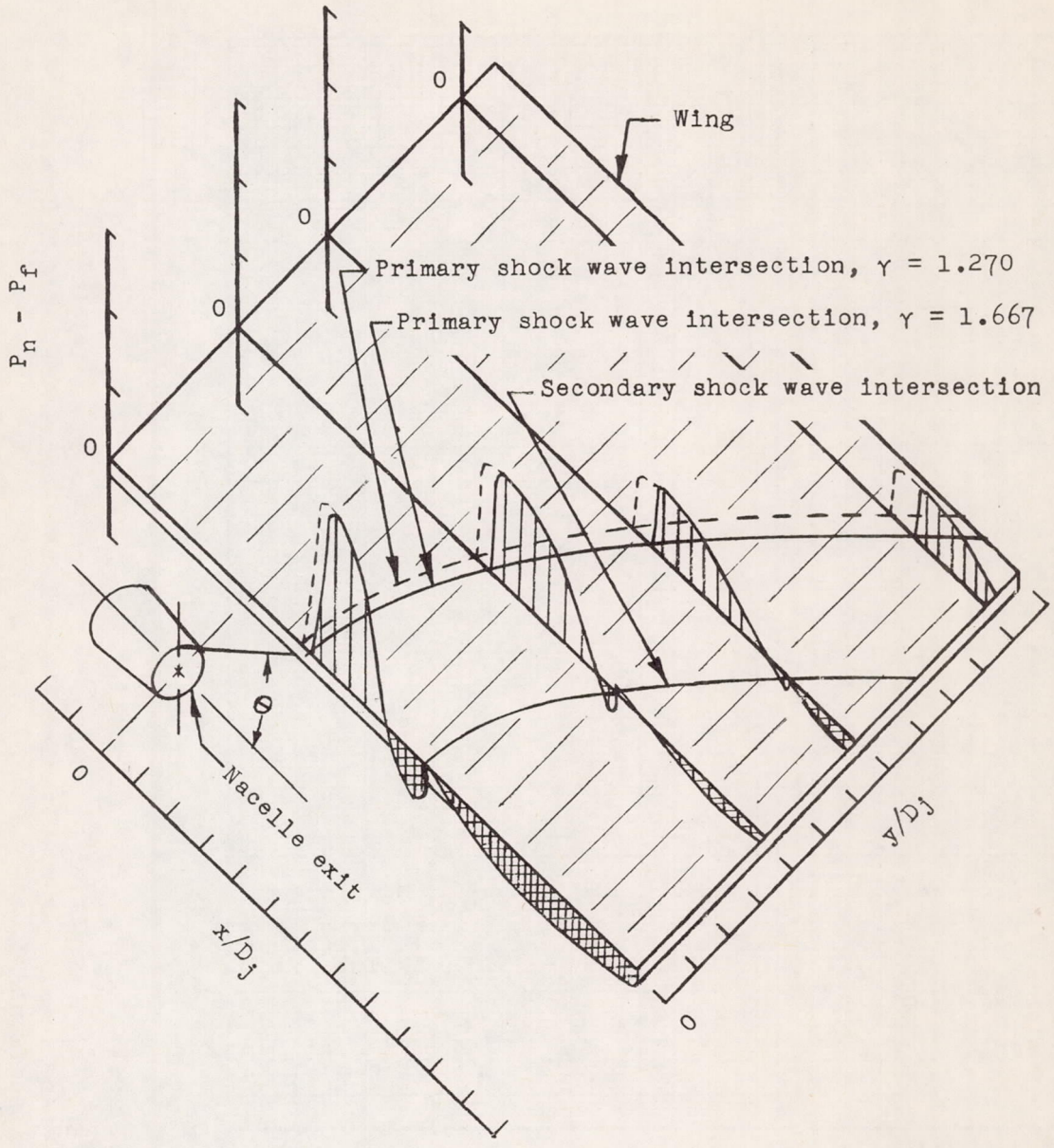


Figure 26.- Typical chordwise and spanwise variation of incremental pressure coefficient $P_n - P_f$.

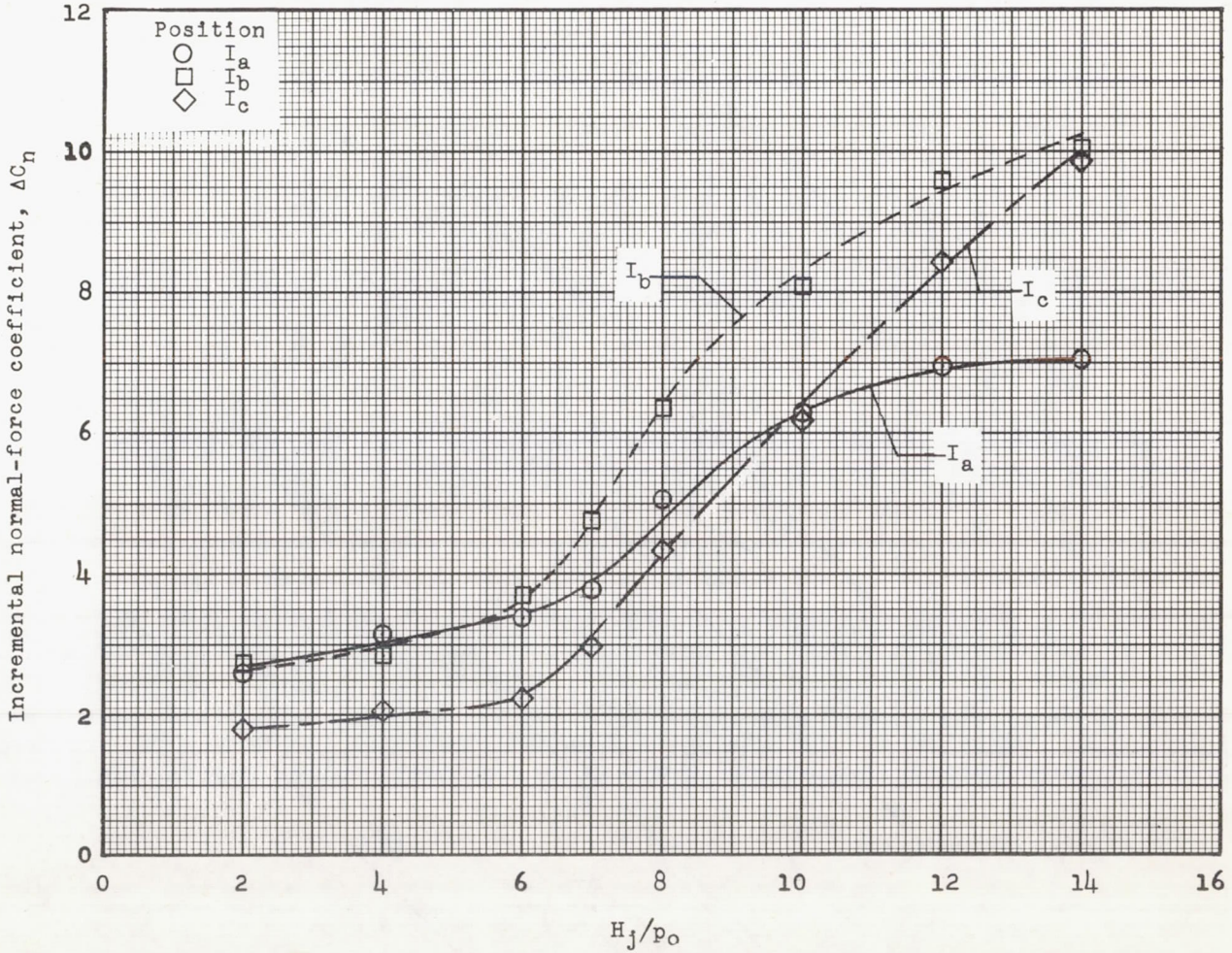


Figure 27.- Variation of incremental normal-force coefficient, based on nacelle exit area, with nacelle-exit total-pressure ratio for test positions I_a, I_b, and I_c.

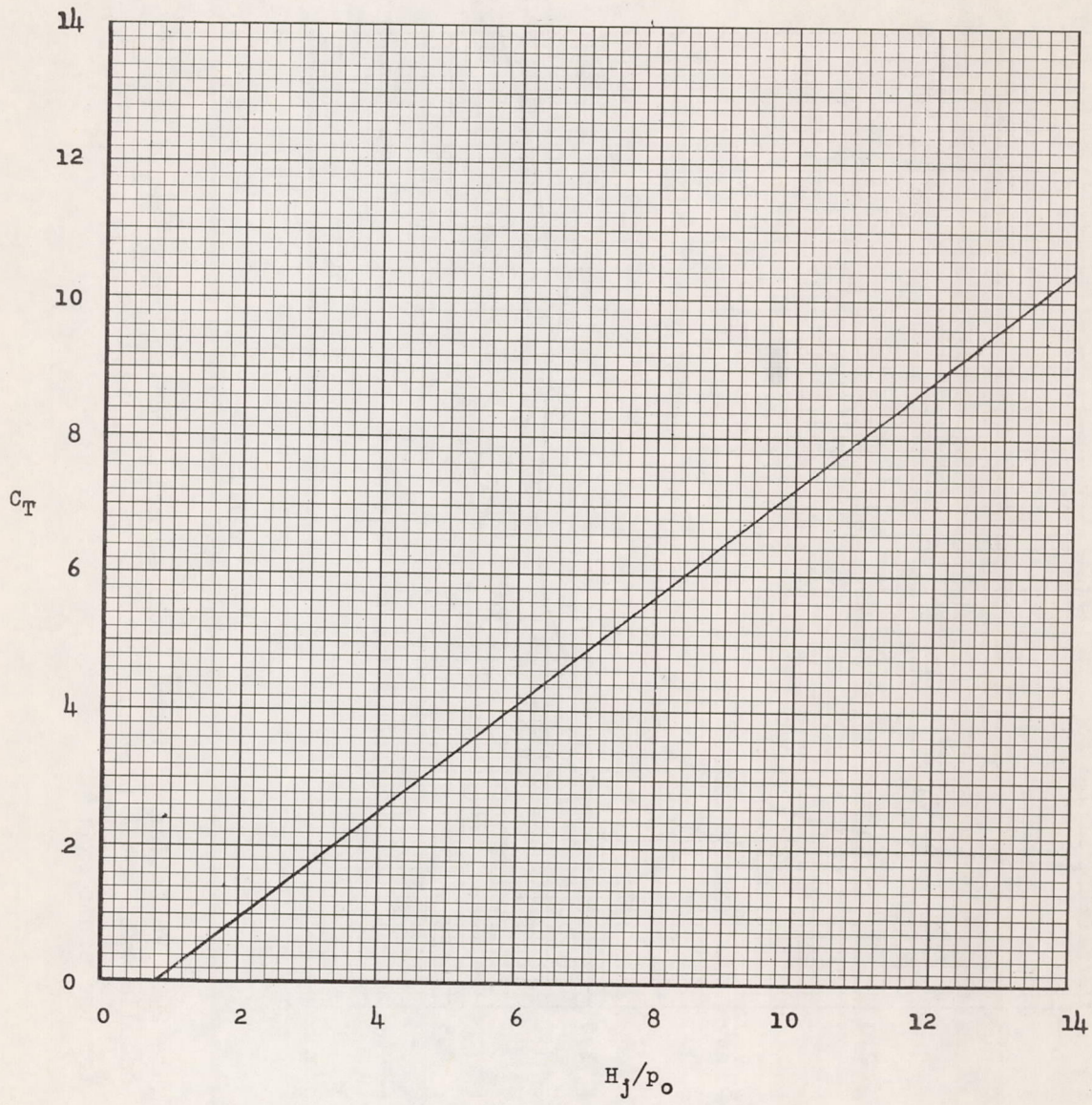


Figure 28.- Variation of gross thrust coefficient with nacelle-exit total-pressure ratio for $\gamma = 1.27$.

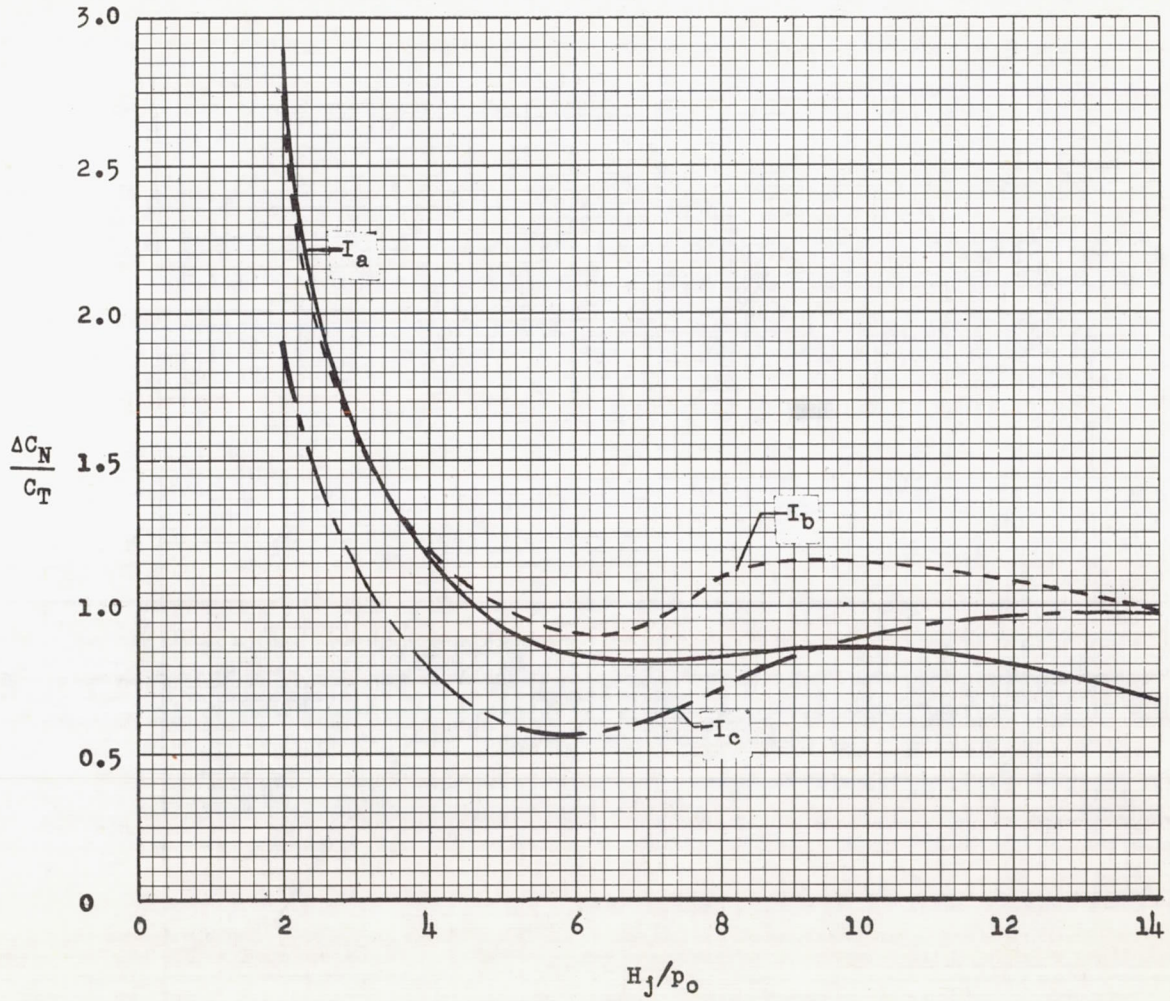


Figure 29.- Variation of incremental normal force to thrust ratio with nacelle-exit total-pressure ratio for test positions I_a, I_b, and I_c for the sonic exit.